MATHEMATICAL MODELS OF HUMAN PILOT BEHAVIOR

Duane T. McRuer, et al

Advisory Group for Aerospace Research and Development
Paris, France

January 1974

DISCLAIMER NOTICE

THIS DOCUMENT IS BEST QUALITY PRACTICABLE. THE COPY FURNISHED TO DTIC CONTAINED A SIGNIFICANT NUMBER OF PAGES WHICH DO NOT REPRODUCE LEGIBLY.

AGARD-AG-188

NORTH ATLANTIC TREATY ORGANIZATION

ADVISORY GROUP FOR AEROSPACE RESEARCH AND DEVELOPMENT

(ORGANISATION DU TRAITE DE L'ATLANTIQUE NORD)

AGARDograph No.188

MATHEMATICAL MODELS OF HUMAN PILOT BEHAVIOR

by

Duane T.McRuer
President and Technical Director
Systems Technology, Inc.
13766 South Hawthorne Boulevard
Hawthorne, California 90250
USA

and

Ezra S.Krendel
Professor of Operations Research
University of Pennsylvania
Philadelphia, Pennsylvania 19174
USA

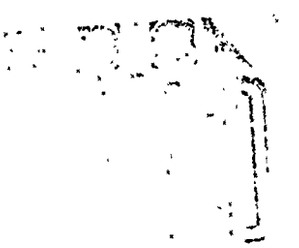

This AGARDograph was prepared at the request of the Aerospace Medical Panel.

THE MISSION OF AGARD

The mission of AGARD is to bring together the leading personalities of the NATO nations in the fields of science and technology relating to aerospace for the following purposes:

Exchanging of scientific and technical information;

Continuously stimulating advances in the aerospace sciences relevant to strengthening the common defence posture;

Improving the co-operation among member nations in aerospace research and development;

Providing scientific and technical advice and assistance to the North Atlantic Military Committee in the field of aerospace research and development;

Rendering scientific and technical assistance, as requested, to other NATO bodies and to member nations in connection with research and development problems in the aerospace field;

Providing assistance to member nations for the purpose of increasing their scientific and technical potential;

Recommending effective ways for the member nations to use their research and development capabilities for the common benefit of the NATO community.

The highest authority within AGARD is the National Delegates Board consisting of officially appointed senior representatives from each member nation. The mission of AGARD is carried out through the Panels which are composed of experts appointed by the National Delegates, the Consultant and Exchange Program and the Aerospace Applications Studies Program. The results of AGARD work are reported to the member nations and the NATO Authorities through the AGARD series of publications of which this is one.

Participation in AGARD activities is by invitation only and is normally limited to citizens of the NATO nations.

Published January 1974

658.3.04 : 629.73.072

Printed by Technical Editing and Reproduction Ltd
Harford House, 7–9 Charlotte St, London. W1P 1HD

SUMMARY

The use of mathematical models of the human pilot in analyses of the pilot/vehicle system has brought a new dimension to the engineering treatment of flying qualities, stability and control, pilot/vehicle integration, and display system considerations. As an introduction to such models, elementary concepts and specific physical examples are used to set the stage for a step-by-step development of what is known about the human pilot as a dynamic control component. In the process, quasi-linear models for single-loop systems with visual stimuli and multiloop systems with visual stimuli are presented and then extended to cover multiloop, multi-modality situations. Empirical connections between the pilot dynamics and pilot ratings are also considered.

Some of the most important nonlinear features of human pilot behavior in adapting to changes in the character of the stimuli are described and tied to the quasi-linear models via the Successive Organization of Perception (SOP) theory, which is reviewed and elaborated. Dual-mode control models needed to describe the pilot's behavior in response to sudden transients are presented, along with pursuit and compensatory elements of the SOP continuum.

The current status of mathematical pilot models is shown to cover random, random-appearing, and transient inputs for single- and multi-loop system configurations. An extensive bibliography of applications and a summary of analysis problems which have been addressed is included, as is a short general status summary and critique of existing models in the form of a listing of shortcomings and problem areas.

CONTENTS

LIST OF FIGURES

LIST OF TABLES

LIST OF SYMBOLS

a_i	Local linear acceleration
A, B	Coefficients of Pilot Rating-Workload Functional
B_m	Effective viscous damper in muscle system
c(t), C(s)	Operator output as a time function and as a Laplace transform, respectively
C_f	Constant of proportionality between motor neuron ensemble firing rate and muscle tension
dB	Decibels, 20 $\log_{10}$ ( )
e(t), E(s)	Error as a time function and as a Laplace transform, respectively
e_n	Error component due to remnant
e_T	Error threshold of the operator
e_v	Visual stimulus
EMG	Electromyogram
f_o	Center frequency of narrowband filter
f_α	Average firing rate
F(t)	Pilot force
G(s)	Open-loop system transfer function; s may be specialized to $s = j\omega$ or $s = -\sigma$
G_m	Muscle/manipulator dynamics describing function
G_N	Neuromuscular system describing function
$G_{ei}(s)$	Closed-loop describing function, error/forcing function
$G_{mi}(s)$	Closed-loop describing function, system output/forcing function
i(t), I(s)	System forcing function as a time function and as a Laplace transform, respectively
i_p	Internally generated pilot command
$j\omega$	Imaginary part of the complex variable, $s = \sigma \pm j\omega$
K	Open-loop gain
K_c	Controlled element gain
K_j	Pilot channel or subsystem gain, particularized by the subscript "j"
K_{p_j}	Pilot gain, particularized by the subscript "j"
m(t), M(s)	System output as a time function and as a Laplace transform, respectively
n	Remnant, referred to pilot output
n_e	Remnant, referred to pilot input
n_z	Normal acceleration
p	Denominator poles
p_x	Amplitude distribution probability density
P_o	Steady-state isometric tension in muscles
P_{sp}	Muscle/spindle tendon organ ensemble lag break frequency
PR	Pilot rating
q_i	Local angular velocity at canals
r	Effective input

R	Pilot rating, particularized by subscript
s	Laplace transform variable, $s = \sigma \pm j\omega$
t	Time
T	First-order time constant, specialized by subscript
T_{d_e}	Effective dwell interval
T_I	General lag time constant of human pilot describing function
T_K, T'_K	Lead and lag time constants, respectively, in precision model of human pilot describing function
T_L	General lead time constant of human pilot describing function, specialized by subscript
$T_{L_{hi}}$	High-frequency pilot lead equalization time constant
T_N	Lag time constant for first-order approximation to neuromuscular dynamics
T_{N_1}	First-order lag time constant of the neuromuscular system
T_R	Aircraft roll subsidence time constant
$\bar{T}_s$	Average sampling interval
u_g	Gust velocity
x, X	Longitudinal displacement
y, Y	Lateral displacement
Y_c	Controlled element transfer function
Y_d	Display transfer function
Y_p	Human pilot describing function
Y_{p_j}	Human pilot describing function operating on the signal j
Y_β	Effective open-loop pilot describing function
z	Numerator zeros
Z	Vertical displacement
Z_{sp}	Muscle spindle/tendon organ ensemble lead break frequency
α	Low-frequency neuromuscular phase lag
α_c, α'_c	Alpha motor neuron command
α_v	Input to oculomotor nucleus
γ, γ'	Gamma motor neuron ensemble command to neuromuscular actuation system, following gamma motor neuron delay
γ_c, γ'_c	Gamma motor neuron ensemble command
δ_a	Control surface deflection (aileron)
δ_e	Control surface deflection (elevator)
δ_r	Control surface deflection (rudder)
δ_{TH}	Throttle deflection
$\underline{\epsilon}$	Environmental variables
ϵ_v	Eyeball position error
ϵ_y	Lateral error
ϵ_z	Vertical error
ζ	Damping ratio
ζ_D	Damping ratio of dutch roll second order

ζ_N	Neuromuscular system damping ratio
η	Disturbance
η_e	Effective dwell fraction
θ	Pitch angle
θ_c	Pitch attitude command
θ_e	Pitch attitude error
θ_i	Pitch angle command
λ_c	Full-attention critical task score
λ_n	Excess control capacity, $\lambda_n = \lambda_s/\lambda_c$
λ_s	Secondary task score
λ_v	Eyeball position
$\underline{\pi}$	Procedural variables
ρ	Correlation coefficient
ρ_{a_c}	Relative remnant at pilot's output
ρ_{a_e}	Relative remnant at error point
σ	Real part of complex variable, $s = \sigma \pm j\omega$
σ	Standard deviation, particularized by subscript
$\underline{\sigma}$	Operator-centered variables
τ	Pure time delay, particularized by subscript
τ_e	Effective pure time delay
τ_{NM}	Time delay of closed-loop neuromuscular system
τ_o	Effective pure time delay for zero forcing function bandwidth
τ_{sp}	Spindle/tendon ensemble pure time delay
ϕ	Roll angle
$\underline{\Phi}$	Physiological outputs
ϕ_M	Phase margin
Φ_{xx}	Continuous component of power spectral density, particularized by the subscript
Φ_{nn}	Closed-loop remnant spectral density, at pilot's output
Φ_{nn_e}	Open-loop remnant spectral density, at system error
Φ_{xy}	Cross-spectral density, particularized by subscripts
Φ_{xx}	Power-spectral density, particularized by subscripts
$\underline{\Psi}$	Psychophysiological outputs
ω	Angular frequency, rad/sec
ω_c	System crossover frequency, i.e., frequency at which $\lvert Y_p Y_c \rvert = 1$
ω_{c_f}	System crossover frequency for foveal viewing
ω_{c_o}	System crossover frequency for zero forcing function bandwidth
ω_{c_p}	System crossover frequency for parafoveal viewing
ω_i	Forcing function bandwidth
ω_{i_e}	Effective bandwidth of forcing function
ω_m	Open-loop neuromuscular system natural frequency
ω_N	Closed-loop neuromuscular system natural frequency

ω_T	Angular velocity threshold
Ω	Ratio of parafoveal to foveal gains, $\Omega = \omega_{cp}/\omega_{cf}$
$\measuredangle$	Phase angle
$\doteq$	Approximately equal to
$(\dot{})$	$d(\ )/dt$
$(\ddot{})$	$d^2(\ )/dt^2$
Σ	Summation
$\int$	Integral
$\lvert\ \rvert$	Magnitude
$\in$	Subset of
$\sim$	Similar to
$\overline{(\ )^2}$	Mean-square quantity

CHAPTER I

INTRODUCTION

A. PURPOSE AND OUTLINE OF THE REPORT

From the authors' standpoint, the genesis of this report was a request from the AGARD Aerospace Medical Panel to prepare a concise and critical review of mathematical modeling of the human pilot as a control element (as distinct from the somewhat parallel technology in passive biodynamic modeling). It was hoped by the Panel that this would highlight the most relevant and reliable conclusions about human operator mathematical modeling to be drawn from the available literature.

Our approach to this task is constructed upon two bases. The first is an indication of what is known about the human pilot as a dynamic control component; and the second is, in the light of this knowledge, what further is needed, or where do we go from here? There is an adequate variety of substantially current surveys of the literature and models readily available to the specialist. Therefore, it is not our intention to contribute another survey. We will, instead, attempt to distill out concepts and models which represent the essence of current generalized empirical knowledge. These are inherently syntheses of models and empirical data based on the efforts of many investigators. Our emphasis will be on quasi-linear descriptions for the most part, since these are the most complete and have been most extensively applied. On the current frontier are nonlinear and non-stationary situations, so these will also be treated to the extent possible. The next sections of this introduction give brief backgrounds of the history, intended nature, and fundamental concepts of human pilot mathematical descriptions. These remarks set the stage for the remainder of this report.

Chapter II presents some elementary concepts for the quantitative description of human dynamic response in closed-loop systems. The intent in this chapter is to introduce the basic concepts and phenomena in a primarily descriptive and intuitively understandable manner. By means of concrete examples, we develop mathematical descriptions (integro-differential equations and transfer functions), the concept of the remnant, and other facets of human operator mathematical descriptions. The physical approach of this presentation is emphasized by reliance on time histories to establish the concepts and approximate mathematical relationships. The data for the several specific cases presented are then synthesized into a simple overall model which characterizes the dynamics of the human and control system. The mathematical implications of this model are then explored in detail to indicate the types of estimates and predictions one could make about control systems which behave in the fashion exhibited by the simple model. Sufficient detail is provided to permit the simple "back of the envelope" calculations so dear to the heart of practical scientists and engineers.

The descriptions of Chapter II are for one pilot subject and the model building there depends on semi-qualitative measurements. Chapter III describes the more general state of affairs which obtains when many subjects are present and when a more respectable mathematical theory is used as the basis for measurement. Thus, the four key types of variable which affect the pilot's action are described in detail, and the nature of quasi-linear measurements is introduced.

Chapters IV and V summarize the current status of quasi-linear models for compensatory situations. We start in Chapter IV with single-loop systems for visual stimuli. The presentation includes an indication of the experimental data available and interpretation of these in terms of the most elaborate current models. Chapter V follows with the extension of the single-loop quasi-linear compensatory model to multi-loop visual input and to multiloop, multi-modality situations. Some empirical connections between pilot dynamics and pilot ratings are considered in both Chapters IV and V.

Chapter VI examines the endpoints of key features of human operator nonlinear behavior, that is, the adaptive changes in behavior induced by changes in the character of the stimulus presented. Pursuit and "precognitive" behavior is introduced and tied together with compensatory behavior via the Successive Organization of Perception (SOP) hypothesis, which is reviewed and elaborated. Step inputs and nearly periodic forcing functions are among those considered, and the dual-mode control model needed to describe the pilot's behavior in response to sudden transients is featured as one element in the SOP continuum.

The status quo summarized by Chapters II-VI provides the prologue to Chapters VII and VIII. Although this report is not intended to provide a survey of applications techniques and examples, part of an adequate status report is an indication of applications. Therefore, Chapter VII briefly summarizes, with the aid of an extensive bibliography, the types of pilot/vehicle analysis problems which have been addressed.

The critique portion of the report follows in Chapter VIII. This takes the form of a listing of deficiencies in the existing models which thereby define shortcomings and problem areas. Some attempt is made to make this critique constructive by noting, where available, analytic or other approaches which might be adopted to alleviate the shortcomings.

B. HISTORICAL BACKGROUND

Piloted aircraft have always required a satisfactory match of the aircraft characteristics and the controller properties of the human pilot. This was explicitly recognized in the December 23, 1907, Signal Corps Specification, No. 486, for a heavier-than-air flying machine, as "....it must be steered in all directions without difficulty and at all times under perfect control and equilibrium." (Ref. 1). But, need for good man-machine integration was thoroughly appreciated even earlier by the Wright Brothers. For instance, in a talk before the Western Society of Engineers in 1901, two years before their first powered flight, Wilbur Wright said (Ref. 2):

> "Men already know how to construct wings or aeroplanes, which when driven through the air at sufficient speed, will not only sustain the weight of the wings themselves, but also that of the engine, and of the engineer as well. Men also know how to build engines and screws of sufficient lightness and power to drive these planes at sustaining speed....Inability to balance and steer still confronts students of the flying problem....When this one feature has been worked out, the age of flying machines will have arrived, for all other difficulties are of minor importance."

Although essential for success, an agreeable marriage between the dynamic properties of the inanimate aircraft and the animate pilot is not spontaneously achieved in the design process. Indeed, the provision of proper aircraft flying qualities has often posed serious problems which the designer must solve. Until fairly recently these solutions relied very heavily on intuitive cut-and-try procedures. Over the years this ad hoc empirical approach fostered many of the adventures and uncertainties of flight testing!

The desire to handle aircraft stability and control problems in a more analytical fashion was recognized long ago. As an illustration, before World War II Koppen stated (Ref. 2):

> "Since the controlled motion of an airplane is a combination of airplane and pilot characteristics, it is necessary to know something about both airplane and pilot characteristics before a satisfactory job of airplane design can be done."

But the central difficulty in understanding controlled motion was recognized earlier still. For example, W. Crowley and Sylvia Skan remarked in a 1920 Aeronautical Research Committee report (Ref. 4):

> "A mathematical investigation of the controlled motion is rendered almost impossible on account of the adaptability of the pilot. Thus if it is found that the pilot operates the controls of a certain machine according to certain laws, and so obtains the best performance, it cannot be assumed that the same pilot would apply the same laws to another machine. He would subconsciously, if not intentionally, change his methods to suit the new conditions, and the various laws possible to a pilot are too numerous for a general analysis."

Actually, matters are even worse than Crowley and Skan recognized; for while much of the pilot's dynamic behavior is governed by the aircraft dynamics, many additional factors also affect his properties.

Psychologists too pointed to variability as the hallmark of human behavior, and organized much of the theory useful in experimental psychology so as to cope with intersubject and intrasubject differences.

But, the biggest problem confronting anyone who wished to study the controlled motion of aircraft — what we would today call pilot/vehicle analysis — was not the human's adaptability and variability but the absence of an underlying quantitative theory on which to erect a structured approach to the manual control of aircraft. What was needed was a theory for feedback control systems, and this became available in a sufficiently mature state in the early 1940s. With feedback control theory available as a paradigm, only a need had to be at hand for attempts to be made to overcome the a priori pessimism. And at the beginning of the '40s there was no end to the needs! Thus, necessity was the mother of human dynamics research. Complex weapons were evolving which could only function in concert with human operators, so an urgent requirement for engineering data arose.

The pioneer in human operator dynamic measurements was Arnold Tustin, the electrical engineer, in England during World War II. Tustin extended the required feedback control theory framework by introducing the concept of "describing function" and "remnant" measures and quasi-linear systems in general (Ref. 5). He then applied the concepts to actual human operations. In reporting on his studies of manual control of a power-driven gun (Refs. 6 and 7):

> "The object of the series of tests was to investigate the nature of the layer's response in a number of particular cases and to attempt to find the laws of relationships of movement to error. In particular, it was hoped that this relationship might be found (within the range of practical requirements) to be approximately linear and so permit the well developed theory of 'linear servomechanisms' to be applied to manual control in the same way as it has already been to automatic following."

Also during the Second World War and responding to the same urgent needs but acting independently of Tustin, A. Sobczyk and R. J. Phillips at the MIT Radiation Laboratory (Ref. 8) and H. K. Weiss (Refs. 9 and 10) at Aberdeen Proving Ground presumed quasi-linear operation in a series of studies on aided tracking of guns.

After the war these seminal efforts, and the hope for a more rational approach to the design of aircraft, led Leo Chattler of the USN Bureau of Aeronautics and Charles Westbrook of the US Air Force Aircraft Laboratory to sponsor some small-scale contract research efforts aimed at determining the dynamic characteristics of human pilots. For the Navy, the Goodyear Aircraft group of R. Meade, L. Diamantides, and A. Cacioppo, headed by R. Wayne, developed excellent analog computer representations for pilots for two specific task-variable situations (Refs. 11-13). The Air-Force-sponsored activity at Franklin Institute (Ref. 14), Princeton University (Refs. 15-18), and Control Specialists, Inc. (Refs. 19 and 19) chose to exploit cross-correlation and cross-spectral techniques to establish human pilot dynamics. Parallel university research was underway at MIT with a remarkable Master's thesis by Lindsey Russell (Ref. 20) and an extensive and useful doctoral dissertation by Jerome Elkind (Ref. 21).

The end of the pioneering era in experimentation can be conveniently put with the publication of "Dynamic Response of Human Operators" (Ref. 19) in October, 1956, and its journal summary in Ref. 22. This volume codified and correlated the available human response data, developed predictive models compatible with these data, and prescribed preferred forms for the operator which permitted specification of "ideal" characteristics for the controlled element compatible with the man in the manual control system.

Since 1957 an enormous number of measurements have been made for single-loop, i.e., single-input/single-output manual control systems of all kinds. Using more and more refined measurement and data reduction techniques, many organizations and individuals have contributed in the U S. and abroad. Many of these will be mentioned later when we attempt to define where we stand today. In terms of the historical record, it is probably fair to say that now much more is known about the input-output characteristics of some kinds of single-loop systems than remains to be learned. The single-loop experience also provided a firm foundation for subsequent extensions.

Going from single-loop to multiloop situations is an enormous step — so large, in fact, that it is still in progress. The first attempts were multi-modality experiments in which a number of fundamental dynamic response measurements were made in aircraft and moving-base simulators to determine the effects of linear and rotary motion cues on the pilot's dynamics. Ordinarily, these studies compared fixed- versus moving-base situations on the basis of effective visual input pilot describing functions. In two or three instances it has been possible to separate uniquely the motion and visual transfer characteristics by using independent forcing functions. As will be seen later, all this amounts to an excellent start, although much of importance is on the docket for the future.

As one might expect from this brief historical account, three decades of joint engineering and experimental psychological attempts to characterize mathematically the dynamic characteristics of human pilots has resulted in an enormous collection of literature. Because most of the work, in the United States at least, has been sponsored by the Government, notably the Air Force Flight Dynamics Laboratory, the National Aeronautics and Space Administration, and the Naval Air Systems Command, or has been the result of university research activities, the complete documentation is predominantly in Government reports and university theses. Stemming from this enormous base, like the visible tip of an iceberg, is a journal literature which is also extensive. Much of the original work is reflected in the IEEE Transactions (Human Factors in Electronics; Man-Machine Systems; Systems, Man, and Cybernetics), the AIAA Journal of Aircraft, the Journal of the Human Factors Society, and Ergonomics. Particularly complete documentation in recent years has come about from the "Annual Manual," officially the Annual Conference on Manual Control, sponsored by NASA and the USAF (Refs. 22-28). These international annual meetings present summaries of the latest word in manual control technology as well as a useful, but incomplete, cross section of applications. Extensive bibliographies are given in Refs. 29-31. This literature reflects the application of almost every conceivable control theory approach to modeling the human operator, as well as the application of appropriate models to the control of almost any imaginable vehicle.

As befits the rapid evolution of mathematical models for the human operator through the past three decades, a series of summary surveys have appeared aperiodically (Refs. 19, 32-38). Thus, not only the dynamic characteristics and models of the human operator but some synthesis, as depicted in summary surveys, are well represented in a readily available literature.

C. MODELING PILOTED SYSTEMS

Engineering models, as we use the terms, comprise analytic and verbal descriptions of the phenomenon of interest so expressed that the key variables are explicit; the ranges and rules of application are well defined; and all of the relevant constructs described in operational terms compatible with such other models as may be pertinent. When this has been done such models are (and to be at all convincing must be) capable of being validated, augmented, or disproved by researchers other than the originators. These models are much more than convenient and efficient summaries of data; they are predictive tools for rational systems synthesis. In fact, the most compelling justification of any model is its capacity to subsume past experimental results and to predict the outcome of future experiments especially contrived to exercise the model beyond its original scope. Once these engineering models have been validated, they serve several purposes. For instance, they:

1. Provide "laws" which can be used to estimate or predict pilot dynamic behavior.

2. Characterize past observations with simple analytical forms, thereby achieving economies in description of experimental data.

3. Quantitatively describe the connections between model parameters and situation variables which affect the pilot.

4. Establish the basis for a rationale which can be used to better "understand" the ways in which the pilot behaves as a control system component.

Because the purpose of engineering models is application, a host of variables which appear to be interesting intuitively can easily turn out to be irrelevant to the particular application and, thereby, to the model. However, whether they be relevant or irrelevant is not an intuitive judgment. The decision follows from a careful, almost tedious, statement of potentially relevant variables and the establishment of their influence either empirically or theoretically, so that these can be made analytically and/or verbally explicit in the model.

We have denoted the relevant variables as key variables and have divided them into four categories: task, environmental, pilot-centered, and procedural. They will be described in detail further along, but the point for now is the need to recognize and take into explicit account the principal factors which underlie human operator variability — thus reducing to a minimum the inevitable component of variability which remains unassigned. The engineering model then becomes more generalizable in that its parameters are affected in an empirically discoverable way by the identified key variables. Further, our understanding of vaguely defined key variable elements, e.g., "motivation" or "fatigue" as typical pilot-centered variables, is further enhanced by associating quantitative changes in measurable pilot parameters with changes introduced in these variables. In summary, an effective model of human dynamic operation must recognize that inter- and intra-subject variability exists and that much of this variability can be assigned as the effects of key variables on the model's parameters.

D. PILOT DYNAMIC BEHAVIOR IN CONTROL TERMS

A pilot's actions are many and their range is broad. We are interested in those actions which exert control on the aircraft, and we will outline the model structure implications of these activities. Subsequently, we will indicate the variety of factors which can influence the resulting performance; for by limiting the conceptual context and defining these factors it becomes possible to convert an unmanageably complicated general problem to a manageably complicated set of specific problems.

The conceptual context derives from the following three fundamental concepts which constitute the essential substance of pilot-in-the-loop systems analysis:

- The establishment of appropriate control loops among the display, pilot, and vehicle system elements.
- The optimization of the loop properties by suitable pilot adaptation.
- The penalties for this adaptive control.

The initial concept is that to accomplish guidance and control functions (as in flying approaches, intercepts, formation, regulating against atmosphere disturbances, etc.) the human pilot establishes a variety of closed loops around the airplane which, by itself, could not accomplish such tasks. The greatest amount of information and experience exists for the single-loop case for which the pilot is applying his full attention to one control task. Because many piloting problems involve one axis dominantly, and because a wide variety of displays, configurations, vehicle dynamics, and manual control mechanisms can be reduced to a single-loop block diagram, concentration on this simplified structure has been highly productive. When multiple inputs and irreducible multiple loops exist, more complicated analysis cannot be avoided. It is often the case that the input data upon which the pilot depends and the loops he elects to close are not immediately obvious and must be deduced from his measured dynamics and performance. After recognizing such data sources and loops it is possible for the system engineer to enhance their utility for the pilot by appropriate design refinements. In this fashion the peculiarly human contributions to the system may be strengthened and the pilot will be treated with more design "respect."

The second major concept is that to be satisfactory these various closed-loop systems have to behave in a suitable fashion, although animate and inanimate components are interacting, the overall system must share certain of the qualitative features of all "good" closed-loop control systems (stability, accuracy, simplicity, etc.). As the adaptive means to accomplish this end, the pilot must make up for any dynamic deficiencies of the effective controlled element as a whole by appropriate adjustments of his own dynamic properties. The view of the pilot is that of an active, sophisticated, and knowledgeable system component, not an afterthought which, in some quasi-mechanistic manner, must fit into the control system. The pilot expresses his operational judgments on criteria for system performance and on satisfactory system stabilization by his actions. In every sense he is in control and serves to enrich the system's task capability repertory.

The third major concept states that there is a cost to the pilot for this adjustment: in workload-induced stress; in concentration of his faculties; and in a reduced potential for coping with the unexpected. The measures of the cost to the pilot are pilot commentary and pilot rating, possible task-associated changes in the pilot's dynamics, and other workload-sensitive physical and psychophysiological measures such as heart rate. The cost to the system is expressible in terms of diminished operational reliability and effectiveness. Since these costs can be high indeed, efforts to predict their onset and magnitude by measures based on the pilot's behavior are of great potential benefit.

CHAPTER II

ELEMENTARY CONCEPTS FOR THE QUANTITATIVE DESCRIPTION OF HUMAN OPERATOR DYNAMICS IN CONTROL SYSTEMS

When a human is successfully engaged as an active element in a feedback control system the combined behavior of man and machine is such as to satisfy overall man/machine system purposes. Machines and their manipulative controls differ; the external environment and surround from which the operator derives sensory input may be highly diverse; and control purposes may bear little resemblance to one another. Yet the human controller counters all this diversity by modifying his characteristics appropriately to match the many possible control situations. The fact of these adjustments and adaptation is characteristic of the human; the consequence is a bewildering range of behavior which makes quantitative description of the human operator enormously complex when viewed in the large. Because the entirety is incomprehensible, in order to gain quantitative understanding it is necessary to partition the whole into parts. If we are lucky, these parts can be selected so as to have behavioral properties which efficiently capture the dominant effects and are susceptible to simple quantitative description. In this way, there is some hope of obtaining an ensemble of reasonably simple quantitative behavioral models, each of which has adequate generality in its restricted sphere. Then, when efficient models, each suitable for one of several related facets, are available, further inductive generalization may be feasible. This is the approach we will pursue here.

The situations which are most susceptible to quantitative description involve control of inanimate elements which have constant characteristics, and an operator who has learned by extensive practice to control the system effectively with little fluctuation in the man/machine system performance measures. When the stimuli impacting on the system are random or random-appearing time-stationary processes, the skilled operator will ultimately adjust so that his control actions (as time signals) have similar random and time-stationary properties, at least over all but a very short or very long period. The simplest manual control system, Fig. 1, which fits these characteristics is the so-called single-loop compensatory system with visual stimulus, which is the paradigm for many much more complicated appearing configurations. The system forcing function, i(t), is a random or random-appearing time function which has stationary or quasi-stationary properties. The compensatory display presents the operator with a visual stimulus which shows only the difference between the system forcing function and the system output. Typically, the operator's task is to minimize this presented error signal, e(t), by trying to keep it superimposed on a stationary point or line on the display. This is accomplished by manipulative control action, c(t), which affects the controlled element and gives rise to the system output, m(t), being controlled. The usual purpose of a system of this nature is to make the system output closely resemble the system forcing function or, in other words, to make the output follow the input. The quality of this following is indicated by the system error which is directly proportional to the operator's visual stimulus.

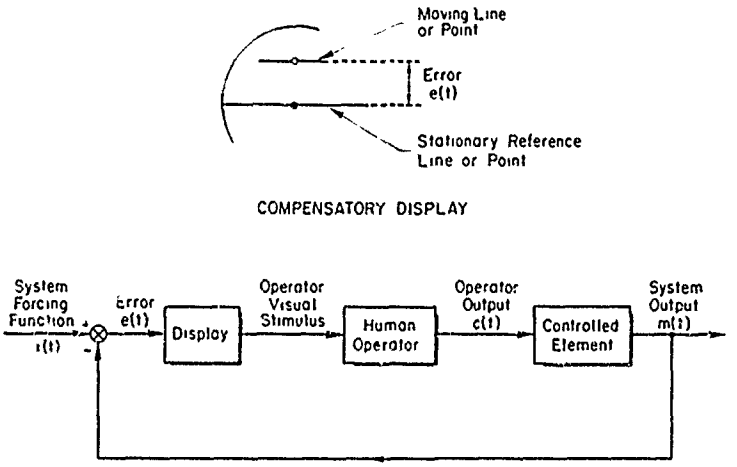

Figure 1. Display and Functional Block Diagram of Simple Compensatory Manual Control System

In order to obtain some physical appreciation for human operator behavior in such systems, we shall consider a few simple cases. Several kinds of human operator dynamic behavior can be evoked by changing the controlled element dynamics while retaining a common control purpose, i.e., minimization of the error for all the control systems studied. For each control situation, a simplified characterization of the human operator will be determined. Then the human operator models for the several specialized control situations will be considered as representative elements of all single-loop compensatory manual control systems subjected to a stationary random-appearing forcing function in an attempt to generalize. The generalization achieved will be a simplified overall model of manual control system dynamics which connects human operator and controlled element dynamic forms by a simple equation. This equation also reveals how the operator's dynamics are affected by controlled element form.

The simple mathematical models for manual control system dynamics developed on this ad hoc basis define a particular form of feedback control system. The mathematical laws for this type of system will then be exercised to illustrate their use in analysis and prediction.

A. APPROXIMATE DESCRIPTION OF HUMAN OPERATOR DYNAMICS FOR ELEMENTARY COMPENSATORY SYSTEMS

In this section we shall consider several pieces of experimental data taken with a single highly trained operator for a variety of controlled element dynamics composed of combinations listed and described in Table 1. To make matters as physical and specific as possible, the experimental data and discussion will emphasize time histories and time domain operations. Nonetheless, the controlled element properties given in Table 1 indicate both time and frequency domain characteristics and illustrate how the element's defining

TABLE 1. ELEMENTARY CONTROLLED ELEMENT DYNAMICS

CONTROLLED ELEMENT DYNAMICS			TIME DOMAIN CHARACTERISTICS		ROOT PLOT	FREQUENCY DOMAIN CHARACTERISTICS
TYPE	EQUATION OF MOTION	TRANSFER FUNCTION	WEIGHTING FUNCTION	INDICIAL RESPONSE		
Proportional	$m(t) = K_c c(t)$	K_c				
Rate or Velocity	$\dot{m}(t) = K_c c(t)$	$\frac{K_c}{s}$				
First-Order Lag	$\dot{m}(t) + am(t) = K_c c(t)$	$\frac{K_c}{s+a}$				
First-Order Divergence	$\dot{m}(t) - \lambda m(t) = K_c c(t)$	$\frac{K_c}{s-\lambda}$				
Acceleration	$\ddot{m}(t) = K_c c(t)$	$\frac{K_c}{s^2}$				

parameters are reflected in each domain. This serves as a convenient introduction to the frequency domain which will be used in subsequent chapters.

Although the controlled element dynamics in Table 1 are very simple, they have many parallels in practical control systems. For example, the rate (velocity) controlled element is an idealization for pitch attitude control with a heavily augmented aircraft, heading control in automobile driving, bank attitude control in an aircraft which has a rapid roll subsidence mode, etc. But the most important feature these elementary controlled elements share with their more complex cousins which represent real-world control situations more adequately is that, with the exception of the proportional type, none of them will stay put by themselves. That is, they respond to an operator input in a dynamic fashion so that the controlled element output, m(t), continues to change or remains non-zero after the operator's output, c(t), has stopped. Thus, to cause the system output to behave as desired, the operator must exert control activities much of the time. In the compensatory situations to be considered here, this control action is inherently of a feedback system nature because the operator's sole stimulus is the error presented on the display. In describing the operator's behavior then, the key question is how the operator, as a dynamic element in the closed-loop system, equalizes, scales, and adjusts quantities derivable from the error signal to form his control output, c(t). In other words, we wish to investigate the dynamic functional relationships between stimulus and response in the closed-loop system context.

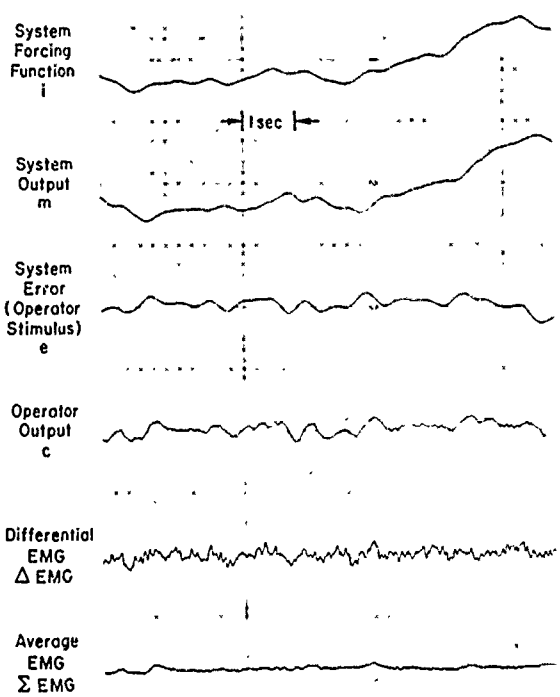

Figure 2. Man/Machine System Response Time Histories; $Y_c = K_c/s$

As a starting point, consider the signals present at various points in the closed loop when the controlled element dynamics are $Y_c = K_c/s$. A sample set of such signals is shown in Fig. 2. These were generated using as a subject a professional instructor pilot who is also highly trained in the controlled tasks to be presented here. The control situation is compensatory (Fig. 1) and involves a random-appearing forcing function which is to be followed by the controlled element output. The system error is presented on a cathode ray tube and the operator manipulates a stiff stick grasped between thumb and forefinger to exert control over the controlled element dynamics generated in an analog computing setup.

The first thing to notice about the typical time histories is that the system output, m, follows the system forcing function, i, very closely. Only a slight time lag keeps the output from being a nearly identical duplicate of the forcing function. The actual difference between these two quantities is shown by the error, which is quite small and fluctuates about zero in a random-like fashion. It is in response to this stimulus that the operator develops his output, c. Here we find a remarkable thing. The operator output tends to look very much like a scaled and delayed version of the error. In fact, if we simply advance the output trace by a time, $\tau_2 = 0.14$ sec, the two signals appear to be directly proportional, with a proportionality constant, K_{p_2}, except for a few tiny "random wiggles" here and there on the output. If we now grace this observation with a quantitative description, we can write that the operator output is approximately related to the system error or operator stimulus by:

$$c(t + \tau_2) \doteq K_{p_2} e(t) \tag{1}$$

or:

$$c(t) \doteq K_{p_2} e(t - \tau_2) \tag{2}$$

If the relationship is considered exact rather than approximate, a transfer function equivalent can be derived by Laplace transforming to obtain:

$$Y_{p_2}(s) \doteq \frac{C(s)}{E(s)} = K_{p_2} e^{-\tau_2 s} \tag{3}$$

These equations all indicate that quantitatively the operator behaves as a proportional controller (pure gain) with pure time delay.

Although it is easy to imagine from Fig. 2 that the delayed proportional relationship between stimulus (cause) and response (effect) obtains, the operator's output is not precisely given by the operation of the transfer function on the stimulus. Instead, there is a slight difference between the delayed and amplified error signal and the actual output. This is a kind of residual, or "remnant," and appears to have a random fluctuating nature akin to a random noise. Since it is generated by the operator, we can consider, for the moment at least, that the remnant is operator-induced noise. Then, the above equations in the time domain can be rewritten with the remnant added and the approximate equality removed.

Besides the major system signals, i(t), e(t), c(t), and m(t), two other time histories appear in Fig. 2. These are the differential EMG, obtained by differencing muscle action potentials from the major agonist and antagonist muscles involved; and the average EMG, found by summing the two muscle action potentials (Fig. 3). The ΔEMG time trace thus represents the operator's neuromuscular system force output which tends to move the manipulator, while the ΣEMG indicates the average tension or tension operating point within the

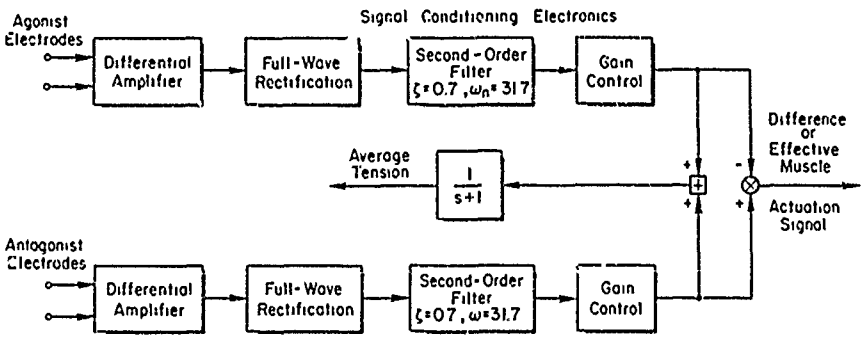

Figure 3. Muscle Action Potential (EMG) Processing to Obtain Effective Muscle Actuation Signal and Average Tension

actuator system. In Fig. 2 the ΔEMG is similar in general trend to the operator's output, with a fairly large nearly-periodic wiggle of about 10-11 Hz superimposed. This oscillatory component is a high-frequency mode in the neuromuscular system. The ΣEMG is fairly constant but not zero, indicating that some steady-state tension is present and that the agonist and antagonist muscle groups are loaded against each other even when no net force output is acting on the manipulator. The neuromuscular system will be discussed later.

If the controlled element free s is moved slightly into the right half plane, a first-order divergence is obtained (fourth type in Table 1). This situation is unstable and requires constant attention to maintain control, although for moderate values of divergence rate the control required is similar to that for $Y_c = K_c/s$. A typical example is shown in Fig. 4, where $Y_c = K_c/(s-2)$. A careful comparison of expanded-scale original records reproduced in reduced form as Figs. 2 and 4 revealed that the operator output is approximately proportional to the system errors for both, but that the delay is much less for the divergent condition, i.e., $\tau_2' \doteq 0.07$ sec as opposed to $\tau_2 = 0.14$ sec. There is also some higher-frequency content to the system output trace, indicating that the system output response reflects the presence of a closed-loop system mode in addition to the system response to the forcing function.

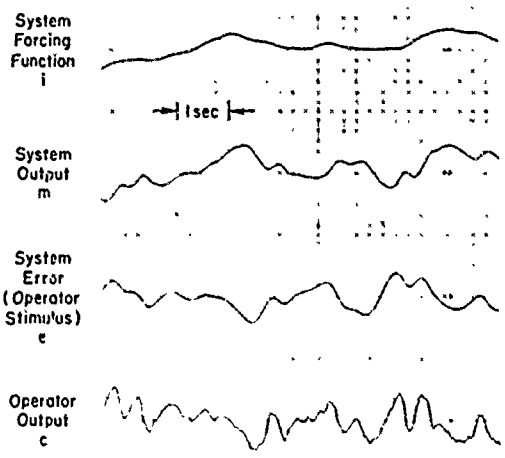

Figure 4. Man/Machine System Response Time Histories; $Y_c = K_c/(s-2)$

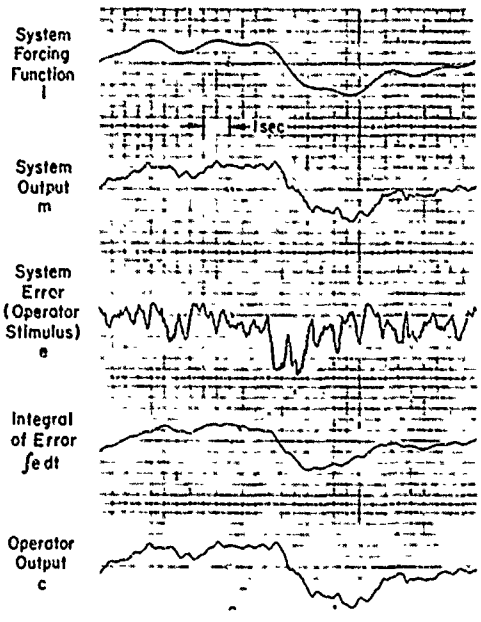

Figure 5. Man/Machine System Response Time Histories, $Y_c = K_c$

Let us turn now to typical data for a proportional controlled element, K_c. These are shown in Fig. 5. (These data are for a different subject than all the rest, a relatively untrained non-pilot.) The system output follows the forcing function in this case very well, but when compared with the $Y_c = K_c/s$ data the high-frequency fluctuation is more apparent. This is because the operator-induced noise is passed directly through the controlled element without any filtering due to the controlled element dynamics. This is also evident from the direct correspondence between the operator's output, c(t), and the system output, m(t).

Because the operator does so well in this kind of system, the error is very small. Consequently, the e(t) trace shown has been amplified to show its nature on a larger scale. If we now examine the relationship between stimulus, e(t), and response, c(t), we find that unlike the rate case, there is little apparent resemblance. So, the human operator is clearly not acting as a proportional controller operating on the error. If, however, the integral of the error is compared with the operator output, we see a great similarity. Again, the output trace has more higher-frequency "wiggles," but the main trend is a near duplicate to the integral of the error, delayed by $\tau_1 = 0.18$ sec. Thus, we can again consider a cause-effect proportional relationship, but this time between the integral of the stimulus and the response. In equation form:

$$c(t + \tau_1) \doteq K_{p_1} \int e(t)\, dt \qquad (5)$$

The equivalent transfer function is:

$$Y_{p_1} \doteq \frac{C(s)}{E(s)} = \frac{K_{p_1} e^{-\tau_1 s}}{s} \qquad (6)$$

This implies that the operator acts as an integration or smoothing filter on the stimulus, which is quite different indeed from the proportional action exhibited in the two previous situations.

For the fourth example, the controlled element dynamics are $Y_c = K_c/s^2$. For this case, as shown in Fig. 6, the system output follows the system forcing

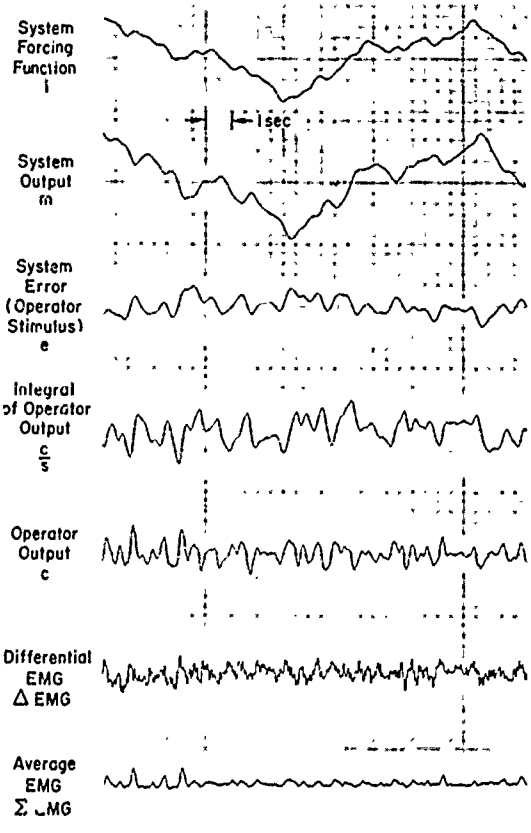

Figure 6. Man/Machine System Response Time Histories; $Y_c = K_c/s^2$

function well enough, in general trend, although with some displacement to the right indicating time delay. But here the point-to-point correspondence is nowhere near as good as for the above examples. Instead, there seems to be an almost periodic function in the system output, m(t), or e(t) and c(t) for that matter, which is not present in the input, as if the closed-loop system possessed an under-damped, relatively high-frequency mode of its own. Except for this, and the $Y_c = K_c/(s-2)$ examples, the output has been a faithful enough representative of the input to suspect that operator-induced noise rather than any closed-loop system dynamics was affecting the match.

Comparison of the error and output reveals little connection between the two except a general oscillatory quality. On the other hand, if the integral of the operator's output is compared with the error, these time traces are similar. A roughly proportional relationship appears to exist when the error is delayed by $\tau_3 = 0.43$ sec and then compared with the integral of the operator's output. So, again, we can demonstrate a roughly proportional relationship between stimulus and some function of the response, i.e.:

$$\int c(t)\,dt \doteq K_{p_3} e(t - \tau_3) \tag{7}$$

As a transfer function, this will be:

$$Y_{p_3} \doteq \frac{C(s)}{E(s)} = K_{p_3} s e^{-\tau_3 s} \tag{8}$$

Thus, the operator behaves as if generating a first-order lead (with a break at a very low frequency) on the stimulus or, alternatively, as if operating as a proportional control on stimulus velocity.

An intermediate example between the rate (K_c/s) and acceleration (K_c/s^2) controlled elements is the second-order system:

$$Y_c = \frac{K_c}{s(Ts + 1)} \tag{8}$$

Time history examples for this controlled element form with $T = 1/3$ sec are given in Fig. 7. The system output follows the forcing function quite well, with the higher input frequencies being somewhat accentuated in the output. The operator output does not correspond at all well with the system error as it would if the controlled element were just a rate control; and, in fact, the integral of the output (not shown) also does not show the type of correspondence expected for the acceleration control. For this intermediate controlled element, the operator output lagged by:

$$(s + 1/T)^{-1} = (s + 3)^{-1}$$

is proportional to the error signal delayed by about 0.16 sec. The operator characteristics as a transfer function would then be:

$$Y_{p_3'} \doteq \frac{C(s)}{E(s)} = K_{p_3'}(s+3)e^{-\tau_3' s} \tag{10}$$

This result implies that the operator develops a lead which is approximately equal to the first-order lag component of the controlled element dynamics.

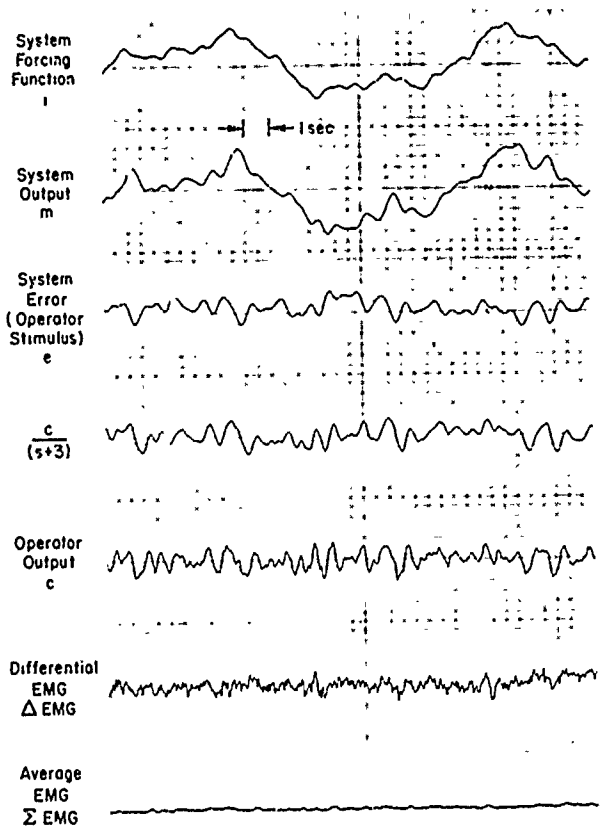

Figure 7. Man/Machine System Response Time Histories; $Y_c = K_c/[s(s/3 + 1)]$

As the sixth and last of the examples, a more complex set of controlled element dynamics will be considered, i.e.:

$$Y_c = \frac{K_c}{(s + \alpha)(s - \lambda)} \tag{11}$$

This is a combination of the first-order lag and first-order divergence elementary controlled element dynamics shown in Table 1. The unstable root, λ, creates an output motion which is always tending to diverge, so the system requires continuous control efforts by the operator. This need for continuous operator attention is not present for $Y_c = K_c$, where the operator's action was motivated primarily by a desire to have output match input. Any lack of operator action in the $Y_c = K_c$ situation will not incur the penalty of a system output divergence. On the other hand, to the extent that the operator

motivation in both systems is error minimization, then his actions will tend to be similar in kind, if not in detail. The actual signals in the control system for this controlled element are depicted in Fig. 8 for $\alpha = 3$ and $\lambda = 1.5$. Again, the output follows the input rather well, with the inevitable delay, but the operator output is not in any recognizable way a proportional function of the stimulus. Yet, if the controller's output signal is passed through a first-order lag with time constant, $T = 1/3$ sec, the result appears to be approximately proportional to the error signal delayed by $\tau_4 = 0.20$ sec. Again, a proportional relationship is reasonable, and the appropriate approximate equations describing the human operator's action are given by the transfer function:

$$Y_{p_4} \doteq \frac{C(s)}{E(s)} = K_{p_4}(s+3)e^{-\tau_4 s} \tag{12}$$

The result is very similar to that obtained in Eq. 10 for the second-order controlled element with the free s^{-1}.

As a final point in this section, we should emphasize that the simplified examples discussed are by no means academic. They are all approximately representative of various flight control circumstances. Some are also applicable to other vehicular control situations, such as automobile driving. Table 2 presents the exemplary controlled element forms considered above with a listing of control situations which these forms idealize.

The several examples described above make plausible the first concept that some linear function of the operator's output can be related approximately to another linear function of the operator's stimulus. The second concept introduced is that these relationships are different from system to system; that in fact they depend explicitly on the controlled element dynamics. The third concept illustrated is that the actual relationship between stimulus and response contains a random component, at least when the operator's output is considered to be predominately linearly connected with the input. These kinds of data form an empirical basis for the description of human operators as quasi-linear systems comprising describing function and remnant components to characterize human behavior. This will be formally pursued in the next chapter. The examples taken in concert can be explored more fully in an attempt to develop some approximate laws of human behavior. This will be done below.

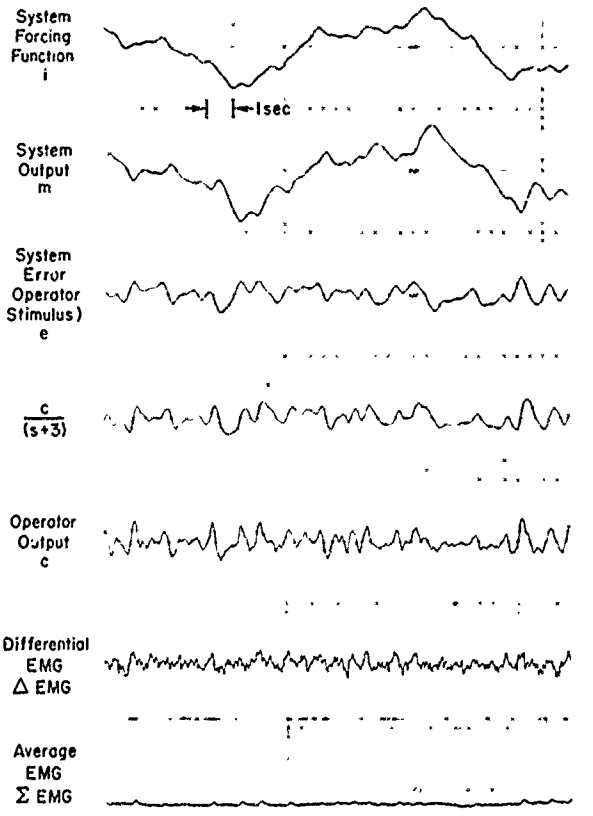

Figure 8. Man/Machine System Response Time Histories; $Y_c = K_c/[(s+3)(s-1.5)]$

B. AN APPROXIMATE CROSSOVER MODEL FOR HUMAN DYNAMIC OPERATIONS IN SINGLE-LOOP COMPENSATORY SYSTEMS

The human operator transfer functions developed for the controlled element set investigated above are compiled in Table 3. As indicated there, the human's transfer function is different for each controlled element, but the open-loop system function, i.e., Y_pY_c, is essentially the same in form for four of the six cases. In fact, in frequency response terms, all the cases fall into the same category for values of frequency greater than λ.

Although the form is common, the components are quite different. As will be seen in subsequent chapters, the "crossover frequency," ω_c, which always contains the operator gain, K_p, as a factor, is different for each of the controlled elements considered. We have not thus far applied the appropriate analytical tools to determine K_p from the data presented, so the ramifications of this point will await more complete development subsequently. For the examples we have described above, the effective time delay has been approximately determined from the time traces by superimposing the two nearly proportional time history quantities and shifting them about until a maximum degree of overlay occurs. This is, of course, an eyeball rather than mathematically based determination. Nonetheless, the effective time delays determined show an interesting ordering across the five controlled elements for which we have data for the same subject. Proportional control action, which is exhibited when the controlled element transfer function itself is an integrator, can be taken, temporarily, as a baseline. When the operator has to generate low-frequency lead, a larger delay is incurred. Even when only moderate amounts

TABLE 2

EXAMPLE APPLICATIONS OF IDEALIZED CONTROLLED ELEMENT FORMS

CONTROLLED ELEMENT FORM	AEROSPACE CONTROL	AUTOMOBILE CONTROL
K_c	Attitude (pitch or roll) control with an attitude command, attitude hold command augmentation system (CAS)	Speed control
$\frac{K_c}{s}$	Attitude (pitch or roll) control with a rate command CAS or with a damper stability augmentation system (SAS)	Heading control at low to moderate speeds
$\frac{K_c}{s(Ts + 1)}$	Roll attitude control of conventional aircraft with roll subsidence time constant, T	
$\frac{K_c}{s^2}$	Attitude (pitch or roll) control of a spacecraft with damper off Limiting case of roll attitude control of conventional aircraft as roll subsidence time constant becomes very large	Longitudinal position control Lateral path control with only positional cues (e.g., local lane markers) and little preview
$\frac{K_c}{s - \lambda}$	Heading control, with rudder, of conventional aircraft spiral mode	
$\frac{K_c}{(s + \alpha)(s - \lambda)}$	Pitch attitude control of unstable short period	Heading control of oversteering car above critical speed

TABLE 3

SUMMARY OF HUMAN OPERATOR APPROXIMATE CHARACTERISTICS

CONTROLLED ELEMENT TRANSFER FUNCTION Y_c	APPROXIMATE HUMAN OPERATOR TRANSFER FUNCTION Y_p	OPEN-LOOP TRANSFER FUNCTION	
		FORM Y_pY_c	EFFECTIVE TIME DELAY τ_e (sec) For the Example Pilot Subject
K_c	$\frac{K_p e^{-\tau_1 s}}{s}$	$\frac{\omega_c e^{-\tau_e s}}{s}$	NA
$\frac{K_c}{s}$	$K_p e^{-\tau_2 s}$	$\frac{\omega_c e^{-\tau_e s}}{s}$	0.14
$\frac{K_c}{s(s + \alpha)}$	$K_p(s + \alpha)e^{-\tau_3' s}$	$\frac{\omega_c e^{-\tau_e s}}{s}$	0.16
$\frac{K_c}{s^2}$	$K_p s e^{-\tau_3 s}$	$\frac{\omega_c e^{-\tau_e s}}{s}$	0.43
$\frac{K_c}{(s - \lambda)}$	$K_p e^{-\tau_2' s}$	$\frac{\omega_c e^{-\tau_e s}}{(s - \lambda)}$ *	0.07
$\frac{K_c}{(s + \alpha)(s - \lambda)}$	$K_p(s + \alpha)e^{-\tau_4 s}$	$\frac{\omega_c e^{-\tau_e s}}{(s - \lambda)}$ *	0.20

*$\lambda << \omega_c$

of operator lead are present, as in the $Y_c = K_c/s(s + a)$ and $Y_c = K_c/(s + \alpha)(s - \lambda)$ cases, the delay is greater than with proportional control. Qualitatively, at least, it thus appears that low-frequency lead equalization of the system which is accomplished by the operator incurs a cost which can be measured in terms of effective time delay introduced. In the other direction, the introduction of a mild divergence in the controlled element resulted in a smaller delay for the operator.

In subsequent chapters, more elaborate mathematical and analysis procedures will be applied to many more complex situations. As a consequence, the operator's dynamic behavior will be quantified in much greater depth and detail than that presented above. Yet, when all is said and done, a common thread through almost all situations which we shall consider, and the only thread which has any pretensions to general applicability, is the form exposed in Table 3 above. This is the "crossover model," which relates the operator and controlled element transfer characteristics by the equation:

$$Y_p(j\omega)Y_c(j\omega) \doteq \frac{\omega_c e^{-j\omega\tau_e}}{j\omega} \tag{13}$$

The reason for the "crossover" appellation is connected with the model's frequency range of validity, which was introduced above in connection with the divergent controlled elements, and which will be elaborated on extensively throughout the report.

C. MATHEMATICS OF THE CROSSOVER MODEL — INTRODUCTION TO MAN/MACHINE SYSTEMS ANALYSIS AND PREDICTION OF HUMAN OPERATIONS IN COMPENSATORY SYSTEMS

One of the results of the first two sections in this chapter is the crossover model as an approximate quantitative description of man/machine system dynamics for single-loop compensatory systems. The model does not distinguish explicitly between controlled element and operator characteristics, although it is plain from what has been presented that the two parameters, ω_c and τ_e, depend on controlled element dynamics. It will later turn out that these quantities are dependent also on other control system task variables and on experimental situation variables which have an impact on the operator. Discussion of these possible dependencies will be deferred while the system dynamics and performance for the crossover model as a control system is derived and discussed. To accomplish this, conventional methods of feedback systems analysis will be used.

The purpose of this exercise is twofold. First, it serves a tutorial function in presenting, by way of an elementary example, some simple methods which are useful in the analytical treatment of manual control systems. Second, all of the generalized data on the dynamics and performance of the crossover model developed can be used to make estimates or interpretations of manual control system properties by specializing the results with particular assignments of τ and ω_c. The answers obtained will be valid for those many circumstances in which the human controller behaves in a fashion similar to that depicted by the crossover model.*

When the loop is closed about the open-loop crossover model, as depicted by the Fig. 9a block diagram, the result is the system dynamics summarized in the system survey of Fig. 9b and c. The survey shows a number of related plots. The most familiar are probably the $G(j\omega)$ Bode plot (or open-loop $j\omega$ Bode) and the conventional root locus. As shown in Fig. 9c, the $j\omega$ Bode diagram gives the open-loop amplitude ratio and phase in dB and degrees, respectively, versus the normalized frequency, $\tau\omega$, on a logarithmic scale. The amplitude ratio plot is a straight line with a slope of −20 dB/decade. The phase lag, while increasing at an ever-increasing rate in these coordinates, is linear with frequency. This diagram represents the open-loop frequency response characteristics, and can be manipulated (e.g., using a Nichols chart, Ref. 8) and interpreted to determine the closed-loop frequency response properties. The conventional root locus shown in Fig. 9b indicates the closed-loop roots of the system. Each closed-loop root corresponds to a different open-loop gain, which is the basic parameter along the loci. Damping ratio is directly indicated for a particular root vector by its angle made with the negative real axis; this angle is $\cos^{-1}\zeta$. On Fig. 9b these ζ values are called out rather than the gains as parameters along the complex locus.

The root locus and $j\omega$ Bode are directly correlated at that value of gain for which the system is neutrally stable. At this point, the phase angle on the Bode plot is −180 deg, and the normalized gain, $\tau\omega_c$, is $\pi/2$. The reference 0 dB line shown in Fig. 9c is constructed for this gain value as it corresponds to neutral stability. The underdamped quadratic locus branches (only the upper one is shown) of the root locus cross the $j\tau\omega$ axis at this value of gain on their way from the left to the right half plane.

The closed-loop system dynamics relating system output and error to the forcing function are given by:

$$G_{mi}(s) = \frac{M(s)}{I(s)} = \frac{G(s)}{1 + G(s)} \longrightarrow 1 \text{ when } |G(s)| \gg 1$$

$$= \frac{\omega_c e^{-\tau s}}{s + \omega_c e^{-\tau s}} \tag{14}$$

*In some cases the operator-induced noise or remnant is large enough to be of major consequence. The answers provided by the crossover model may still be valid, but only to provide the linearly correlated (with forcing functions or disturbances) components of signals within the control loop. The remnant introduces another source of system excitation which must be taken into account.

$$G_{ei}(s) = \frac{E(s)}{I(s)} = \frac{1}{1 + G(s)}$$

$$\rightarrow \frac{1}{G(s)} \text{ when } |G(s)| \gg 1 \qquad (15)$$

$$= \frac{s}{s + \omega_c e^{-\tau s}}$$

Perhaps the most significant property of feedback systems is that which obtains when the open-loop transfer characteristic is much larger than 1, for then the system output is almost exactly equal to the system input and the system error is very small. From examination of the $G(j\omega)$ Bode plot it can be seen that this occurs at low frequencies and is, of course, the reason that the system output and system forcing function were similar in all the examples given thus far. At high frequencies $|G(j\omega)| \ll 1$, so the closed-loop relationship between $M(j\omega)$ and $I(j\omega)$ is substantially the same as the open-loop, i.e., the feedback loop is effectively inoperative. For the crossover model, the frequency which divides these two regimes of near-ideal following of the forcing function and little or no feedback action is the crossover frequency, ω_c. In Fig. 9c this is the intersection of the 0 dB line established for a particular gain with the $G(j\omega)$ Bode plot. The name "crossover frequency" comes from this crossover intersection of the 0 dB line by the open-loop frequency response characteristic. For stable operation of the system the normalized crossover frequency, $\tau\omega_c$, can range from 0 to $\pi/2$.

When $\tau\omega_c$ is relatively small compared to $\pi/2$, then $\tau\omega_c$ is also tantamount to the closed-loop system "bandwidth" (the frequency at which the output amplitude is 3 dB less than the amplitude of an input sinusoid) For higher crossover frequencies this direct equivalence between $\tau\omega_c$ and system bandwidth degrades because of a peaking in the closed-loop frequency response near the crossover frequency, but even for this kind of a system $\tau\omega_c$ is always equal to or less than the bandwidth and thus provides a lower bound.

While the conventional $G(j\omega)$ Bode plot is useful in frequency domain descriptions to illustrate the fundamental properties of feedback as it affects output/input relationships, the root locus best emphasizes the closed-loop system roots. The root locus plot shown in Fig. 9b indicates that the root which starts at the origin for open-loop (zero gain) conditions progresses further into the left half plane as the gain $\tau\omega_c$ is increased. At the point $\tau\sigma = -1$ (for which $\tau\omega_c = 1/e$), this branch of the locus meets with the first of an infinity of branches present because of the $e^{-\tau s}$ term (the other branches are not shown). The quadratic formed by the two branches then increases in undamped natural frequency and decreases in damping as gain is increased until neutral stability occurs at the gain $\tau\omega_c = \pi/2$.

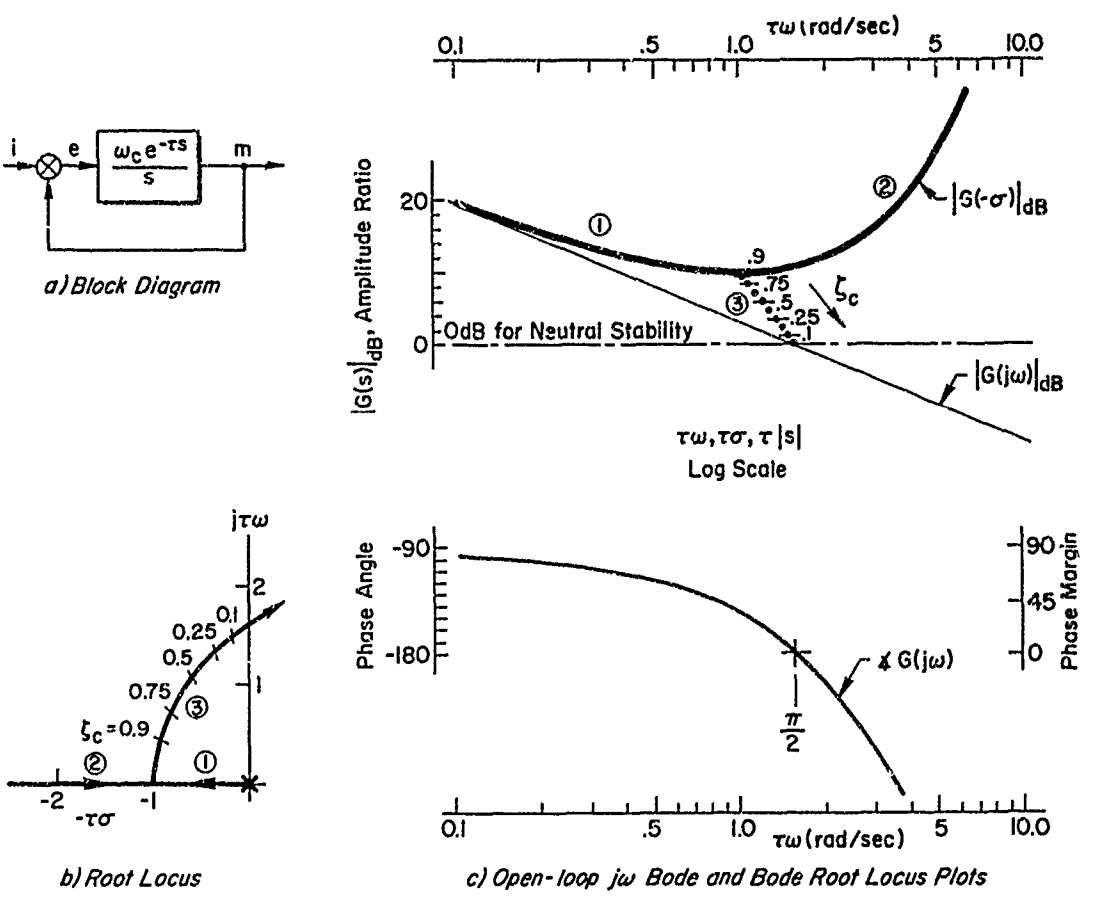

Figure 9. System Survey for Crossover Model

The connections between the dominant closed-loop second-order mode and open-loop parameters are readily developed. The damping ratio can be related directly to the phase margin from the $G(j\omega)$ Bode plots. For a particular open-loop gain, $\tau\omega_c$, the phase margin is given by:

$$\varphi_M = \frac{\pi}{2} - \tau\omega_c \qquad (16)$$

The relationship between closed-loop damping ratio, ζ_c, and phase margin, φ_M, is shown in Fig. 10 (with open-loop gain as an alternate ordinate). This could also be expressed in terms of the gain margin, $|G_M|_{dB}$, which is:

$$\left|\left[1 - (2\varphi_M/\pi)\right]^{-1}\right|_{dB}$$

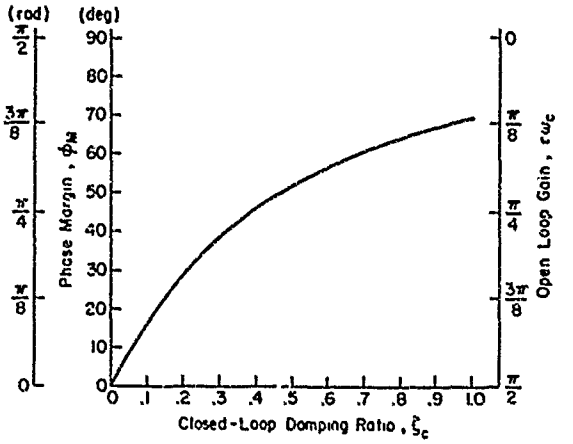

Figure 10. Phase Margin as a Function of Closed-Loop Damping Ratio

It is apparent from the Bode root locus (Fig. 9c) that for the values of normalized gain, $\tau\omega_c$, which result in an underdamped closed-loop system dominant mode, the logarithm of the closed-loop undamped natural frequency of the quadratic modes is linearly related to the logarithm of the crossover frequency (or gain in dB). The actual relationship can be shown to be:

$$\tau\omega_n = (e\tau\omega_c)^{\frac{\ln \pi/2}{1+\ln \pi/2}} = (e\tau\omega_c)^{\frac{\ln \pi/2}{\ln e\pi/2}} = (e\tau\omega_c)^{0.311} \qquad (17)$$

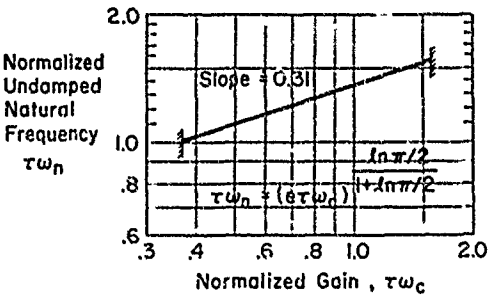

Figure 11. Closed-Loop Undamped Natural Frequency as a Function of Crossover Frequency

Thus, the relationship between closed-loop undamped natural frequency and open-loop gain is a straight line in logarithmic coordinates. This is illustrated in Fig. 11 for the range of $\tau\omega_n$ from 1 (at the rendezvous point on the root locus) to $\pi/2$ at neutral stability.

The same information available on the conventional root locus is also present in the so-called Bode root locus. This comprises two elements: the "siggy plot" of $|G(-\sigma)|_{dB}$ versus $\tau\sigma$; and the complex branch plotted as a dotted line versus $\tau|s|$. The direct correspondence between the two root locus plots is indicated on Figs. 9b and 9c by the labeling of the branches 1, 2, and 3. On the Bode root locus, ζ_c is a parameter and gain is the ordinate; whereas on the conventional root locus gain is a parameter. The Bode root locus places on one common figure both the frequency response and closed-loop pole-zero relationships.

In system dynamic operations, the system output response will contain two components. The first is the forced response, i.e., an output which derives from the system operating upon the forcing function. The second output component is the natural modes of the system as transients excited by the forcing function. For the crossover model these modes are an overdamped second order (i.e., two first orders) for $\tau\omega_c$ less than 1/e, and an oscillatory second order from that gain to the stability limit, $\tau\omega_c = \pi/2$. When the system dynamics are relatively well damped and the forcing function bandwidth is low compared with the crossover frequency, then the system output will very closely resemble the system forcing function alone. When the closed-loop system dynamics are more oscillatory, the presence of the natural modes will also be seen in the system output because this component then does not rapidly damp out and is constantly being excited by the forcing function.

If we now view some of the example cases studied in the first section we will recall two forms of following responses. For several of the systems the system output follows the forcing function quite precisely (except for a very-high-frequency component in the output which is not explained by the crossover model). For some of the other systems, the output followed the forcing function fairly well, but another mode also appeared to be present. We can identify this with the basic closed-loop mode when it is oscillatory in nature. Thus, for those cases which show this quality in the responses, the closed-loop damping ratio was on the low side, corresponding to a high gain and a low phase margin.

When the forcing function is a stationary random or a harmonic process, it can be characterized by a power spectral density, Φ_{ii}. Then the system's steady-state performance in response to such a forcing function will be:

$$\overline{e^2} = \frac{1}{2\pi}\int_0^\infty \Phi_{ee}\, d\omega = \frac{1}{2\pi}\int_0^\infty |G_{ei}|^2 \Phi_{ii}\, d\omega \qquad (18)$$

where G_{ei} is the transfer characteristic between the forcing function and the error (Eq. 15). For a rectangular power spectral density input with bandwidth ω_i and variance σ_i^2 this becomes:

$$\frac{\overline{e^2}}{\sigma_i^2} = \frac{1}{\omega_i}\int_0^{\omega_i} |G_{ei}|^2 \, d\omega$$

$$= \frac{1}{\omega_i}\int_0^{\omega_i} \frac{\omega^2 \, d\omega}{\omega^2 - 2\omega\omega_c \sin \omega\tau + \omega_c^2} \tag{19}$$

This integral is not readily evaluated analytically. However, if $\sin \omega\tau \doteq \omega\tau$, which is an approximation good when $\omega_i\tau \ll 1$, then:

$$\frac{\overline{e^2}}{\sigma_i^2} = \frac{1}{\omega_i}\int_0^{\omega_i} \frac{\omega^2 \, d\omega}{\omega^2(1 - 2\omega_c\tau) + \omega_c^2}$$

$$= \frac{1}{(2\omega_c\tau - 1)}\left[1 - \frac{\omega_c/\omega_i}{\sqrt{2\omega_c\tau - 1}} \tanh^{-1} \frac{\omega_i}{\omega_c}\sqrt{2\omega_c\tau - 1}\right] \tag{20}$$

If the $\tanh^{-1}$ is expanded and carried only to the second term, the extremely simple "1/3 Law" results, i.e.:

$$\frac{\overline{e^2}}{\sigma_i^2} \doteq \frac{1}{3}\left(\frac{\omega_i}{\omega_c}\right)^2 \tag{21}$$

This gives remarkably good results for a large number of practical control systems. When more precise answers are needed the exact results, obtained by integrating Eq. 19, shown in Fig. 12 can be used.

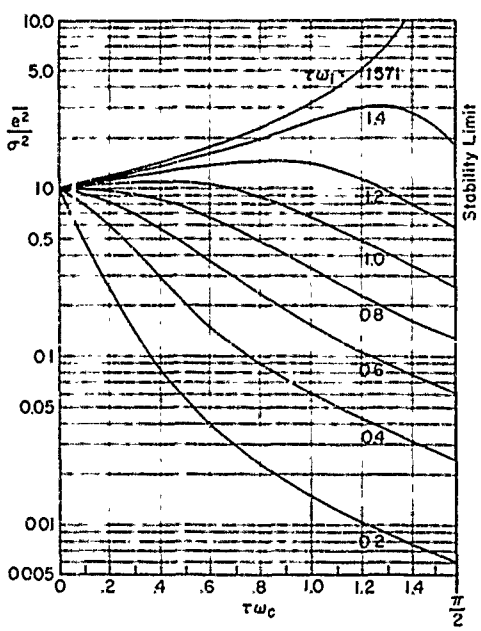

Figure 12. Crosssover Model Steady-State Performance for Inputs with Rectangular Spectral Densities

CHAPTER III

KEY VARIABLES AND MEASUREMENTS

A. KEY VARIABLES WHICH AFFECT THE PILOT'S BEHAVIOR

As our discussion of the origins of human dynamics theory has indicated, engineering needs provided the impetus and engineering techniques the methods for much of the early research. The nature and characteristics of this approach is exemplified qualitatively by the presentation of Chapter II. In fact, the use there of a single subject, with the tacit assumption that single-run segments are representative responses, exposes the obvious need for detailed consideration of intrasubject and intersubject differences. Here, psychological thinking has had a major impact in calling attention to the many variables which might affect the intra- and inter-subject variability of human dynamic performance and, by so doing, influencing the design of experiments. A strong traditional viewpoint in experimental psychology has been oriented to the description of behavior in terms of discrete events rather than to the interacting continuous description demanded by a closed-loop analysis. As a consequence, much effort in psychomotor research in psychological laboratories was devoted to specifying stimulus and response pairs in motor behavior under constrained conditions. Response latencies and simple performance measures were favored measurements, and the description and parameters of learning were common objects of study. It required the introduction of closed-loop analysis, which even in simplified form provides a greatly enriched characterization of human psychomotor properties, to enable the wealth of sophisticated behavior which the human can generate to be revealed, understood, and applied to the rational design of control tasks. Two examples are the analysis of what were previously discrete reaction time measures into components arising from the plant dynamics, the neuromusculature, and the processing time requirements of the human controller; and the description of the exploitation of the human ability to discern temporal patterns of signals in improving the performance of a variety of skilled tasks.

Although human controller variabilities can be magnified or minimized depending on what measurements are taken and where the measurement points lie, there is a need to specify appropriate ranges of reliable application for human dynamic findings. To fill this need we begin by classifying the plethora of physical, psychological, physiological, and experimental effects which can affect the human's relevant outputs. This organization is illustrated in Fig. 13 where the variables — in some cases really parameters — are subsumed under four categories as follows.

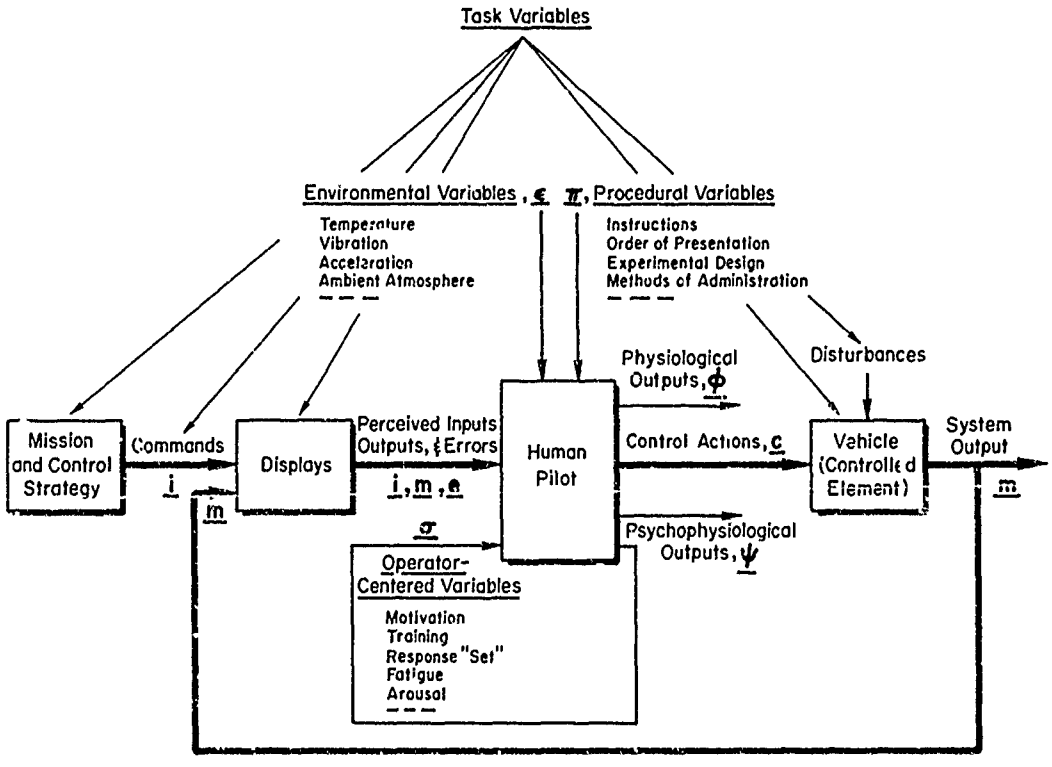

Figure 13. Variables Affecting the Pilot/Vehicle System

1. Task Variables

Task variables comprise all the system inputs and those control system elements external to the pilot which enter directly and explicitly into the pilot's control task. Stability of the closed-loop system is always a necessary, though not sufficient, control strategy. Consequently, the pilot's dynamics are profoundly affected by the display and controlled element dynamics, because his properties must be adapted to provide the necessary loop stability. The general nature of these adaptations has been illustrated in Chapter II. The characteristics of the other task variables,

i.e., disturbance inputs and command inputs related to the mission and control strategy, also exert direct influences on the pilot dynamics, although their effects are more in the nature of adjustment and emphasis than of change in fundamental dynamic form.

These variables constitute an enormous range of possible conditions. As a practical convention interest is often focused on a limited number of input signals having well-defined amplitude distribution, shape, and bandwidth, on a selection of controlled element dynamics which represent or idealize practical vehicles, and on a restricted range of both functional and physical displays. The abstraction of these task variables was accomplished by a combination of engineering insights (the variables were similar to gust disturbance, the dynamics were similar to aircraft dynamics, etc.) with the need to make accurate measurements over a usefully broad range of frequencies (the use of subdued high-frequency signals, the selection of appropriate run lengths, etc.).

2. **Environmental Variables**

The state of the environment external to the pilot is shown in Fig. 13 as the vector $\underline{\epsilon}$. Included as components of this vector are such factors as ambient illumination, vibration, temperature, acceleration (to the extent that this is superimposed on, rather than controlled by, the pilot), noise, ambient atmosphere, etc.

3. **Procedural Variables**

The procedural variables, denoted by the vector $\underline{\pi}$, include such aspects of experimental procedure as instructions and background indoctrination, training schedule, order of presentation of trials, and so forth. For those experiments for which the subjects are experienced engineering test pilots, a carefully planned indoctrination briefing can serve to heighten their motivation as well as to enable them to generate an appropriate mode of response. In many cases, the experimental control device is structurally a highly abstracted version of the actual aircraft being simulated and a careful indoctrination can help avoid a situation in which the pilot's control responses are more appropriate to a pinball machine than to the flying of an aircraft. There is, however, a danger that in motivating a subject he will become so involved in the experiment that despite his intentions to the contrary he will influence the results to conform with what he perceives are the experimenter's hopes. Instructions and indoctrination serve either explicitly or by means of the mission to establish the performance criterion which the subject will use.

The experimental design and the statistical analyses used can serve to obscure actual effects or "reveal" behavioral phenomena which are in truth artifacts of improper technique. Meticulous attention must be paid to counterbalancing time-dependent effects on subjects and to making assumptions explicit. In view of the generally small number of subjects and runs generated by human dynamics experiments, it is necessary to develop techniques for controlling extraneous variables rather than depending on randomization over a large number of subjects and conditions in the experimental design.

4. **Pilot-Centered Variables**

The operator-centered variables, denoted by the vector $\underline{\sigma}$, include the characteristics the pilot brings to the control task: training, motivation, "set" to respond, physical condition, etc. Many of these factors are difficult to quantify in terms meaningful to a given experiment. They can, however, at least be qualitatively graded by pretest, interview, etc., or controlled or modified by procedures (therefore there is some interaction between $\underline{\pi}$ and $\underline{\sigma}$). "Set" to respond, for example, as established by a particular set of experimental experiences can be compensated for by counterbalancing the order in which subjects are tested. The subject's performance criteria are another pilot-centered variable which can be modified by procedures.

B. DESCRIPTION OF HUMAN PILOT BEHAVIOR

The most obvious aspect of human dynamic behavior in a control task is the pilot's control actions within that task. There exist precedents from the analysis of inanimate systems for specifying which control actions should be measured for a description of the controller's behavior. Such measurements do not tell the complete story for a human controller, since associated with the control actions are physiological and psychophysiological outputs, the vectors $\underline{\varphi}$ and $\underline{\psi}$. These include status indicators of the human's internal environmental control systems, such as respiratory rate and volume, heart rate and blood pressure, rate of sweating and body temperature, etc., as well as such highly structured but nonetheless subjective indications of workload and pilot behavior as Cooper-Harper pilot ratings.

Both the measures derived from inanimate control device description and the peculiarly human outputs listed above can be used to provide operational definitions for a variety of verbal concepts commonly associated with human behavior. Skill, for example, is a concept which has been described in such intuitive terms as "sequence of deftly timed responses" and "the outstanding character of rapid adaptation" (Ref. 39). The availability of dynamic descriptions of human control actions enable us to quantify "deftly timed" in a fashion not otherwise possible. Similarly, the human ability to adapt can be reduced to readily quantifiable changes in the mathematical form of the description of the control actions.

To make these general statements more concrete presume, for the moment, that the crossover model developed in Chapter II was a complete description of operations in a single-loop manual control system. Then, the equations of motion for a specific system would be:

$$\begin{aligned} e(t) &= i(t) - m(t) \\ \dot{m}(t) &= \omega_c e(t - \tau) \end{aligned} \tag{22}$$

The first of these equations applies for all compensatory situations; whereas the second requires that the crossover model be valid. The corresponding open-loop transfer function is:

$$\frac{M(s)}{E(s)} = Y_p(s)Y_c(s) = \frac{\omega_c e^{-\tau s}}{s} \tag{23}$$

The human pilot's adaptation to controlled element dynamics is implicit in this relationship, i.e., for a particular set of controlled element dynamics defined by $Y_c(s)$, the human will adopt a transfer function:

$$Y_p(s) = \frac{\omega_c e^{-\tau s}}{sY_c(s)} \tag{24}$$

The general form of the human's response would thus be determined by the specifics of Y_c, and a change in this task variable evokes a change in Y_p such that the crossover model open-loop transfer function is conserved. The effects of changes in other task variables, or in the environmental and operator-centered variables, will be to modify ω_c or τ. These ω_c and τ modifications are themselves the quantification of changes or differences in key variables on the pilot's control action. In measuring the effects of training, for instance, ω_c increases with trials until stable conditions are obtained for that particular subject and set of constant task and environmental variables. For circumstances in which the 1/3 Law applies (Eq. 21), an increase in ω_c with trials will be reflected by a hyperbolic decrease in the system rms error. Thus, in the context of this hypothetical example in which the crossover model is a total representation of human control actions, the human's control action will be quantified in terms of the crossover model gain, ω_c, and/or effective time delay, τ.

The human pilot's actions are unfortunately not as readily described, in general, as this hypothetical example. For one thing, the effects of environmental stresses and operator-centered variables may manifest themselves in the $\underline{\Phi}$ and $\underline{\Psi}$ vectors, as well as in changes in the control actions. Further, the human pilot is a multi-input, multi-output device of enormous complexity rather than a single-channel control mechanism. Nonetheless, it should be plain from both the hypothetical and real-data examples discussed thus far that a great amount of verbally expressed descriptive material and concepts can be quantified and reduced to operationally usable terms by virtue of a control engineering approach.

A complete and detailed descriptor of a human in this context is one which relates control, physiological, and psychophysiological outputs to control and environmentally-derived inputs. For a large number of practical cases, however, the $\underline{\Phi}$ and $\underline{\Psi}$ outputs are of secondary interest and the $\underline{\epsilon}$ inputs are parameters over the measurement period. When attention is focused on control actions as the major interest, and as shall be done henceforth, the pilot's control activity is capable of being described as a short-time stationary process for a very large number of circumstances.

When the key variables are fixed and the signals in the control loop are approximately time stationary over an interval of interest, the pilot/vehicle system can be modeled as a quasi-linear system. Quasi-linearization is one of the most fruitful approaches to the description of those nonlinear time-varying systems in which the relationships between pertinent measures of system input and output signals have some linear correlation in spite of the possible existence of nonlinearities and short-term (relative to the observation interval) time variations. The description is valid for only the specific situation; when conditions (e.g., inputs) are changed a different quasi-linear description is needed.

In a quasi-linear system the response for a given input is divided into two parts — describing function components which correspond to the responses of equivalent linear elements driven by that input, and a "remnant" component, which represents the difference between the response of the actual system and an equivalent system based on the linear element (Ref. 40). Quasi-linear models consisting of describing function plus remnant descriptions for random-appearing inputs and disturbances have been the basis for the vast majority of man/machine systems analyses and have also received the lion's share of experimental effort.

The most important class of situations in closed-loop control of aircraft are compensatory tasks in which the pilot acts on displayed error quantities, $\underline{e}$, between desired command inputs, $\underline{i}$, and comparable vehicle output motions, $\underline{m}$, to produce control actions, $\underline{c}$. This class is illustrated in Fig. 14. In this block diagram the dynamics of the equivalent controlled element and displays are described by a matrix of transfer functions, $\{Y_c(j\omega)\}$. The signals in this general block diagram, $\underline{i}$, $\underline{e}$, $\underline{c}$, and $\underline{m}$, as well as the remnant, n_e (considered as a quantity injected at the pilot's input) are all, in general, vector quantities. Finally, the transfer characteristics of the pilot are represented by the matrix of quasi-linear describing functions, $\{Y_p\}$. The describing functions and remnant depend explicitly on the task variables, as noted in the functional notation. (While an explicit functional dependence is not shown, the remnant and transfer characteristics are also functions of the operator-centered, procedural, and environmental variables.)

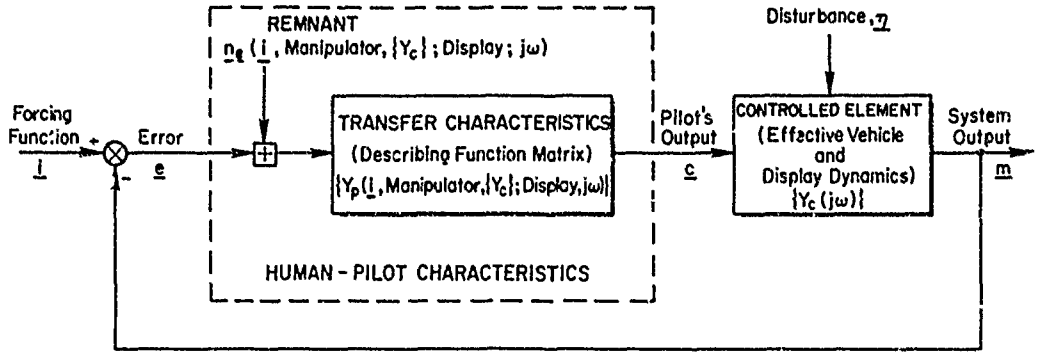

Figure 14. Quasi-Linear Paradigm for the Human Pilot

C. MEASUREMENT FUNDAMENTALS

The detailed nature of typical measurements in manual control systems is most easily introduced by simplifying the general block diagram of Fig. 14 to a single-loop situation. Such a figure appears at the top of Table 4. Here, the pilot's properties are divided into actuation-load dynamics and sensory and equalization dynamics blocks. The manipulator task variable is intrinsically included in the former. The signals throughout the loop are characterized in several ways: as a time function, $x(t)$; as a mean-squared value, $\overline{x^2(t)}$; as an amplitude distribution probability density, p_x, where $p_x\,dx = \text{Prob}(x_1 < x < x_2)$; and as a power-spectral density, $\Phi_{xx}(\omega)$. The time functions, i, e, c, and m, are ordinarily available; whereas special means (e.g., see Fig. 3) are needed to obtain EMG signals proportional to the pilot's force, $F(t)$, which drives the actuation and load dynamics.

For stationary situations the forcing function signal $i(t)$ may, in principle, have two components, random and periodic. As power-spectral densities these correspond to a continuous power-spectral density function, $\Phi_{ii}(\omega)$, and a sum of line spectra. In responding to this excitation, the pilot's output power-spectral density will also have, in general, random and line spectra elements, but not all of the output will be linearly correlated with the forcing function. Accordingly, the remnant spectral density, $\Phi_{nn}(\omega)$, constitutes the difference between the linearly-correlated and total pilot output power-spectral density. In principle, the remnant spectrum may also have random and line-spectra components; although the spectral lines will not appear at the discrete line spectra frequencies, ω_m, present in the forcing function. The spectral formulas in Table 4 represent these statements mathematically.

The pilot's dynamics as a transfer element are given by the open-loop describing function, Y_p, which is also represented along with the controlled element transfer function in the closed-loop describing function, H. These are, in general, obtained using cross-spectral measurements as shown in the table. Noted there is the sometimes used estimate for Y_p of Φ_{ec}/Φ_{ee}. As can be appreciated from the formula, this measurement can give good results at frequencies where the forcing function power and its consequences are much larger than the remnant power and its consequences. On the other hand, when the forcing function effects are not dominant, the answer obtained approaches $-1/Y_c$. Techniques which help circumvent problems caused with low forcing function power levels are given in Refs. 41-43.

The "linear correlation" and signal-to-noise ratio are useful as indicators of the nature of pilot operations and as a means for the determination of remnant. These quantities depend on the effective bandwidth, ω_b, of the measuring apparatus or data processing procedure. Clearly, as this becomes more narrow, the value of ρ increases regardless of the magnitude of the remnant, approaching 1 as ω_b approaches zero.

Finally, relative remnant measures finish off the Table 4 summary.

The principles and practices of measuring pilot characteristics are extremely well developed and have an extensive literature. A representative cross section, which includes both time domain and frequency domain considerations, is given in Refs. 40, 44-54. There are many pitfalls for the unwary in practical application of these methods, with the $-1/Y_c$ example noted above being perhaps the most common. The references cited offer a cross section of others.

A measurement detail of considerable importance is the character of the forcing function or disturbance. When compensatory behavior is to be measured the ideal attributes include:

1. Random appearance so that the operator cannot detect any internal coherence in the forcing function and thereby adopt a higher level of behavior (unless the intent is to induce that higher level).

2. Frequency content which encompasses the bandwidth of the manual control system under test, thus insuring that all significant modes of the system are excited.

3. Evoked outputs easily recognized and distinctly different from constant-coefficient linear, nonlinear, constant-rate sampled, and other idealized system forms which may offer a mathematical basis for human pilot modeling.

4. Precisely known statistics, to the extent possible, thereby eliminating a source of uncertainty in experimental results.

TABLE 4. MEASUREMENT SUMMARY

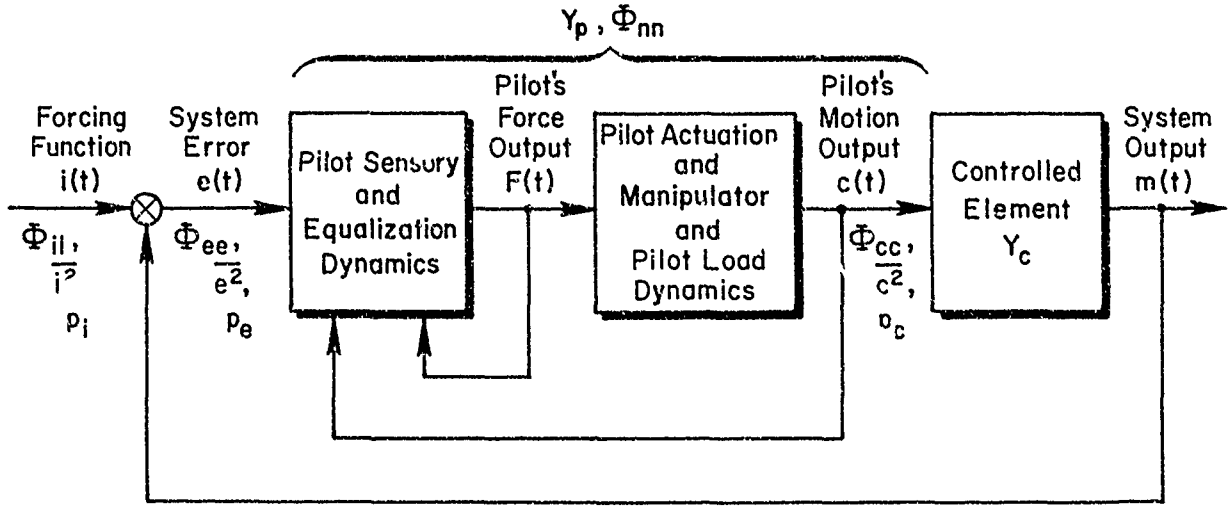

SPECTRA

Forcing Function: $\Phi_{ii}(\omega) = \underbrace{\varphi_{ii}(\omega)}_{\text{Random}} + \underbrace{\pi \sum_{m=1}^{M} \varphi_i^2(\omega_m)\delta(\omega - \omega_m)}_{\text{Line}}$

Pilot Output: $\Phi_{cc}(\omega) = \underbrace{|H|^2 \Phi_{ii}}_{\text{Linearly Correlated}} + \underbrace{\Phi_{nn}(\omega)}_{\text{Remnant}}$

$$\overbrace{\left[\varphi_{cc}(\omega) + \pi \sum_{m=1}^{M} \varphi_c^2(\omega_m)\delta(\omega - \omega_m)\right]}^{\text{Linearly Correlated}} + \overbrace{\Phi_{nn}(\omega)}^{\text{Remnant}}$$

DESCRIBING FUNCTIONS

Closed Loop: $H = \dfrac{\varphi_{ic}(j\omega)}{\Phi_{ii}(\omega)} = \dfrac{Y_p}{1 + Y_p Y_c}$

Pilot: $Y_p = \dfrac{\Phi_{ic}(j\omega)}{\Phi_{ie}(j\omega)}$; Note: $\dfrac{\Phi_{ec}(j\omega)}{\Phi_{ee}(\omega)} = \dfrac{Y_p \Phi_{ii}(\omega) - Y_c^* \Phi_{nn}(\omega)}{\Phi_{ii}(\omega) + |Y_c|^2 \Phi_{nn}(\omega)}$

Controlled Element: $Y_c = \dfrac{\Phi_{im}(j\omega)}{\Phi_{ic}(j\omega)} = \dfrac{\Phi_{mm}(\omega)}{\Phi_{mc}(j\omega)} = \dfrac{\Phi_{cm}(j\omega)}{\Phi_{cc}(\omega)}$

LINEAR CORRELATION AND SIGNAL/NOISE

$$\rho^2(\omega_m) = \frac{1}{1 + \dfrac{\displaystyle\int_{\omega_m - \omega_b/2}^{\omega_m + \omega_b/2} \Phi_{nn}(\omega)\, d\omega}{\pi\varphi_c^2(\omega_m) + \displaystyle\int_{\omega_m - \omega_b/2}^{\omega_m + \omega_b/2} \varphi_{cc}(\omega)\, d\omega}} \doteq \frac{1}{1 + \dfrac{\omega_b \varphi_{nn}(\omega_m)}{\pi\varphi_c^2 + \omega_b \varphi_{cc}(\omega_m)}}$$

$$S/N = \frac{\rho^2(\omega_m)}{1 - \rho^2(\omega_m)} \doteq \frac{\pi\varphi_c^2 + \omega_b \varphi_{cc}(\omega_m)}{\omega_b \varphi_{nn}(\omega_m)}$$

RELATIVE REMNANT

$$\rho_{a_c}^2 = 1 - \frac{\overline{n^2}}{\overline{c^2}} \quad \text{(Output)} \quad ; \quad \rho_{a_e}^2 = 1 - \frac{\overline{e_n^2}}{\overline{e^2}} \quad \text{(Error)}$$

5. Repeatability to permit reproduction of meaningful tests under varying conditions.

6. Representation of physical signals such as turbulence, radar noise, evasive targets, with which the pilot must contend.

7. Pseudo-randomness so that the forcing function will appear ergodic when its time average is taken over a specified interval.

8. A Gaussian amplitude distribution so that Gaussian input describing function theory may be used.

A forcing function comprising a properly selected sum of sinusoids which have frequencies that are integral multiples of the run length is perhaps the best approach to achieving these desirable features. In second place would be a recorded, and hence repeatable, noise source with precisely known statistics. Sometimes, special functions or disturbances cannot be used, and the experimenter must then make do with whatever excitation sources are available, with the concomitant reduction in quality.

The third desirable feature listed above can be especially valuable in providing insights as to the most appropriate mathematical models to use to describe the pilot's actions. Table 5 lists the features of some system types which would be revealed by measurements of the kind summarized in Table 4 when subjected to a periodic input with frequency ω_0 and amplitude σ_i. Careful examination of data for inputs with sums of sinusoids in the context of the differences indicated in this table can go a long way in selecting the best paradigm. Many of these insights are lost if a forcing function with a continuous power-spectral density is used. In this case, the remnant for all but the linear constant-coefficient system will also be a continuous power-spectral density.

TABLE 5

PROPERTIES OF VARIOUS SYSTEMS

TYPE OF SYSTEM	DESCRIBING FUNCTION	REMNANT	ρ^2	ρ^2_{ac} or ρ^2_{ae}
Linear, Constant Coefficient	Y_p	0	1	1
Linear, Sampled Data (Constant Frequency)	Y_p	Line Spectra $k\sigma_i^2\delta(\omega_0 \pm m\omega_s)$	1	< 1
Linear, Random Time Variations	Y_p	Continuous Spectra $k\sigma_i^2\varphi(\omega)$	< 1	< 1
Nonlinear Constant Coefficient	$Y_p(\sigma_i)$	Line Spectra $kf(\sigma_i)\delta(m\omega_0)$	1	< 1
System with Noise Injection		Line or Continuous $\Phi_{nn} \neq f(\sigma_i)$	≤ 1	< 1

TABLE 6. SUMMARY OF SINGLE-LOOP COMPENSATORY SYSTEM DESCRIBING FUNCTION PLUS REMNANT DATA

INVESTIGATOR (Reference)	NUMBER OF RANDOM-APPEARING FORC. FUNC. TYPES INVEST.	NUMBER OF CONTROLLED ELEMENT FORMS INVESTIGATED	MANIPULATOR	CONTROLLED ELEMENT DYNAMICS; REMARKS
Tustin (7)	?	?	Spade grip, spring restraint	Simulated tank gun turret tracking; both $Y_c \doteq K_c/s$.
Russell (20)	?	6	Handwheel, no restraint	$Y_c \doteq K_c$, K_c/s, $K_c(s+z)/(s+p)$.
Goodyear (12, 14)	?	?	Aircraft control stick	Simulated aircraft pitch attitude control in both stationary and pitching simulator.
Krendel, et al. (15, 19)	3	3	Aircraft control stick	Simulated control of aircraft lateral and longitudinal axes in tail-chase, with and without airframe dynamics: two-dimensional input.
Elkind (21)	20		Pencil-like stylus, no restraint	$Y_c = K_c$; single-dimensional input; some remnant data.
Seckel, et al. (17)	1	1	Aircraft control wheel	Attitude control of aircraft lateral and longitudinal axes in both flight and fixed-base simulator; two-dimensional input.
Hall (17, 18, 24)	4	5	Aircraft control wheel	Simulated aircraft pitch attitude control while also controlling a fixed set of lateral characteristics; many Y_c parameter variations; two-dimensional input.
McRuer, et al. (16)	3	5	Lateral side stick	Control of a wide range of idealized dynamics contrived to evoke a complete range of operator transfer characteristics; many Y_c parameter variations; good remnant data.
Stapleford, et al. (17)	1	1	Lateral side stick	Simulated aircraft lateral control in a tail-chase; two-dimensional input.
Magdaleno and McRuer (18, 19)	2		Longitudinal side stick; various restraints	$Y_c = K_c$, K_c/s, K_c/s^2; extreme ranges of manipulator restraints.
Jex and McDonnell (60, 61)	?	?	Rigid side stick	First- and second-order subcritical tasks. Good remnant data.
Smith, et al. (62, 63)		7	Aircraft control stick	Lateral bank angle control; simultaneous longitudinal stabilization; both flight and fixed-base simulator; single-dimensional input.
Newell, et al. (63, 64)		2	Aircraft control stick	Lateral bank angle control; simultaneous longitudinal stabilization; both flight and fixed-base simulator; single-dimensional input.
Levison and Elkind (65)	3	3	Spring restrained side stick	$Y_c = K_c$, K_c/s, and K_c/s^2; single-axis base runs for two-axis experiments; good remnant data.
Shirley (66)		4	Spring restrained stick	Simulated lateral aircraft control; many Y_c parameter variations; complete remnant data.
Allen and Jex (67)		2	Lateral side stick	$Y_c = K_c/s$ and K_c/s^2; compensatory base runs for pursuit/compensatory comparison.
Gordon-Smith (68)	2		Free-moving and pressure center sticks	$Y_c = K_c/s$ dynamics; good high-frequency neuromuscular actuation system data.
Stapleford, et al. (69)	1		Aircraft control stick	Simulated aircraft pitch attitude control; base runs for multiloop/single-loop comparison.
Magdaleno and McRuer (71)	1	3	Lateral side stick; rudder pedals	First-, second-, and third-order subcritical tasks; good neuromuscular actuation system data.

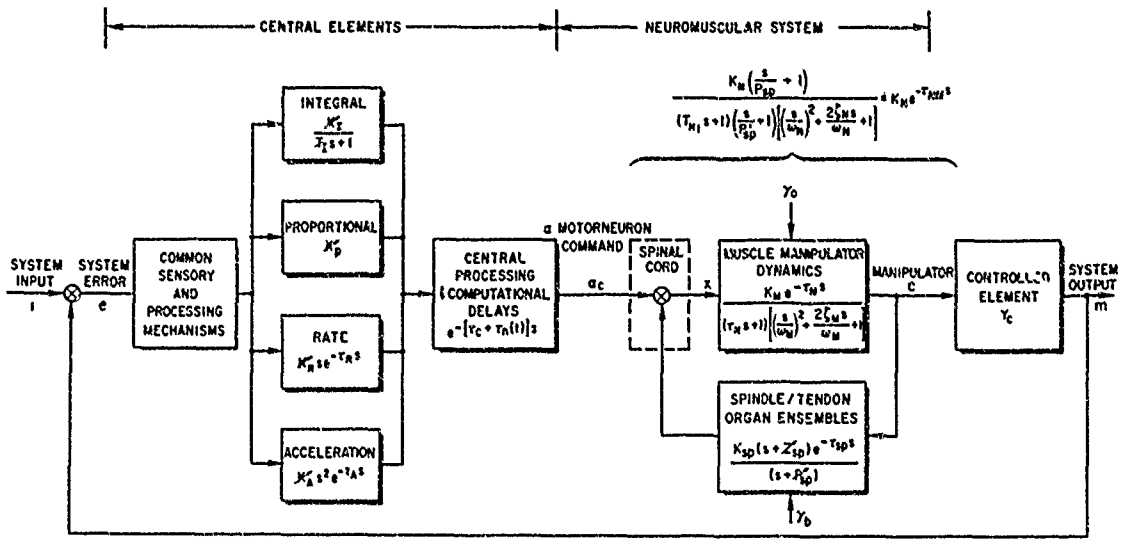

Figure 15. Model for Human Pilot Dynamics in Single-Loop Compensatory System with Random-Appearing Inputs

neuromuscular system shown in Fig. 15 has a feedback element labeled as spindle and tendon ensembles, although spindle characteristics may well be predominant for the small motion and relatively light forces involved in most measurements thus far accomplished. The effective dynamics of the closed-loop neuromuscular system, from the alpha motor neuron command signals to manipulator force, can be approximated over a wide frequency range by the third-order transfer function shown. This form is also compatible with small perturbation dynamics based on analytical models of muscle and manipulator characteristics (Refs. 68, 71, 73-75). The parameter values are strongly dependent upon the steady-state neuromuscular tension, γ_0, due to the gamma motor system. The gamma system also affects the dynamics of the spindle ensembles. This is depicted by the arrows indicating variation in the P'_{sp} and P_{sp} factors in the neuromuscular system feedback block.

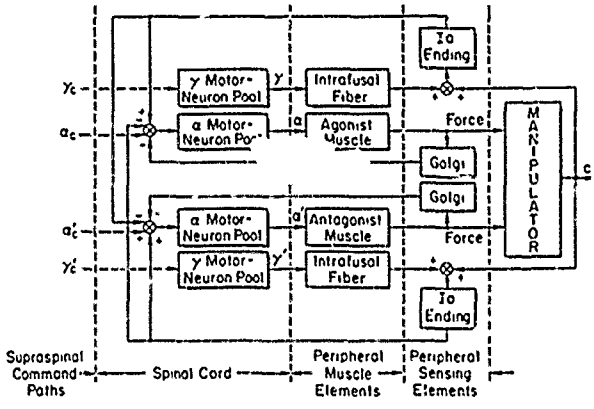

Figure 16. Functional Diagram of Elemental Agonist/Antagonist Neuromuscular System Elements Involved in Tracking

This degree of model complexity is a minimum to have even marginal value in physiological descriptions. It is also often needed for the study of limb/manipulator system dynamics in aircraft control, as in determining the effects of bobweights and primary control system hysteresis on pilot-induced oscillations. For other aspects of pilot/aircraft analysis the neuromuscular dynamics are so high in frequency as to be relatively unimportant in their details. For these cases a pure time delay, τ_{NM}, or a first-order lag can be used as a low-frequency approximation (at frequencies lower than any of the neuromuscular system breakpoints). This delay will be given by:

$$\tau_{NM} \doteq T_{N_1} + \frac{2\zeta_N}{\omega_N} + \frac{1}{P'_{sp}} - \frac{1}{P_{sp}} \qquad (\quad)$$

Turn now to the central and input elements at the left of Fig. 15. As shown there, the pilot can develop a neuromuscular system input command which is the summation of a lag, proportional, lead, or double-lead function of the system error. The integral and proportional channels have a basic time delay, τ_C, associated with them. The higher derivative channels have additional incremental delays. These incremental time delays constitute the dynamic cost of pilot lead generation. They are about 1/5 sec for rate (τ_R) and greater than 1/2 sec for the acceleration channel (τ_A).

It is primarily because of the latency differences for proportional, rate, and acceleration low-frequency lead equalization that these are shown as separate parallel channels. The independence schematized is oversimplified, for common neurological apparatus is undoubtedly present for each function. These are modeled here by the common sensory pathway block following the system error and the central processing and computational block following the four parallel channels. A slight difference, not shown, in integral and proportional channel effective latencies is indicated by existing data but conceivably these channels could be combined into a single-channel adjustable lag-lead element.

Besides the different effective time delays, the other evidence for parallel channels is the difference in response quality as a function of low-frequency equalization supplied by the pilot. When proportional,

integral, or a lag-lead combination is exhibited, the pilot's output amplitude distributions are Gaussian when the input amplitude is Gaussian. On the other hand, when very-low-frequency leads are present, as if operations were through the rate or acceleration channels, the pilot's output distirbutions are distinctly non-Gaussian. Typically, these are bimodal, as illustrated in Fig. 17. Time traces tend to appear more discrete and pulselike as well. This characteristic difference is also reflected in changes in the remnant.

The association of incremental latencies with differences in the neural pathways and apparatus takes us back a century or more to the very earliest work in the reaction time studies of Helmholtz, Wundt, and others (Ref. 76). They examined a large number of situations which exhibited different reaction times and tried to assign these differences to various component functions. In their day, their attributions often turned out to be wrong, and we can only hope that those indicated here do not repeat that history!

The channel gains and the time constant, T_I, are all shown as variable quantities. To a first approximation, they are adjusted such that the crossover model applies. To a higher order of approximation the adjustments obey the Analytical/Verbal model. Both models are discussed further below.

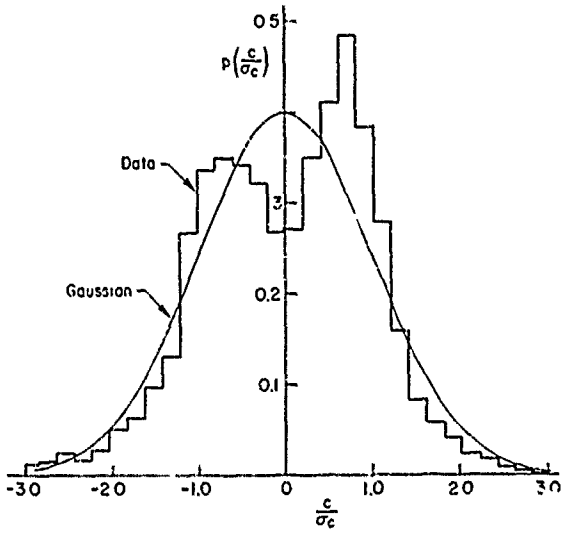

Figure 17. Example of Bimodal Amplitude Distribution for Pilot Output for $Y_c = K_c/s^2$

C. CROSSOVER MODEL FOR SINGLE-LOOP SYSTEMS

Consider the crossover model first. Typical data for velocity, first-order subcritical divergence, and acceleration controlled elements are shown in Fig. 18 with ±1σ bands. These data are more or less typical of any of the rate and acceleration controlled element data listed in Table 6. Further, the $|\omega_c/j\omega|_{dB}$ amplitude ratio trend in the region of crossover is characteristically present in much of the Table 6 data with more complex controlled elements. In fact, for those data sources from the last decade, there exists a remarkable consistency. In most cases, investigators have taken pains to show tie-ins with earlier results from other investigators. For instance, typical comparisons made in Ref. 66 for the controlled elements $Y_c = K_c$, K_c/s, and K_c/s^2, which cover three widely varying modes of control behavior from the pilot, are reproduced in Fig. 19a-c. Other comparison data are shown, for example, in Refs. 56, 60, and 62-69. For a given controlled element such differences as do exist between data sets are ordinarily attributable to differences in forcing function or manipulator task variables. In other cases, the experimental conditions are such as to permit the differences to be ascribed directly to the effects environmental or operator-centered variables.

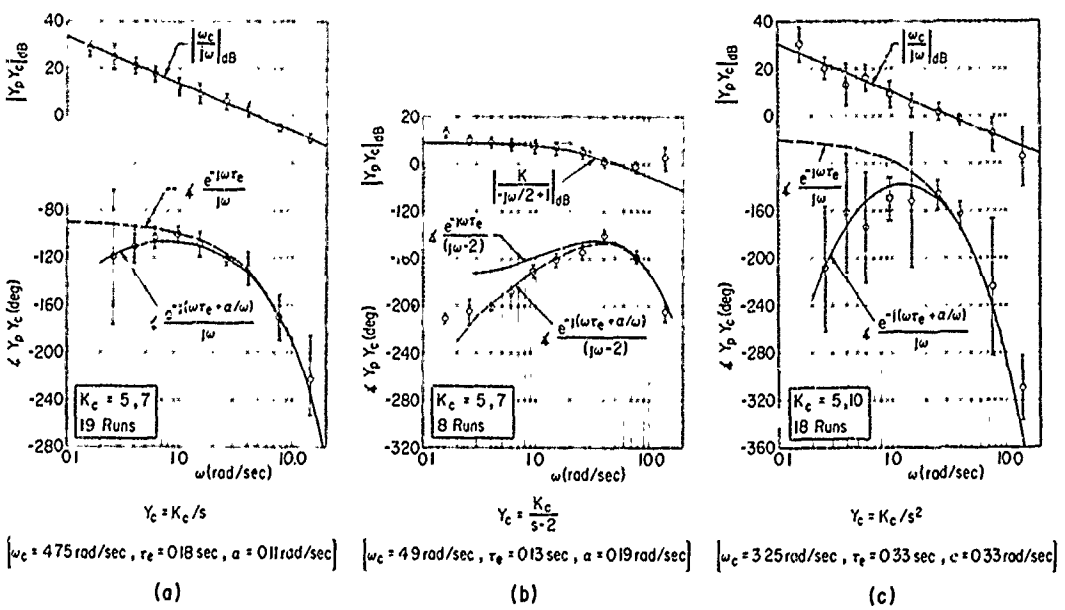

Figure 18. Data, Simple Crossover Models, and α Crossover Models for Elementary Controlled Elements; ω_1 = 2.5 rad/sec (Ref. 56)

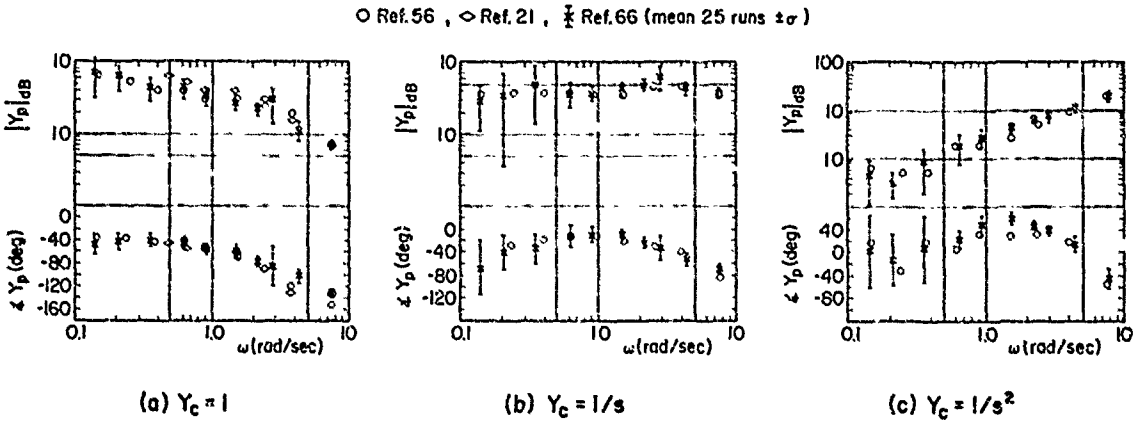

Figure 19. Comparisons of Typical Data from Different Investigators (from Ref. 66)

Visual examination of the data shown in Figs. 18 and 19 indicates that, to a first order at least, the simple crossover model developed in Chapter II from "eyeball" fitting of time traces is also applicable when the more sophisticated spectral analysis procedures are used. The model is apparently a better description of amplitude ratio than of phase characteristics. Also, the amplitude ratio for $Y_c = K_c/(j\omega - 2)$, in Fig. 18b, tends to be somewhat flatter than −20 dB/decade.

For the Table 6 data in general the crossover model is neither appropriate nor accurate at frequencies much less than or much greater than the crossover frequencies. Nonetheless, it usually leads to essentially correct closed-loop dynamic characteristics because the actual shape of the open-loop describing function far from the crossover region usually has little effect on the dominant closed-loop dynamics (see Eqs. 14, 15, and 21).

Although the basic Y_pY_c approximate form is the same for the Figs. 18 and 19 data, and for most of the cases listed in Table 6 as well, the numerical values of crossover frequency and effective time delay are not. These are both functions of the task variables. For low-pass forcing functions, idealized as rectangular power-spectral densities with bandwidth ω_i and rms value σ_i, the crossover frequency and effective time delay can be represented (Ref. 56) as:

$$\begin{aligned} \omega_c &\doteq \omega_{c_o}(Y_c) + \Delta\omega_c(\omega_i) \quad , \quad \Delta\omega_c(0) = 0 \\ \tau_e &\doteq \tau_o(Y_c) - \Delta\tau_e(\omega_i) \quad , \quad \Delta\tau_e(0) = 0 \end{aligned} \tag{26}$$

As the forcing function bandwidth is reduced the phase margin also decreases, becoming approximately zero for $\omega_i = 0$. Although this trend towards zero phase margin can only be demonstrated directly for $\omega_i \neq 0$, it is a common observation that signals circulate throughout the manual control loop without any forcing function as long as the operator is in active control. In the absence of other inputs or disturbances, the presence of these signals implies an on-the-average condition of zero phase margin. So, both the direct and indirect evidence indicates that phase margin is zero when ω_i is zero. Then, the neutrally stable crossover frequency, ω_{c_o}, and the basic time delay, τ_o, are related by:

$$\tau_o\omega_{c_o} \doteq \frac{\pi}{2} \tag{27}$$

To a first approximation, $\partial\omega_c/\partial\omega_i$ is nearly zero (i.e., $\Delta\omega_c \doteq 0$) for controlled element forms encountered in aircraft (although it is not quite true for $Y_c = K_c$). If this approximation is taken to be exact for simplicity, then the principal variations in the crossover model are those of τ_o with controlled element characteristics and $\Delta\tau_e$ with forcing function bandwidth.

In general, τ_o consists of effective transport lags due to both the pilot and the controlled element. The controlled element contribution will be approximately the difference between the controlled element high-frequency (much greater than crossover) lags and leads. With this assumed negligible or otherwise accounted for, the net τ_o depends on the amount of lead generation required of the pilot to establish the approximate −20 dB/decade slope in the region of crossover. When the lead required has been determined, the latency can be estimated from Fig. 20a. The curve shown there represents a grand average from a very large number of experiments, essentially all of those involving crossover region data and spring-restrained manipulators listed in Table 6. Zero lead units is a pure-gain proportional control; plus-one units is first-order lead or rate control; plus-two units second-order lead, etc. The time delays shown include the effective dynamics of the neuromuscular system as an additive component to the central latencies. The total effective low-frequency time delay ranges from about 0.3 sec for the pure integral control case (−1 lead units) through 0.8 sec for the acceleration control. The time delays are plotted as inverse functions because in this form they are normally distributed and the variability of the inverse time delay is a constant.

Figure 20b shows the remaining variation of Eq. 26, that of the incremental latency, $\Delta\tau_e$, with ω_i. This result is based primarily on data taken by several investigators with the so-called STI forcing

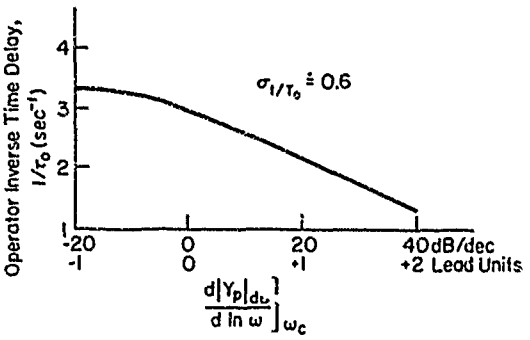

Figure 20a. Variation of Crossover Model Dynamic Stimulus-Response Latency with Degree of Pilot Lead Equalization

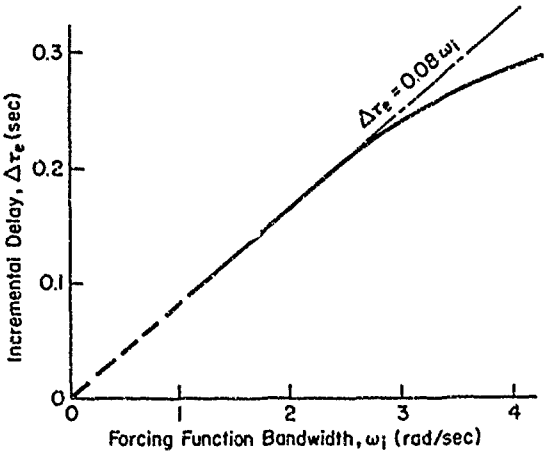

Figure 20b. Variation of Crossover Model Incremental Latency with Forcing Function Bandwidth

function spectrum made up of 10 sinusoids (Ref. 56). With other forcing function types a somewhat more complicated adjustment is made. This will be discussed in connection with the "precision model" presented in the next section. With the approximations made thus far, the $\Delta\tau_e$ variation in Fig. 20b is proportional to the phase margin variation with ω_i since $\gamma_M \doteq \omega_{c_O}\Delta\tau_e$. This reduction in effective time delay as forcing function bandwidth is increased is due primarily to an increase in steady-state neuromuscular tension, γ_o, (shown entering the neuromuscular block in Fig. 15). Thus, the decreased delay is predominantly a change in the neuromuscular dynamics which would be reflected in the low-frequency approximation, τ_{NM}, to those dynamics.

The foregoing has related the parameters of the crossover model to the task variables, primarily ω_i and Y_c. The numerical values were obtained under test conditions — specified in terms of operator-centered, σ, procedural, κ, and environmental, ϵ, variables as discussed in Chapter 3 — so as to insure that Y_p determinations would be useful for system analysis and design. The operators, pilots or well-coordinated simulator pilots, were highly motivated, well-trained males paying full attention to the control tasks. The procedural variables were selected to enhance generalizability. Hostile or disruptive environmental variables were avoided. Consequently, the foregoing data are representative of the best high-dynamic performance, low-variability parameter values which pilot can be expected to generate. For usual, flight-encountered situations the values of ω_c are high, of τ_e low.

Ample evidence exists for the dependence of crossover model parameters on σ variables. An increase in gain and decrease in τ_e occurs with training and has been noted by several investigators — for example, Ref. 86. The pilot's performance criteria affect measurements of Y_p by determining where he can afford to relax control and where he must conform strictly to the system's demands. Thus, for example Ref. 56, large run-to-run variability is exhibited by a pilot in Y_p in the low-frequency range for control of K_c/s or K_c/s^2; however, this variability becomes confined to a very tight band in and about ω_c where good performance demands become contraining. Similarly, the variability expressed by the same pilot is practically negligible when Y_c is an unforgiving divergence. Interestingly, pilots exhibit individualized consistent departures from the crossover model at low frequencies where performance and stability are scarcely affected. Such behavior is in the nature of personal "style," and in effect it represents decisions on where to apply trim control.

When it is desired to measure the effects of σ or ϵ variables upon Y_p, the pilot must be constrained so that his dynamics are tightly related to the selected variables. A highly effective manner for accomplishing this is by employing controlled elements of the form $Y_c = \lambda/s^k(s-\lambda)$, $k = 0, 1, 2$. Since this divergent controlled element tightly constrains the allowable pilot equalization near the region of gain crossover, these critical tasks leave the pilot's effective time delay, τ_e, as the sole determinant of system stability. When the divergence is gradually increased until control is lost, this "critical" divergence time constant is a measure of τ_e (Ref. 61).

These tasks provide a sensitive method for reflecting σ or ϵ variables onto a restricted measure of the pilot's dynamic performance. This technique is being exploited in several laboratories (a representative group can be found by scanning Refs. 2, 26-28) to study a variety of such ϵ variables as heat and noise, and σ variables such as induced by amphetamine, alcohol, and other drugs; task-induced stresses, fatigue, enforced bedrest, etc.; and even certain task variables related to displays. The application of the critical task to measure pilot workload and to aid in understanding pilot opinion ratings will be presented later in this chapter.

The simplified crossover model discussed above is deficient in two major respects. First, for the controlled elements with non-zero poles, the open-loop describing function in the region of crossover tends to be somewhat less than -20 dB/decade. For these cases the data are better fitted with open-loop describing functions which contain the controlled element dynamics explicitly, as illustrated, for example, in Fig. 18b. Second, the phase at low frequencies is not described too well by the simple delay. These phase lags at low frequencies usually do not substantially affect the closed-loop characteristics because magnitude $|Y_pY_c|$ is much greater than unity at the frequencies where the lags are present. However, the

ubiquitous nature of the low-frequency phase lags, and their occasional importance on closed-loop dynamics, demands attention.

This can be accomplished simply by adding a catch-all increment to the low-frequency phase which takes into account dynamics having amplitude ratio breakpoints below, or in the lowest-frequency portion of, the measurement bandwidth. The approximation derives from considering that the low-frequency phase lag is due to an equal number of lags and leads having breakpoints ordinarily below the lower frequencies at which the crossover model applies. Thus, for M leads and lags occurring at $1/T_{lead_i}$ and $1/T_{lag_i}$, the phase will be:

$$\Delta\varphi_{low} = \sum_{i=1}^{M} \tan^{-1} T_{lead_i}\omega - \sum_{i=1}^{M} \tan^{-1} T_{lag_i}\omega \tag{28}$$

When all of the breakpoints occur below the measurement bandwidth or otherwise outside the bandwidth of crossover model validity, the phase angle within the measurement or validity bandwidth will be approximately:

$$\begin{aligned}\Delta\varphi_{low} &\doteq \sum_{i=1}^{M} \left(\frac{\pi}{2} - \frac{1}{\omega T_{lead}}\right)_i - \sum_{i=1}^{M} \left(\frac{\pi}{2} - \frac{1}{\omega T_{lag}}\right)_i \\ &\doteq \frac{1}{\omega} \sum_{i=1}^{M} \left(\frac{1}{T_{lag}} - \frac{1}{T_{lead}}\right)_i \\ &\doteq -\frac{\alpha}{\omega}\end{aligned} \tag{29}$$

where

$$\alpha = \sum_{i=1}^{M} \left(\frac{1}{T_{lead}} - \frac{1}{T_{lag}}\right)_i \tag{30}$$

The effective time constant, $1/\alpha$, describes the effect, within the crossover region, of leads and lags below that frequency band. In this sense it is analogous to τ_e, which lumps high-frequency phenomena into a simple low-frequency approximation suitable within the measurement bandwidth. In the describing function the low-frequency term is represented as $e^{-j\alpha/\omega}$.

The open-loop describing functions of Fig. 18 are curve-fitted using both the simple and the α crossover models, which differ only in whether or not they include the low-frequency phase correction. The range of validity for the α component is obviously less than the lower frequency at which the phase margin will be zero.

The relationship of the crossover model and Fig. 15 for simple controlled elements is summarized in Table 7. For more complex controlled elements the channels are appropriately combined to achieve the

TABLE 7

CONNECTION BETWEEN COMPLETE AND CROSSOVER PILOT MODELS

CONTROLLED ELEMENT CHARACTERISTICS	PRIMARY PILOT CHANNEL ACTIVATED	CROSSOVER REGION PILOT AMPLITUDE RATIO	EFFECTIVE PILOT TIME DELAY
K_c	Integral	$\frac{K_I}{T_I j\omega}$	$\tau_c + \tau_{NM}$
$\frac{K_c}{s}$	Proportional	K_p	$\tau_c + \tau_{NM}$
$\frac{K_c}{s^2}$	Rate	$K_R j\omega$	$\tau_R + \tau_c + \tau_{NM}$
$\frac{K_c}{s^2}$	Acceleration	$K_A(j\omega)^2$	$\tau_A + \tau_c + \tau_{NM}$

crossover model properties. Thus, when a lag-lead equalization is needed, the integral and proportional channels can both be used to give a net equalization given by:

$$\frac{K_I}{T_I s + 1} + K_p = \frac{(K_p + K_I)\left[\frac{K_p}{K_p + K_I} T_I s + 1\right]}{(T_I s + 1)} \tag{31}$$

Similarly, when a lead characteristic is required, the proportional and rate channels can be used together. Remarkably, there is very little evidence that more than two channels are used simultaneously to create complex equalization. This observation may well be an artifact of the particular experiments which have thus far been accomplished, for in almost all of these the crossover model characteristic can be achieved with no more than two channels.

D. PRECISION MODEL FOR SINGLE-LOOP SYSTEMS

In order to cover a broader frequency range than permitted by the crossover model, a so-called precision model is used. The pilot's operation of his acceleration channel is extremely difficult, cannot long be maintained, and is associated with extremely unfavorable subjective ratings and excessive workload. Because of these features, this channel is probably never useful on aircraft-like controlled elements. Consequently, the precision model need not take it into account. With this proviso, the general describing function form which describes the transfer characteristics of the human pilot in single-loop compensatory situations for all of the Table 6 data base is given by:

	GAIN	PURE TIME DELAY	SERIES EQUALIZATION	VERY-LOW-FREQUENCY LAG-LEAD	NEUROMUSCULAR ACTUATION SYSTEM

$$Y_p = K_p \; e^{-j\omega\tau} \left(\frac{T_L j\omega + 1}{T_I j\omega + 1}\right) \underbrace{\left[\frac{T_K j\omega + 1}{T_K' j\omega + 1}\right]}_{e^{-j\alpha/\omega}} \underbrace{\left\{\frac{1}{(T_{N_1} j\omega + 1)\left[\left(\frac{j\omega}{\omega_N}\right)^2 + \frac{2\zeta_N s}{\omega_N} j\omega + 1\right]}\right\}}_{\frac{1}{T_N j\omega + 1} \text{ or } e^{-j\omega T_N}} \tag{32}$$

where:

$$\alpha \doteq \frac{1}{T_K} - \frac{1}{T_K'}$$

and:

$$T_N \doteq T_{N_1} + \frac{2\zeta_N}{\omega_N}$$

The neuromuscular actuation portion presumes the neglect of the very-high-frequency lead-lag of the spindle/tendon organ ensembles implied in Fig. 15. It can, of course, be approximated at low frequencies by the first-order neuromuscular lag or, at even lower frequencies still, by the pure time delay. The very-low-frequency lag-lead is occasionally indicated in very-low-frequency data by at least the low-frequency lead breakpoint, $1/T_K$. It can also be approximated by the single parameter, α. There is evidence that α and T_N are covarying quantities (Ref. 77) with forcing function bandwidth and/or neuromuscular average tension. Therefore, the effect represented by the very-low-frequency lag-lead may be neuromuscular in origin; although no physiological connections have yet been established.

The major mid-frequency action elements of the precision model are the gain, K_p, latency, τ, and the adjustable lead-lag or lag-lead represented by the ratio $(T_L j\omega + 1)/(T_I j\omega + 1)$. These, of course, derive from various approximate summations of the "central elements" channels of Fig. 15.

Commonly used simplifications for the precision model take advantage of the very-low- and high-frequency approximations indicated. For conditionally stable systems the low-frequency phase can be an important feature of the manual control system, and an appropriate simplified version of Eq. 32 is then:

$$Y_p \doteq K_p \left(\frac{T_L j\omega + 1}{T_I j\omega + 1}\right) e^{-j[\omega(\tau + T_N) + \alpha/\omega]} \tag{33}$$

This form is also adequate for most other systems as well. For systems wherein low-frequency performance is essentially unaffected by the low-frequency phase lag term, $e^{-j\alpha/\omega}$, Eq. 33 can be simplified to:

$$Y_p \doteq K_p \left(\frac{T_L j\omega + 1}{T_I j\omega + 1}\right) e^{-j\omega(\tau + T_N)} \tag{34}$$

In either of Eqs. 33 or 34 the $e^{-j\omega T_N}$ is interchangeable with $(T_N j\omega + 1)^{-1}$. Furthermore, if $\omega T \leq 1$, $e^{-j\omega T} \doteq -[(T/2)j\omega - 1] / [(T/2)j\omega + 1]$.

Essentially all the components of the precision model and its simplified versions are adjusted as functions of the controlled element dynamics and forcing function spectra. The latter can have many shapes and sizes, yet we have thus far emphasized spectra which can adequately be defined by a bandwidth, ω_i, and a forcing function rms amplitude, σ_i. These are unambiguous quantities only when the forcing function has a rectangular spectrum, achieved by using many sinusoids as in Ref. 21, or an essentially rectangular spectrum plus a very limited number of extremely low-amplitude sinusoids at higher frequencies, as with the STI forcing function. For other spectral shapes the bandwidth can be defined in several ways. The best metric yet found (Ref. 35) to put different shapes on a comparable effective bandwidth basis is:

$$\omega_{i_e} = \frac{\left[\int_0^\infty \Phi_{ii}(\omega)\, d\omega\right]^2}{\int_0^\infty \left[\Phi_{ii}(\omega)\right]^2 d\omega} \tag{35}$$

This definition for effective forcing function bandwidth works very well as a means to consolidate data for the 20 forcing function spectral shapes considered in Ref. 35. It also reduces to ω_i for rectangular spectra.

To specialize the precision model to a particular controlled element and forcing function combination, the adjustment rules are applied. Those given below are similar to the Ref. 72 set, modified by conclusions based on data of Refs. 68 and 78 and the analysis of Ref. 79.

Equalization selection and adjustment. A particular equalization is selected from the general form $K(T_L j\omega + 1)/(T_I j\omega + 1)$ such that the following properties obtain:

(a) The system can be stabilized by proper selection of gain, preferably over a very broad region.

(b) Over a considerable frequency range in the crossover region (that frequency band centered on the crossover frequency, ω_c) $|Y_p Y_c|_{dB}$ has approximately a −20 dB/decade slope.

(c) $|Y_p Y_c| >> 1$ at low frequencies to provide good low-frequency closed-loop response to system forcing functions (commands).

Examples of form selection and basic adjustment are provided in Table 8.

TABLE 8

TYPICAL PILOT EQUALIZATION CHARACTERISTICS

CONTROLLED ELEMENT APPROXIMATE TRANSFER FUNCTION IN CROSSOVER REGION	PILOT EQUALIZER FORM	EQUALIZER ADJUSTMENTS		
		LOW-FREQUENCY ($\omega << \omega_c$)	MID-FREQUENCY (ω_c Region)	HIGH-FREQUENCY ($\omega > \omega_c$)
K_c	Lag-Lead	$\frac{1}{T_I}$	—	T_L to partially offset $\tau + T_N$
$\frac{K_c}{j\omega}$	High-Frequency Lead	—	—	T_L to partially offset $\tau + T_N$ ($T_I\omega_c < 1$)
$\frac{K_c}{(j\omega)^2}$	Low-Frequency Lead	$\frac{1}{T_L}$	—	T_L not available to offset $\tau + T_N$
$\frac{K_c}{j\omega(Tj\omega + 1)}$	Mid-Frequency Lead ($T > \tau$)	—	$T_L \doteq T$	—
	High-Frequency Lead ($T < \tau$)	—	—	T_L to partially offset $\tau + T_N + T$
$\frac{K_c}{\left(\frac{j\omega}{\omega_n}\right)^2 + \frac{2\zeta}{\omega_n} j\omega + 1}$	Low-Frequency Lead $\omega_n << \frac{1}{\tau}$	$\frac{1}{T_L}$	—	—
	Lag-Lead $\omega_n >> \frac{1}{\tau}$	$\frac{1}{T_I}$	—	T_L to partially offset $\tau + T_N$

Effective time delay. After the appropriate equalization form has been adopted, the net effect in the region of crossover of high-frequency (relative to crossover) leads and lags can be approximated by replacing these terms in Eqs. 32-34 with a pure time delay term, $e^{-j\omega\tau_e}$. The effective time delay, τ_e, is the sum of all the human pilot's pure time delays and high-frequency lags less the high-frequency leads, i.e.,

$$\tau_e \doteq \tau + T_{N_1} + \frac{2\zeta_N}{\omega_N} - T_{L_{hi}} \qquad \text{(for the crossover model)}$$

$$\doteq \tau + T_N - T_{L_{hi}} \qquad \text{(for Eqs. 33 and 34)}$$

The notation $T_{L_{hi}}$ means that only those T_L's used to partially compensate for high-frequency phase lags (e.g., see Table 8) are involved; otherwise, $T_{L_{hi}} = 0$. In general, τ_e depends on both the controlled element dynamics and the forcing function bandwidth. These dependencies are approximately serial, viz.,

$$\tau_e(Y_c, \omega_i) = \tau_o(Y_c) - \Delta\tau_e(\omega_{i_e}) \qquad \text{where } \Delta\tau_e(0) = 0$$

(a) **Estimation of τ_o.** τ_o can be estimated from the effective order of Y_c in the crossover region using Fig. 20a.

(b) **Incremental τ_e due to forcing function.** τ_e is essentially equal to τ_o when the forcing function bandwidth, ω_i, is zero or very small. As ω_i is increased the neuromuscular lag, T_N, and/or the equalizer lead, $T_{L_{hi}}$, are adjusted to reduce the net value of τ_e. A first-order approximation for this effect, good for all controlled elements, is given in Fig. 20b or by:

$$\Delta\tau_e \doteq 0.08\omega_{i_e} \qquad (36)$$

where $\Delta\tau_e$ is in seconds and ω_{i_e} is in radians/second.

Crossover frequency, ω_c.

(a) **Rectangular and quasi-rectangular forcing function spectra** (discrete power-spectral densities which are essentially rectangular and low-pass continuous spectra with a high-frequency cutoff equivalent to a third or higher order lag filter).

(1) **Basic crossover frequency, ω_{c_o}.** The basic crossover frequency for quasi-rectangular forcing function spectra is found by adding the phase angle, $-\omega\tau_o$, due to the base effective time delay, to the phase angles of the controlled element and the previously estimated Y_p equalizer characteristics. Estimates for ω_{c_o} and the associated pilot gain are then made from the conditions for neutral stability.

(2) **Phase margin.** The phase margin for this forcing function category corresponds to the incremental time delay, $\Delta\tau_e$, of Eq. 36:

$$\phi_M \doteq (0.08\omega_{i_e})\omega_{c_o} \qquad (37)$$

(b) **Low-pass with a roll-off of less than third order and augmented (shelf-type) continuous input spectra.**

(1) **Nominal crossover frequency, ω_c.** With equalization and effective time delay, τ_e, selected as above, the nominal crossover frequency, ω_c, and associated pilot gain is estimated from the condition to provide minimum mean-squared error.

(c) **ω_c regression.** When ω_{i_e} nears or becomes greater than $0.8\ \omega_{c_o}$ for the quasi-rectangular forcing function case or when ω_{i_e}/ω_c is greater than 1 for the low-pass and augmented low-pass spectra, then the crossover frequency regresses to values much lower than ω_{c_o} and ω_c, respectively.

(d) **ω_c invariance properties.**

(1) **ω_c — K_c independence.** After initial adjustment, changes in controlled element gain, K_c, are offset by changes in pilot gain, K_p; i.e., system crossover frequency, ω_c, is invariant with K_c.

(2) $\omega_c - \omega_i$ **independence.** System crossover frequency increases only slightly with forcing function bandwidth until crossover frequency regression occurs.

(e) **Threshold properties.** With very low stimulus amplitudes, a threshold characteristic should be included in series with the pilot's describing function. Also, when full-attention, nearly continuous control actions are not required, an indifference threshold is likely to be present. Both of these lower ω_c from what would be estimated using the above adjustment rules.

The ω_c regression phenomenon mentioned in the adjustment rules refers to a reduction of pilot gain and, hence, of crossover frequency when the forcing function bandwidth becomes too large. The physical reason underlying this phenomenon is best described by referring to Fig. 12. Here, it is seen that for a normalized forcing function bandwidth, $\tau\omega_i$ less than about $0.08\omega_c$, an increase in gain results in a decrease in normalized mean-squared error. When this approximate inequality is reversed, the normalized mean-squared error becomes greater than 1 as gain is increased. In fact, ideally, for the assumed rectangular forcing function spectra used to compute Fig. 12, a gain of zero would be indicated to minimize the error for these cases. This result is academic for pilot/vehicle control systems, because some pilot gain is needed to maintain control; but the trend, nonetheless, for high forcing function bandwidths is to reduce gain. The same regression effect can occur for other than rectangular forcing function spectra (Refs. 68, 78, 79). This regression effect has practical consequences whenever the pilot is required to track broadband signals.

The adjustment rules given above are generally adequate for the pilot's lower-frequency dynamics in tasks with spring-restrained manipulators. The higher-frequency properties due primarily to the neuromuscular actuation system are included only to the extent that τ_{NM} is a component of τ_e. The complete model of Fig. 15 provides for a much more elaborate characterization of the neuromuscular system, subject only to the proviso that these dynamics reduce to the τ_{NM} when viewed from the low-frequency end.

Recent data (Refs. 68 and 71) and modeling efforts (e.g., Refs. 71 and 73-75) can be used to estimate more completely the neuromuscular actuation system dynamics for a given set of manipulator characteristics. An example of what can be involved for the muscle-manipulator dynamics (the forward loop element in the neuromuscular system of Fig. 15) is indicated in the simplified schematic diagram of the muscle and manipulator elements shown in Fig. 21. There the effective driving force, $C_f\Delta f_\alpha$, is proportional to the change in average firing rate, Δf_α, of the alpha motor neuron ensembles involved. This is essentially the signal x in Fig. 15. The muscle characteristics are shown as functions of P_o, the steady-state isometric tension of the muscle system operating point. The changes in this average tension are caused primarily by changes in the gamma motor neuron system discharge, γ_o. The tension changes result in a modified τ_{NM} and thus underlie the variation of τ_e with, for example, ω_{ie}. Typical describing function data for the muscle/manipulator dynamics are shown in Fig. 22a and b for rudder pedals and a hand manipulator, respectively (Ref. 71). These data indicate that the muscle/manipulator dynamics for rudder pedals and hand manipulators are similar in form and numerically, in spite of the difference in limb size and function. The data also provide an exemplary indication of the numerical values involved in this neuromuscular system component.

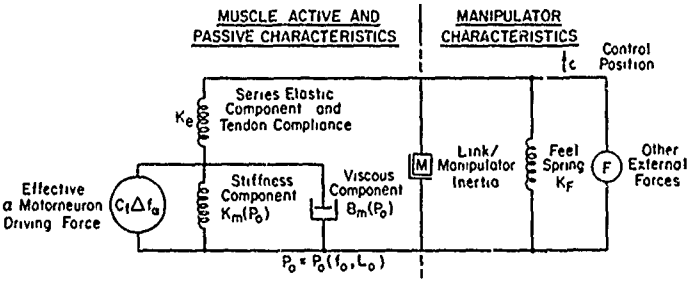

Figure 21. Schematic of Limb/Manipulator

When the neuromuscular system feedback elements (the spindle/tendon organ ensembles of Fig. 15 with specific numerical values Z_{sp} = 11 rad/sec, P_{sp} = 40 rad/sec, and $\tau_{sp} \doteq 40$ msec as given in Ref. 71) are combined with the muscle/manipulator dynamics (Fig. 22a) into a closed-loop system, the resulting neuromuscular system dynamics are shown as the curves in Fig. 23. The data points on the figure are those for the total human operator describing function, Y_p, measured for this controlled element. The closed-loop neuromuscular system curves provide excellent curve fits to these data at the higher frequencies. On Fig. 23 the closed-loop neuromuscular system dynamics are $1/T_{N_1} \doteq 12$ rad/sec, $\omega_N \doteq 19$ rad/sec, and $\zeta_N \doteq 0.13$. These are representative values for stiff spring-restrained, nearly-isometric situations with very low-inertia manipulators.

The neuromuscular system dynamics will change markedly as the manipulator load dynamics are modified. One of the most important of these possible modifications is reduction in stiffness of the spring restraints. This is a common feature of aileron controls, as opposed to elevator and rudder controls. When the spring forces are light the manipulator approaches the free-moving (isotonic) extreme. In these cases, the spindle/tendon organ ensemble feedback elements are joined by joint receptor ensembles. These feed back to higher centers than the spindle organs before they influence the alpha motor neuron commands. They accordingly introduce into the neuromuscular system dynamics additional delays which are not present with the isometric situation. Available data from Refs. 59, 68, and 71 indicate that the effect of this proprioceptive feedback required of the pilot when the manipulator is free-moving is to increase the effective time delay by approximately 0.1 sec. This can be added directly to the previously discussed time delay, τ_o, of Fig. 20a. It amounts to an additional time delay cost incurred by forcing the pilot to close a positional loop about the manipulator.

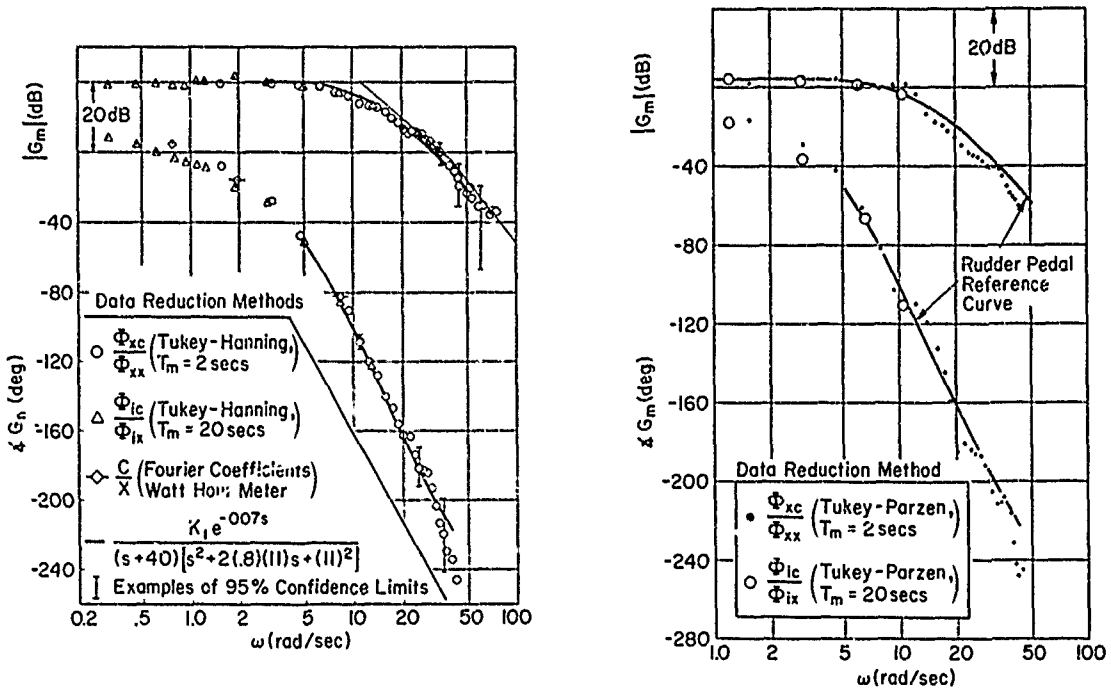

(a) Rudder Pedal (b) Hand Manipulator

Figure 22. Muscle/Manipulator Describing Function, G_m, for $Y_c = 1/(s-1)$

E. REMNANT CHARACTERISTICS

The remnant component of the human pilot's response is generally defined as that portion not accounted for by his describing function. When all of the system elements other than the pilot can be described mathematically in constant coefficient linear and time-stationary terms, remnant must arise from the pilot's action alone. Then, in principle, remnant could result from the following sources:

1. Pilot responses to inputs other than the supposed system forcing function.
2. Nonlinear transfer behavior.
3. Non-steady behavior.
4. Injection of "noise" into the loop.

The first can be ignored for the single-loop situations with a solitary forcing function. For the others, the best data to consider are those taken with a limited number of sinuoids. Then the considerations of Table 5 apply. Existing remnant and describing function data obtained with this type of forcing function indicate that:

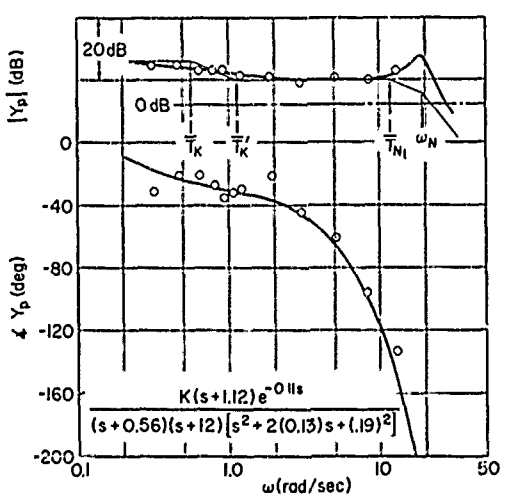

Figure 23. Closed-Loop Neuromuscular System Model and Total Y_p Data; Rudder Pedal, $Y_c = 1/(s-1)$

1. Remnant is a continuous and reasonably smooth spectrum indicating no spectral lines which might be associated with periodic sampling or strongly nonlinear behavior (Ref. 56).
2. For full-attention, continuous-control operations there is very little nonlinear dependence of the describing function on forcing function amplitude over a wide range, i.e., $Y_p \neq Y_p(\sigma_i)$ (Refs. 21 and 56). Threshold phenomena are present with low-velocity stimuli (Ref. 74), and at very low display gains (Refs. 136). An "indifference" threshold (Refs. 14 and 19) has also been observed. These can be significant in special circumstances.
3. The remnant data for a wide variety of controlled elements and forcing function amplitudes coalesce best when all the remnant is reflected to the pilot's input (Ref. 56).

4. When open-loop input-referred remnant is normalized by the variance of the system error, the remnant data tend to coalesce further (Refs. 80-82). A sometimes-refined normalization is with respect to the variance of the principal pilot channel being exercised, e.g., $\sigma_{\dot{e}}^2$, when the rate channel is used to control $Y_c = K/s^2$, has also been observed (Refs. 80-81).

5. The major sources of remnant appear to be located in the human operator prior to the neuromuscular system (Refs. 71 and 83). This is indicated in Fig. 22a by the interleaving of open- and closed-loop cross-spectral measurements based on x and the forcing function as references. These measurements are analogous to the two expressions for Y_p presented in Table 4.

6. Some evidence for pulsing behavior when very-low-frequency lead generation is required is present from output amplitude distributions and time traces (Ref. 56).

When these findings are compared with the entries in Table 5, the conclusion is obvious that some variety of random time-varying behavior is present in the central elements of the pilot. That this is the most likely source of remnant is indirectly corroborated by other studies (e.g., Refs. 84-87). The time variation could comprise fluctuations in gains and/or in the time delays. Figure 15 indicates the latter, as shown by the $\tau_N(t)$. This tentative assignment of the fluctuations to the effective delay is consistent with trial-to-trial variations exhibited in reaction time measurements but is otherwise somewhat arbitrary. By considering it a random change in the delay, the remnant cause can be interpreted as a random change in phase, akin to a random frequency modulation, or to variations of sampling rate in a sampled data interpretation of the pilot (Ref. 88).

When interest is centered primarily on power-spectral densities or their time domain covariance equivalents and the quantities derivable therefrom, the effect of any remnant source associated with the transfer characteristic can be modeled as an injected noise, just as shown in Fig. 14. Remnant power spectra are, therefore, most conveniently inserted at this point and are often referred to accordingly as "observation noise." While this use of the remnant as an inserted noise source is adequate for calculations of mean-squared error if finer-grained detail is needed, such as the probability distributions of signal amplitudes throughout the pilot/vehicle system, more attention has to be paid to the actual remnant-generating process as a random time-varying delay or gain.

For single-loop systems an approximation to the remnant form, Φ_{nn_e}, when reflected to the pilot's input, is given as (Ref. 89):

$$\frac{\Phi_{nn_e}}{\sigma_e^2} \doteq \frac{(0.1 \text{ to } 0.5)}{(\omega^2 + 3^2)} \qquad \text{when integral and proportional channels are used}$$

$$\frac{\Phi_{nn_e}}{\sigma_e^2} \doteq \frac{(0.1 \text{ to } 0.5)}{(\omega^2 + 1)} \qquad \text{when the rate channel is used} \qquad (38)$$

As demonstrated in Fig. 24 these analytical forms bound most of the available data. Note that the remnant is smaller, although somewhat more broadband, when low-frequency lead is not required of the pilot. Thus, another penalty for low-frequency lead generation is seen to be an increased remnant. The high-frequency asymptotes for both no-lead and high-lead situations are common. Consequently, the remnant increase when lead equalization is necessary is subsumed here primarily by the reduction in break frequency.

As already explained, because the kind of remnant described scales with pilot-stimulus variance, it clearly derives from some signal conditioning operations within the pilot such as the time-varying time delay. Accordingly, this component of remnant is a "processing noise." In Chapter V another remnant component due to scanning will be introduced, which adds to the processing noise in multiloop situations.

If remnant were totally of a processing noise variety, it would disappear when no forcing function or disturbance is present. There is a great deal of evidence, however (e.g., Ref. 61), that some remnant remains. This is wideband and independent of the stimulus signal variance. This "residual remnant" is the "motor" which keeps the signals throughout the loop fluctuating in the absence of any external driving source.

Another occasionally observed remnant component is dither, that is, a sinusoidal-like oscillation inserted by the pilot (Refs. 14 and 90). This consciously-applied input is often present as an attempt on the part of the pilot to effectively linearize control system nonlinearities.

Although the primary source of remnant is the effective stochastic variation of pilot characteristics throughout the measurement run, threshold nonlinearities are occasionally important as well. One type (Ref. 136) can be significant as a stimulus resolution feature when display gains are very low. Another, more severe, variety is a task-dependent "indifference threshold." For many flight control situations the pilot's control task is intermittent adjustments of controls when the aircraft-alone has departed too far from some preconceived, mission-oriented level. The main effect here is a substantial reduction in gain if the operation is viewed as a continuous process. Oftentimes it may be more pertinent to treat these adjustments as discrete, using one of the models presented in Chapter VI.

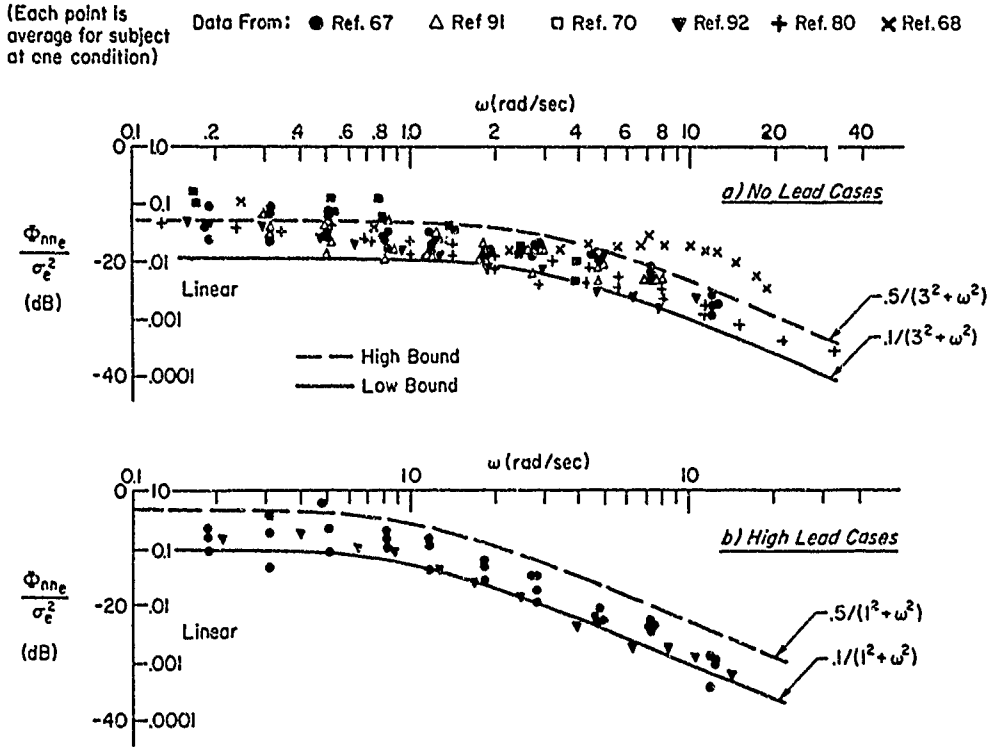

Figure 24. Normalized Remnant Spectra for Various Experiments and First-Order Model Bounds

F. CONNECTIONS BETWEEN PILOT RATING, WORKLOAD, AND PILOT DYNAMICS FOR SINGLE-LOOP SYSTEMS

The previous sections have provided a comprehensive review of the dynamic properties of single-loop pilot models. These are sufficient, in themselves, for a mathematical analysis of pilot/aircraft systems. But pilots are vocal as well as dynamic elements — they toil, and spin, and talk! And for many systems the talk is what counts, rather than the dynamic details of the toiling and spinning. Accordingly, we will present an introduction to pilot rating and workload connections with pilot dynamics. The discussion will be short to keep matters as concise as possible; artistic because ratings are fundamentally ordinal scales subjectively applied and hence difficult to quantify; and incomplete because that portion of the data base which contains pilot dynamics and pilot ratings and/or comments is very small indeed.

To develop closed-loop analysis procedures which permit the assessment of flying qualities, system accuracy, etc., as quantities to be traded off with pilot dynamics and workload requires some generalized criteria. That is, the assessment procedures should, as a minimum, cover:

- Measures of mission/task performance
- Pilot workload
- Effects of aircraft dynamics
- Effects of control augmentation systems

These are the kinds of factors which are taken into account by a skilled test pilot in providing a pilot commentary and an associated rating using, for example, the Cooper-Harper Scale (Ref. 93), part of which is shown in Fig. 25. It is apparent from Fig. 25 that pilot compensation (equalization) and effort (workload) are key factors in the rating scale. The scale is especially useful as an index for comparing competing vehicles on a workload, pilot compensation, basis.

Closed-loop tasks are ordinarily critical from the standpoint of pilot compensation or skill required, and are often critically involved in high workload phases of flight. Consequently, we can expect some connections between subjective ratings and the pilot and pilot/vehicle system dynamics and performance. These connections are intrinsically empirical, and correlations are made somewhat awkward because the rating scale is ordinal. The latter point can be circumvented because the Cooper-Harper scale can be related to an interval scale (Ref. 95), thereby permitting the use of parametric statistics when using and discussing ratings. There are many other features of pilot ratings that are important to the analyst; these are well covered from the pilot's viewpoint in Ref. 93, and from a theoretical standpoint in Ref. 95.

When the tasks being rated can be treated as frozen conditions or are otherwise more or less time stationary (if only for a short interval), a general form of rating functional which explicitly contains some, and implicitly contains all, of the desired features is given by:

Mission/Task Performance: Dominant Aircraft Motion Quantities and Task Measures

Pilot Workload: Pilot Activity (Scale of Pilot Effort); Pilot Equalization (Dynamic Quality of Pilot Effort)

$$R = R\left[\ \lambda_i \overline{q_i^2}\ ;\ \overline{\delta_j^2}\ ;\ \left.\frac{d|Y_p|_{dB}}{d(\ln\omega)}\right|_{\omega_{1_k}}\ ;\ \ldots\ \right]_{i,j,k} \qquad (39)$$

AIRCRAFT CHARACTERISTICS	DEMANDS ON THE PILOT IN SELECTED TASK OR REQUIRED OPERATION*	PILOT RATING
Excellent Highly desirable	Pilot compensation not a factor for desired performance	1
Good Negligible deficiencies	Pilot compensation not a factor for desired performance	2
Fair — Some mildly unpleasant deficiencies	Minimal pilot compensation required for desired performance	3
Minor but annoying deficiencies	Desired performance requires moderate pilot compensation	4
Moderately objectionable deficiencies	Adequate performance requires considerable pilot compensation	5
Very objectionable but tolerable deficiencies	Adequate performance requires extensive pilot compensation	6
Major deficiencies	Adequate performance not attainable with maximum tolerable pilot compensation. Controllability not in question	7
Major deficiencies	Considerable pilot compensation is required for control	8
Major deficiencies	Intense pilot compensation is required to retain control	9
Major deficiencies	Control will be lost during some portion of required operation	10

* Definition of required operation involves designation of flight phase and or subphases with accompanying conditions

Figure 25. Cooper-Harper Handling Qualities Rating Scale

The subscript notation used here implies that $i \in I$ motion and task measures are controlled by $k \in K$ pilot loops actuating $j \in J$ control points. As displayed in Eq. 39 the functional form is general enough to include the existing (e.g., Refs. 94-100) approaches to quantitative flying qualities rating criteria functions. The key closed-loop system quantities in the rating functional are measures of mission and task performance. These are conveniently described by a set of dominant weighted (via λ_i) aircraft motion deviations and total task accuracy or error indications.

The pilot activity component of pilot effort, $\overline{\delta_j^2}$, is particularly dependent on the level of pilot gain. For a given gain, $\overline{\delta_j^2}$ increases directly with gust disturbance spectrum amplitude and remnant amplitude. Accordingly, both $\overline{\delta_j^2}$ and the $\overline{q_i^2}$ quantities will reflect turbulence and remnant levels.

The pilot equalization component of pilot workload is represented in Eq. 39 by the slope (in dB per octave or decade) of the pilot's amplitude ratio evaluated at a particular frequency (generally near crossover). This is by no means the only measure available to describe the dynamic quality of the pilot's effort. References 96-100, for example, use pilot lead time constants as measures; for particular situations with a sufficient data base, this may be a desirable alternative. Then, the rating functional can take a form such as illustrated in Fig. 26.

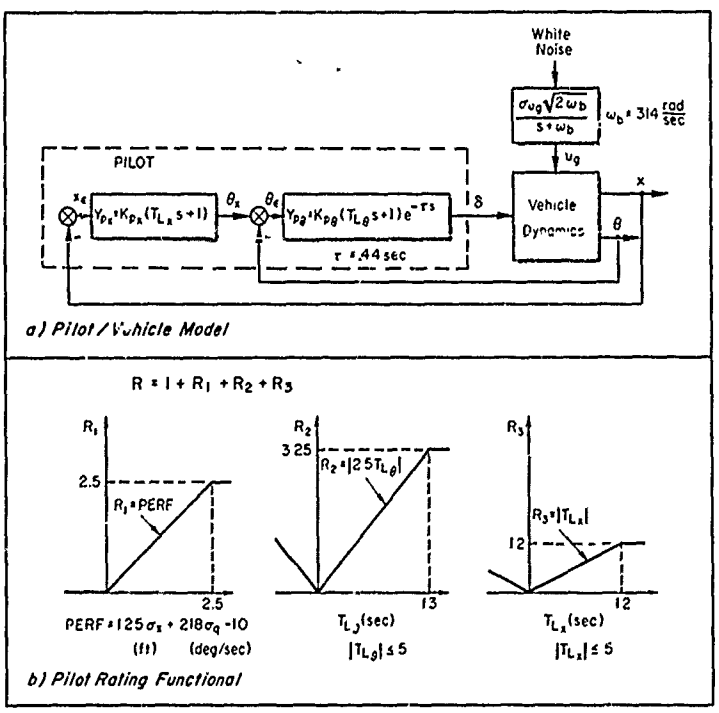

Figure 26. Typical Pilot/Vehicle Model and Form of Pilot Rating Functional (Specific Values for Hover Task, Refs. 96-97) (Refs. 5-6)

Unfortunately, there do not now exist for all closed-loop tasks sets of pilot rating, system performance, and pilot equalization data. Consequently, for many situations we must rely on available correlations which do not include quantities like the q_1^2.

The pilot adapts to the vehicle and forcing function characteristics. He therefore reflects in his adapted describing function form many, if not all, of the vehicle dynamic characteristics and closed-loop pilot/vehicle system properties. Consequently, as a first approximation, a functional relationship can be set up between pilot ratings and the objective system factors in terms of the pilot dynamic characteristics alone. In this connection, it has been found that the dominant rating-sensitive pilot parameters are the low-frequency lead equalization and the crossover gain. Typical relations of this nature are shown in Fig. 27. These can be used directly to estimate pilot rating once the pilot dynamics estimates are made.

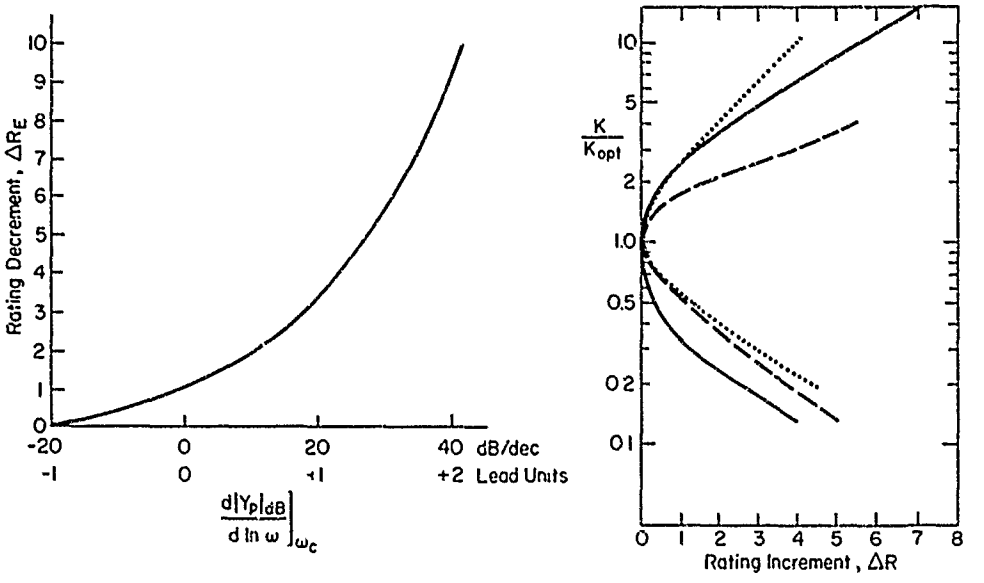

Figure 27. Pilot Rating Decrements as Functions of Lead Equalization and Gain

The descriptive phrases listed under "Demands on the Pilot in Selected Task or Required Operation" in the Cooper-Harper Scale (Fig. 5) directly parallel the correlations with pilot lead equalization. There is also a strong connotation of increasing pilot effort and workload in the scale phrases. But, workload is difficult to define and, consequently, to quantify. In the spirit of offering a general definition which can be measured and predicted, it has been suggested (Ref. 101) that workload margin be defined as the ability (or capacity) to accomplish additional (expected or unexpected) tasks. For example, the pilot opinion rating scale satisfies this definition up to its "uncontrollable" limit point. Furthermore, a number of auxiliary tasks also satisfy this definition of workload in that the decrements in auxiliary task scores give an index of demand on the primary task. One particular measure offers, at the moment, unusual promise in integrating many of the measures into one basic context. This is excess control capacity, a major connector with pilot rating and main task effective time delay(s).

The notion that among the causal factors of pilot rating is the pilot's attention or effort needed to maintain performance is supported by an experiment which measured a parameter uniquely related to excess control capacity (Ref. 9). A secondary subcritical tracking task was used to "load" the pilot so that his performance on the primary task began to deteriorate. A block diagram of these tasks is shown in Fig. 28. The difficulty of the secondary task was made proportional to primary task performance. Thus, when the pilot was keeping primary task error performance less than a criterion value, the secondary task difficulty was automatically increased by increasing the rate of divergence of the secondary instability. Conversely, when the pilot was so busy with the secondary task that primary error was larger than the criterion value, the secondary task difficulty automatically decreased. The final stationary level of secondary difficulty was determined by the sensitivity of the primary task performance to loading. The final "score" is λ_s, the stationary value of the secondary unstable pole (λ) in rad/sec. The scores obtained from this cross-coupled secondary task represent its degree of difficulty; consequently, they also represent the "degree of ease" of the primary task or the excess control capacity available with respect to the primary task.

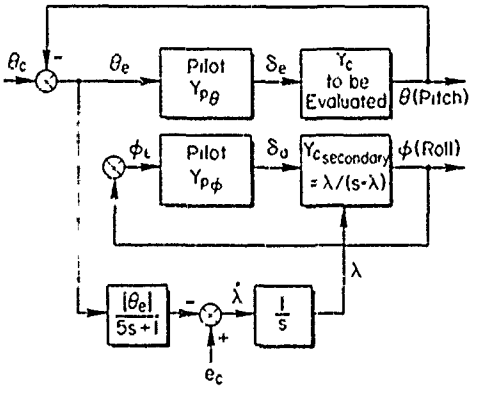

Figure 28. Single-Loop Primary Task with Secondary Cross-Coupled Loading Task

The achievement of the critical limiting score for which $\lambda_c = 1/\tau_e$ in the cross-coupled secondary task indicates a condition of maximum available excess control capacity. We speak of the secondary task as a

"critical" task in this limiting case where τ_e is the sole determinant of system stability. Thus, any activity by the pilot which demands an increase on τ_e on the whole task can be expected to prevent him from achieving his critical limiting score on the cross-coupled secondary task.

Secondary scores obtained for a variety of primary controlled elements are presented in Ref. 95. Figure 29 shows how the scores for the best gain configurations of each controlled element compare with the Cooper ratings. The agreement is extremely good. Even the subcritical task itself in the role of the primary task, which has been a notable culprit in other correlations, seems to be correlated linearly with the other data. In Fig. 29 a score $\lambda_s = 0$ corresponds to 100 percent of the pilot's attention being devoted to the primary task or no excess control capacity, whereas a limiting score ($\lambda_s \doteq 5.5$) means that no attention is required to maintain primary task performance or that 100 percent excess control capacity is available.

These limited experimental data offer a compelling direct connection of pilot rating to measures of workload, thereby quantifying ordinal scale pilot ratings in these workload terms for continuous control tasks. The particular experiment on which these nice correlations are based is, unfortunately, difficult to perform and generalize. A simpler form wherein the side task is not cross-coupled but instead is used to set a series of subsidiary workload levels, each calibrated by a value of λ_s, is much easier to apply.

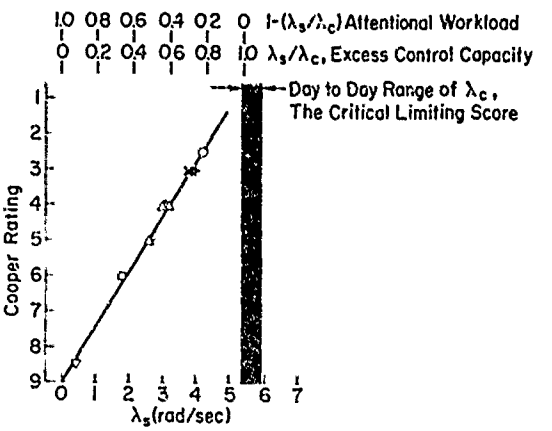

Figure 29. Subjective Pilot Rating Versus First-Order Cross-Coupled Instability Score

CHAPTER V

QUASI-LINEAR MODELS FOR COMPENSATORY MULTILOOP SYSTEMS

The multiloop system pilot models discussed in this chapter are fundamentally extensions of the quasi-linear models for compensatory single-loop systems treated in Chapter IV. To ease the transition from the single-loop case we will first describe some of the needs for multiloop control in aircraft. This will be followed by a review of the data base for visual inputs. A continuous-attention multiloop model for non-scanning visual situations is then presented, with emphasis on the adjustment of the multiloop structure. This basic multiloop model has several variants, depending on the nature of its perceptual stages in a particular instance or, in plain words, depending on how much scanning is involved. The first modification to the multiloop model takes scanning into account in a first-order fashion via modifications to loop gains and remnant.

The second modification to the basic multiloop model differs from the first in that the feedbacks derive from proprioceptive-vestibular signals associated with vehicle motion. This is essentially a particular "multimodality" model where pilot motion inputs join vision in providing control cues on which the pilot can operate.

Unlike the single-loop models which are based on three decades of evolutionary improvement, some features and adjustment rules for the multiloop models are quite new and not yet firmly based on extensive data. Consequently, we can expect much that is written here to change in the next few years. Perhaps nowhere is this more likely to occur than with the very tentative connections of multiloop pilot dynamics with pilot rating described in the section of the chapter. Nonetheless, the quasi-linear pilot models for multiloop systems described here "fly" tracking stages (via multiloop describing functions which close loops about the airplane), introduce pilot-induced noise (remnant) in the process, look about to gather information and, incidentally, add more noise (scanning traffic and scanning remnant), have some workload margin (excess control capacity), and "speak" rationally (pilot rating).

A. NEED FOR MULTILOOP CONTROL

At the outset it is desirable to define what we mean by multiloop. This can, perhaps, best be accomplished with the aid of Fig. 30 (Ref. 57). The first block diagram, Fig. 30a, depicts the single-loop

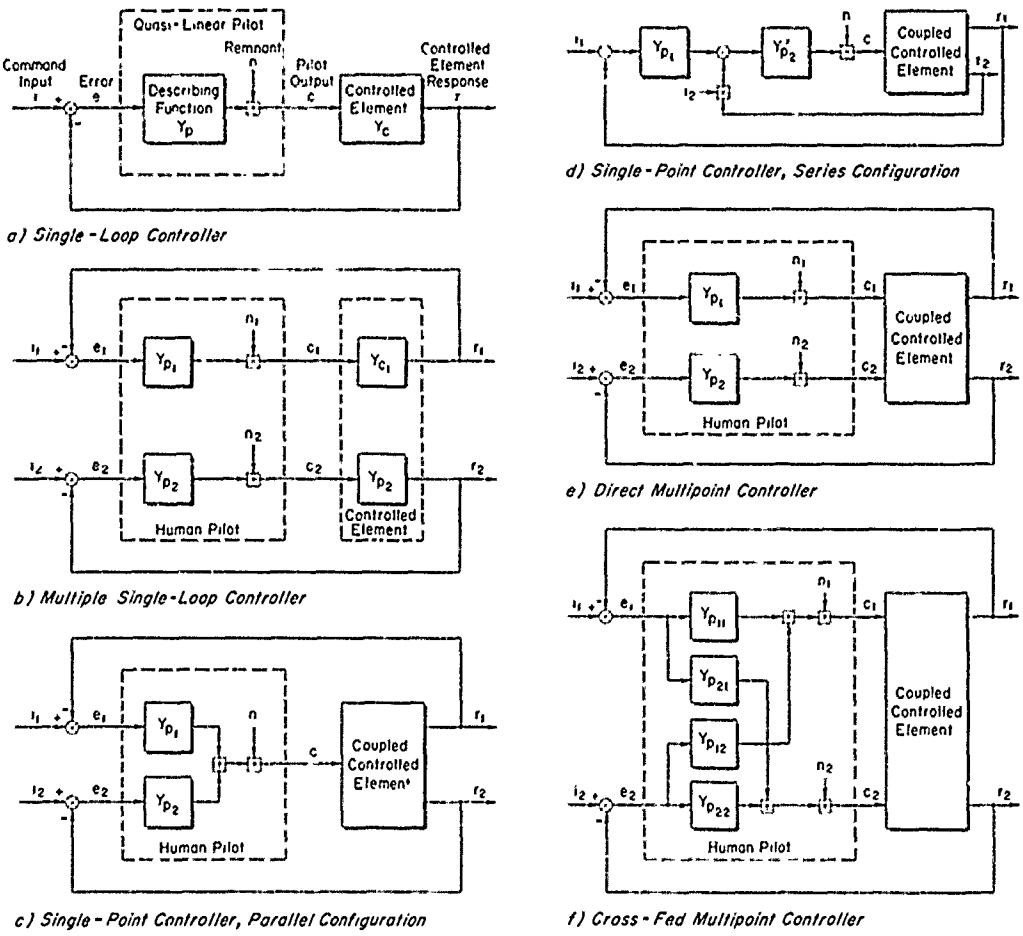

Figure 30. Examples of Single and Multiloop Manual Control Systems

configuration. The second system shown consists of two single-loop compensatory systems with no coupling in the controlled element. A typical example of such a multiaxis situation is longitudinal and lateral stabilization of an aircraft in straight, wings-level, horizontal flight using aileron and elevator. A number of the studies contained in Table C were for controlled elements of this nature (Refs. 19, 16-18, 2[illegible], 62-64, and 69). This multiple single-loop structure was assumed (for data analysis purposes) and demonstrated to be appropriate (as based on data results) for these cases. Multiloop systems differ from multiple single-loop systems in that interaxis coupling is inherent in the controller or the controlled element dynamics, as indicated in Fig. 30c-f. These kinds of systems represent a higher level of pilot/vehicle complexity but are, nonetheless, required for many piloting tasks.

Fundamentally, there are three inspirations for multiloop control. The first is a desire to exert control over more than one variable; in general, this requires one point of control application per control variable as well as meeting controllability and observability limitations. Although this desire could hypothetically be met with multiple single-loop systems, a true multiloop control is often the practical result.

The second reason is the use of auxiliary quantities (controlled element outputs) as feedbacks in lieu of series compensation of primary quantities. Common examples of this parallel (feedback) equalization are the use of pitch attitude (instead of altitude rate) to supply path damping in an altitude control system, and bank angle (instead of heading rate) to provide path damping for a heading control system. Often, the auxiliary feedback will have advantages in other respects. For instance, it may provide a more stable feedback for other than the primary modes considered, may be easier to sense, may suffer less from noise contamination, or may be itself a suitable outer-loop feedback for some flight control system mode. For piloted control systems, the auxiliary feedback in lieu of series compensation can be profoundly important. This is perhaps best appreciated by recalling that pilot generation of lead equalization incurs penalties in incremental time delay, increased remnant, decreased system performance, increased pilot workload, and poorer pilot ratings.

The third reason for multiloop control is to achieve coupling or decoupling purposes. This is a modification of the effective controlled element transfer function numerators by auxiliary control from another control point.

Because this list of inspirations for multiloop control is particularly favorable for manual control, piloted situations may more often be multiloop than corresponding automatic conditions.

The key to multiloop pilot models and actions is also the first fundamental concept of pilot/vehicle analysis: that the pilot "constructs" feedback loops about the effective controlled element. The feedback quantities actually selected by the pilot will be those necessary to satisfy the guidance and control needs and certain pilot-centered requirements. The guidance and control needs are situation-specific. Satisfaction of these needs always involves a task- or purpose-centered outer loop, with possible subsidiary inner-loop and other axis closures as needed to make the principal feedbacks work. Examples of appropriate outer and subsidiary loop structures for typical precision tracking and precise flight path control tasks are given in Fig. 31. Illustrated there are system configurations pertinent to air-to-air combat and/or weapon delivery and to formation flight. The task and purpose-centered outer loops are shown with solid lines in this figure, whereas the subsidiary inner loops are shown with dashed lines. For the tasks noted, the figures may not contain all the inner loops and they do not indicate the crossfeeds or other-axis closures which might be desirable from the standpoint of guidance and control needs. These additional features are, more often than not, highly vehicle-specific. Nonetheless, the unlabeled blocks, each of which represents pilot actions and thus a describing function, are sufficiently large in number to imply an enormously complex analysis and measurement situation. Fortunately, the analytical complexity is more apparent than real, since there are efficient analytical techniques available specifically designed to handle these types of systems (Ref. 102).

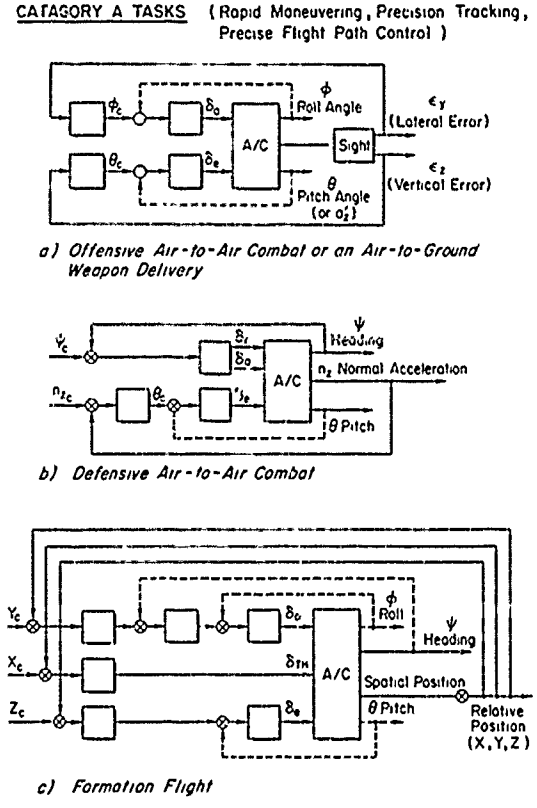

Figure 31. Illustration of Outer and Subsidiary Loops for Typical Precision Tracking and Precise Flight Path Control Tasks

In multiloop pilot/aircraft control systems, the essential features of the system structures are the feedbacks themselves and their equalization. For successful systems, i.e., systems which demonstrate uniform, reliable, high-quality performance in a given task, etc., the possible feedback structures are very limited. They derive primarily from guidance, control, and regulation demands, and secondarily from dynamic response characteristics desired by the pilot. From the systems view it is the satisfaction of these requirements that is important rather than the means employed. In other words, the feedback loops closed is the central issue, whether the closures are accomplished automatically or manually.

Stated verbally, the key guidance and control requirements for most pilot/aircraft precision control tasks may include:

- Establish and maintain the aircraft on some specified spatial pathway or beam (e.g., localizer and glide path).
- Reduce flight path errors to zero in a stable, well-damped, and rapidly responding manner.
- Establish a (perhaps accelerating) equilibrium flight condition.
- Limit the speed or angle of attack excursions from this established equilibrium flight condition.

The regulation requirements are similar, i.e.:

- Maintain the established flight path in the presence of disturbances such as gusts, crosswinds, and wind shears.
- Provide a degree of short-time attitude stability in the presence of disturbances.

These requirements relate primarily to the relatively low-frequency path modes of the pilot/aircraft system. In essence, they define outer control loops involving those vehicle motion quantities which define the desired equilibrium state of motion. More often than not, such outer loops, when closed about unmodified aircraft dynamics, do not result in stable, well-damped, rapidly responding systems. Instead, as already remarked, equalization of either a series or a parallel nature is needed to assist. Parallel equalization is most common and is achieved by the use of inner loops which feed back such quantities as attitude, angular velocity, and sometimes linear acceleration. These inner loops dominate the high-frequency characteristics of the aircraft/controller system.

B. MULTILOOP DATA BASE

The data base available for the construction of mathematical pilot models for multiloop compensatory situations with visual inputs is given in Table 9. Because of the instrumental measurement and analytical difficulties (Ref. 79) inherent in finding unique pilot describing functions in multiloop systems, only these three studies have been accomplished. However, their combined scope is sufficient to cover many cases of pilot/aircraft system interest, both laterally and longitudinally. Several other experimental series avoid some of the measurement and analysis difficulties by assuming adjustable fixed-form pilot characteristics (e.g., Refs. 100, 10 -109). These provide useful, and in some cases definitive, data even though the pilot dynamic characteristics are not uniquely defined.

Another aspect of the Table 9 data which significantly enhances their utility and broadens their scope is that each series was preceded by an extensive pre-experimental analysis activity. These preliminary studies estimated the pilot dynamics and pilot/vehicle system dynamics and performance before the experiments were conducted using the then best available version of the multiloop pilot model. The estimates were used both to help configure critical aspects of the experiments and as the basis for the setup of analog pilots to permit the assessment of measurement and data analysis techniques. After the experiments had been completed and the data analyzed, it was possible to compare the pre-experimental estimates with the actual experimental results. Differences between expectation and realization then lead to rectification in terms of the model, as well as to a more direct understanding of the results. This application of pilot/vehicle system analysis to provide a pre-experimental estimate of what to expect and for post-experimental rationalization of what occured is, of course, one of the principal uses of pilot-vehicle analysis; but nowhere is this more advantageous than when dealing with new model development.

C. MULTILOOP VISUAL COMPENSATORY SYSTEM PILOT MODEL

As a consequence of the kinds of studies referred to in the last section, a series of adjustment rules similar to those used for the single-loop model can be stated. These are listed below.

1. The multiloop situation with full visual field is similar to that shown in Fig. 1[illegible] if the signals i, e, c, and m are interpreted as vector quantities, and with the understanding that the perceptual portions of the central elements for each stimulus used operate in parallel.

2. The feedback quantities available to the pilot for possible use consist of those:
   a. Directly sensed within the general visual field.
   b. Observable via visual displays.
   c. Directly sensed using modalities other than vision.

   Quantities which can be perceived from the full visual field or other modalities will show no scanning penalties whereas those which require instrument scan or modification of the eye fixation point will introduce decrements (described later).

3. The feedback loops preferred are those which:
   a. Can be closed with minimum pilot equalization.
   b. Require minimum scanning to sense the feedback quantity.
   c. Permit wide latitude in the pilot's adapted characteristics.

TABLE 9. SUMMARY OF MULTILOOP, VISUAL, COMPENSATORY SYSTEM DESCRIBING FUNCTION AND REMNANT DATA

INVESTIGATOR	CONTROLLED ELEMENT DYNAMICS AND CONTROL TASK(S)	GENERAL RESULTS AND REMARKS
Stapleford, McRuer, and Magdaleno (Ref. 77)	Single-input, two-control point, integrated display aircraft lateral control. Bank angle tracking with good lateral (roll subsidence $1/T_R \doteq 5$) dynamics and 3 different levels of dutch roll damping ratios: $\zeta_D = 0.75$ (single-loop control), PR = 4; $\zeta_D = -0.075$ (marginal multiloop required), PR ≐ 6; and $\zeta_D = -0.35$ (near multiloop control limits), PR ≐ 8. Effective system was Fig. 30f with $i_2 = Y_{p_{12}} = 0$.	1. Single-loop pilot model is applicable to multiloop system command (outer) loop and, with possible reservation, to inner loops as well. 2. When several feedback possibilities are present, the pilot will select those which permit best dynamic performance with least pilot equalization and effort. 3. Control crossfeeds were adopted to reduce inadvertent oscillation of subsidiary mode. 4. Pilot outer-loop dynamics for all configurations were similar, but ratings degraded as required level of multiloop activity increased.
Stapleford, Craig, and Tennant (Ref. 69)	Two-input, single-control point, integrated display, aircraft longitudinal control. Altitude (approach) control in the presence of attitude and gust disturbances. Effective system was Fig. 30d.	1. Attitude-alone (single-loop task) and attitude inner-loop (multiloop task) closures were very similar. 2. Successive closure of single-loop models are appropriate for multiloop situations. 3. Series (Fig. 30d) closure model is most appropriate in that describing function data then take their simplest form.
Weir and McRuer (Ref. 107)	Single-loop, single-control point, integrated display, pitch attitude control; effective system Fig. 30a. 2 single-loop, two-control point, integrated (flight director) plus full panel display all-axis approach task; effective system Fig. 30b with scanning added. Multi-input, single-control point, full panel display, longitudinal approach control in the presence of attitude and gust disturbances (lateral axes under autopilot control); effective system Fig. 30d with scanning added. Multi-input, two-control point, full panel display, all-axis approach task with attitude and gust disturbances; effective systems for lateral and longitudinal each correspond to Fig. 30d with scanning added. Eye movements measured as well as dynamic properties.	1. Pitch attitude-alone data are consistent with single-loop model, but lower in gain than the Ref. 69 results. 2. Data for pitch attitude-alone, flight director all-axis control, and one longitudinal control cases are reasonably well fitted by crossover model forms. 3. The two pilot subjects exhibited different styles: relatively low-gain inner and high-gain outer loops as contrasted to high-gain inner and low-gain outer loops. 4. Results were consistent with satisfying the guidance and control requirements. 5. Series (Fig. 30d) structures appear pertinent for both lateral and longitudinal control operations. 6. Both inner and outer loop gains for this study were lower than the comparable Ref. 69 results. 7. The major contributor to remnant appears to be inner-loop operation.

4. Where distinct inner- and outer-loop closures can be defined by ordering the bandwidths (e.g., the higher the bandwidth, the more inner the loop), a series multiloop structure applies.

5. Pilot equalization for the outer loop of multiloop systems is adjusted per the crossover model, with the proviso that the effective controlled element transfer function include the effects of all the inner-loop closures. The crossover model is also directly applicable to many inner-loop closures.

6. Crossfeeds are commonly adopted by the pilot to directly negate the excitation of subsidiary coupled modes.

7. The adjustment of the variable gains in each of the loops is, in general, such as to achieve basically simple (i.e., effectively second- or third-order) well-damped dominant modes, and nearly uncoupled sets of aircraft responses. Outer-loop gains, in particular, may be lower than maximum bandwidth for this reason.

8. When scanning is not present, the remnant is primarily associated with the inner loop and is essentially the same as that for a single-loop system equivalent to the inner loop alone. (Scanning remnant is discussed below.)

Although scanning is avoided where possible, multiple fixations are sometimes required to sense the appropriate controlled element output quantities. The basic process of scanning during multiloop control tasks, sampling the fixated and parafoveal information, and reconstructing the scanned signal is very complex and little understood in detail. However, the essence of past work in this area (Refs. 91, 103, 110-113) shows that in the process of extracting the feedback information from the displays:

1. A fairly stationary scanning strategy evolves for a given task and full field/instrument array.

2. The pilot's output control motions are much more continuous than a discrete sampling of input signals coincident with eye fixations would seem to imply from the pure stimulus-response sequence.

3. The first-order effects of scanning are to reduce the pilot gain and increase remnant in the scanned channels.

The development of multiloop pilot models complete with scanning effects has gone through several stages of theoretical analysis and experimental validation. Many of the phenomena observed empirically can be modeled theoretically with two different multi-input, multi-output pilot model forms called, respectively, the "switched gain" model and the "reconstruction hold" model. The current version of these models is described in Ref. 106. We shall consider here the gist of the switched gain model only, because it is appropriate to most critical multiloop piloting situations where scanning is relatively limited. This model is also conceptually the simpler of the two.

This form of scanning model is termed switched gain because it incorporates a quasi-random, finite-dwell sampling or switching process between the pilot's foveal gain and his effective parafoveal gain on each of the several displays involved. Figure 32 illustrates the model with a block diagram. The foveal path is closed during the foveal dwell interval, and the parafoveal path is closed during the foveal interrupt interval. Each of these paths will, in general, exhibit different gains, equalization and effective time delays before the paths are combined in the higher neural centers to send a signal to the actuation describing function.

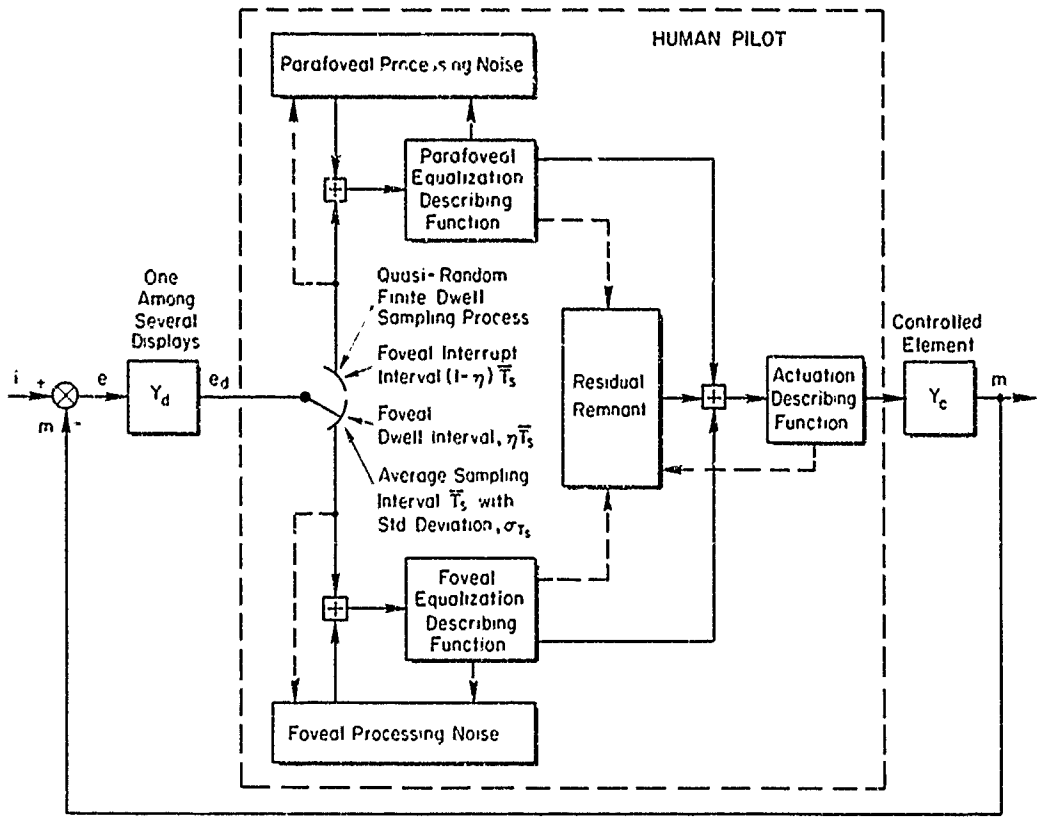

Figure 32. "Switched Gain" Multiaxis Scanning Model for Compensatory Multiaxis Tracking with One Among Several Displays

The conceptual block diagram in Fig. 32 can be remarkably simplified by recalling (Ref. 114) that any quasi-randomly sampled and processed signal can be modeled by: 1) replacing the sampling or switching process by a continuous transmission path, and 2) adding an uncorrelated wideband noise process which has a power-spectral density proportional to the variance of the (displayed) signal before sampling. Since the quasi-random scanning process has a finite foveal dwell interval, the wideband noise process will exhibit a low-pass power spectrum with a first-order break frequency which is inversely proportional to the average foveal dwell interval (Ref. 112). The power-spectral density of this foveal/parafoveal switched gain scanning remnant is given in simplified terms by:

$$\Phi_{nn_S}(\omega) = \frac{\overline{T}_S(1-\overline{\eta}_e)(1-\delta)\sigma^2}{\pi\left[1+\left(\frac{\omega\overline{T}_{d_e}}{2}\right)^2\right]} \quad \left(\frac{\text{units}^2}{\text{rad/sec}}\right) \tag{40}$$

where:

σ^2	is mean-squared value of the signal scanned
$\overline{T}_S$	is mean scanning interval
$\overline{\eta}_e$	is effective dwell fraction = $\overline{T}_{d_e}/\overline{T}_S$
$\overline{T}_{d_e}$	is effective dwell interval
σ_{T_S}	is standard deviation in T_S
$(1-\delta)$	is approximately $\sigma_{T_S}/\overline{T}_S$, the scanning variability ratio

Measurements of this switched gain remnant in Ref. 91 have shown that it is so predominant compared with the other sources of remnant that the other sources cannot even be identified. This makes for great simplification of the remnant in the equivalent switched gain model.

Representation of the pilot's describing function in the switched gain model can also be greatly simplified. The foveal gain exceeds the parafoveal gain in all measurements which have been made (Refs. 91, 110-111). This is probably because of the large displacement and increased rate thresholds in parafoveal perception by comparison with foveal perception. The switched gain model is represented simply by multiplying the ratio of parafoveal gain to foveal gain (Ω) by the interrupt fraction ($1-\eta$) and adding the product to the dwell fraction (η) to obtain the effective dwell fraction, viz.:

$$\eta_e = \eta + \Omega(1-\eta) \tag{41}$$

where $\Omega = \omega c_p/\omega c_f$ = ratio of crossover gains for continuous parafoveal tracking relative to continuous foveal tracking ($0 \leq \Omega \leq 1$). The effective crossover gain for the equivalent switched gain model for one foveal/parafoveal channel is $\eta_e \omega c_f$, where ωc_f is the foveal crossover gain in continuous single-axis tracking of the same display and controlled element constrained by the same task variables. (For a step-by-step application of the scanning model see Ref. 137.)

There are no apparent phase penalties associated with switched gain scanning as long as parafoveal perception is not completely inhibited. Inhibition can occur either by requiring a multitude of different widely-separated fixations with a time constraint or by inducing "tunnel vision" on one or two displays. Even so, measurements reported in Ref. 91, where parafoveal perception was inhibited by blanking the parafoveally-viewed display, show only small effective time delay increments ($\Delta\tau_S$) on the order of 0.05 to 0.15 sec attributable to scanning as the parafoveal-to-foveal gain ratio (Ω) approached zero.

The switched gain model has been quite successful in modeling behavior on a main task in laboratory experiments with induced natural scanning between a primary tracking task and a secondary subcritical tracking task (Ref. 91) and on foveal and parafoveally-viewed displays (Refs. 110-111). For most critical multiloop aircraft control tasks the scanning involved ordinarily needs to consider only two or three major elements (e.g., other aircraft in tail chase, own wing man) within the scan pattern, so this model should be very useful.

The principal effects of scanning are thus seen to be loop gain reductions and remnant increases. Both factors separately degrade performance, and their combined effect can be devastating. Limiting conditions of complete saturation can readily be approached when only a very few loop closures are achieved via scanning.

D. MULTIMODALITY PILOT MODEL CHARACTERISTICS

The description of pilot dynamics to this point has explicitly assumed fixed-base conditions. Many important piloting tasks include accelerating and rotating flight. Consequently, the effects of motion cues on the pilot's dynamic response can be very important. Generally speaking, these can be divided into five categories:

- The motion may provide an alerting and triggering stimulus which activates an internal command generator. This operates in conjunction with the parallel quasi-optimal control path of the dual-mode model (next chapter). It is perhaps most important for recovery maneuvers.
- Motions indicative of status, such as buffet or stick shaking, provide alerting and a consequent increase in neuromuscular tension. This has the effect of reducing the effective time delay in the neuromuscular system, τ_{NM}, thereby permitting the pilot to operate with a higher gain.
- Essentially steady-state, moderate g levels can improve the pilot's dynamic response potential via a neuromuscular tension increase similar in effect to that noted above. At higher g levels the pilot's dynamic capabilities are generally degraded, e.g., gains are decreased.

- Motion effects which conflict with the visual modality can cause illusions which distort the pilot's perception of the state of affairs. These can be so severe as to affect the pilot's control capability (Refs. 74 and 115).

- The vehicle motions sensed by the pilot are used as the basis for closed-loop control (Ref. 70).

The first three of the effects noted above are taken care of in the multiloop model described above either as a stimulus or as an adjustment in one of the model parameters. The last two effects are more complicated and require more extended discussion. For this purpose, we will draw heavily on Ref. 70, which, in turn, relies extensively on data from Refs. 116 and 117. To start, recognize that the pilot contains neurological elements capable of sensing rotary and linear accelerations. The primary neurological elements involved as sensors are in the vestibular apparatus, although other sensors and pathways may also be involved.

The rotary motion sensor, usually associated with the semicircular canals, has a basic second-order response to angular velocity. As shown in Fig. 33a, it is in essence a highly overdamped angular accelerometer. Over the frequency range from 0.2 to 10 rad/sec, the output signal is proportional to angular rate, so the sensor can function as a "rate gyro." For prolonged turning the signal washes out; thus, spurious sensations occur in steady rotations or when the turning motion stops. The threshold element shown in Fig. 33a is somewhat of an oversimplification since the threshold value, ω_T, has both inter-axis and inter-subject variability and is also dependent on the magnitude and time character of the input acceleration. It is of the order of 1-3 deg per sec, which is sufficiently low to assure the presence in the pilot control loops of the rotary motion sensors in large amplitude recovery maneuvers, yet perhaps large enough to make closed-loop motion effects unimportant for precision control near the stall.

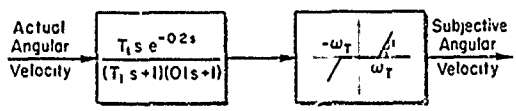

AXIS	T_1(sec)	ω_T(deg/sec)
Roll	6.5	3.2
Pitch	5.3	2.6
Yaw	8.0	1.1

a) Angular Motion Sensing Dynamics

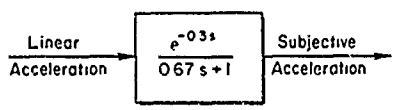

b) Linear Motion Sensing Dynamics

Figure 33. Angular and Linear Motion Sensing Dynamics (Ref. 70)

Because the rotary motion-sensing apparatus gives rise to a rate-gyro-like cue, the necessity for visually-generated attitude lead is reduced. This is particularly important (and has been well demonstrated in Ref. 70) when the effective controlled element dynamics are K/s^2-like or worse. It is also worth mentioning that the primary effect of the rotary motion feedback can be converted into an equivalent visual-only or fixed-base situation. For instance, a fixed-base crossover model can be applied to moving-base tracking by modifying the effective time delay and resulting crossover frequency. Specifically, the phase lag is reduced roughly equivalent to a time delay reduction of 0.1 to 0.2 sec, and the magnitude of the pilot describing function, Y_p, is increased to provide a crossover frequency increase of 0.5 to 1.5 rad/sec. This means of accounting for the rotary motion cues is both effective and extremely simple to apply in analysis.

The linear acceleration sensors are ordinarily associated with the utricles. Less is known about the dynamics of this sensory apparatus, although the effective model between linear acceleration and the pilot's output acting on that linear acceleration is indicated in Fig. 33b. The thresholds in this pathway are very small, of the order of 0.01 g or less, and therefore have a negligible effect in most vehicular control situations. On the other hand, the lag time constant of about 2/3 sec is more often than not too large for the signal to be useful for continuous closed-loop control purposes. Further, the utility for control purposes of acceleration cues is highly dependent on the pilot's location. Consequently, while experiments have demonstrated the significant advantages of rotary cues for control purposes, only very limited situations have done the same for linear accelerations (Ref. 118). Nonetheless, every situation where a linear acceleration feedback of this nature would be advantageous to the pilot shows some evidence of its use. The point is that there are few such situations.

To structure a multimodality multiloop pilot model, the motion cue pathways illustrated in Fig. 33 are simply added to the vector version of Fig. 15.

In the discussion above, the linear and angular motion sensors are treated as if they are parallel pathways to the visual modality. This is only part of the story, as is shown in Fig. 34. There, the "nystagmus crossfeeds" from the canals and utricle to the oculomotor system will be noted. The nystagmus crossfeeds produce involuntary eye motions as a function of the excitation of the vestibular apparatus. Such motions are important in disorientation and illusions which result from the initiation or sudden cessation of large amplitude maneuvers. There are also other flight operations which have no ordinary earthbound equivalent and which give rise to similar illusory phenomena. Several of these are of great importance in producing conflicting cues for flight control. Some examples are given in Table 10. Most of these phenomena have only qualitative connections with even the most sophisticated versions of the multimodality multiloop pilot model.

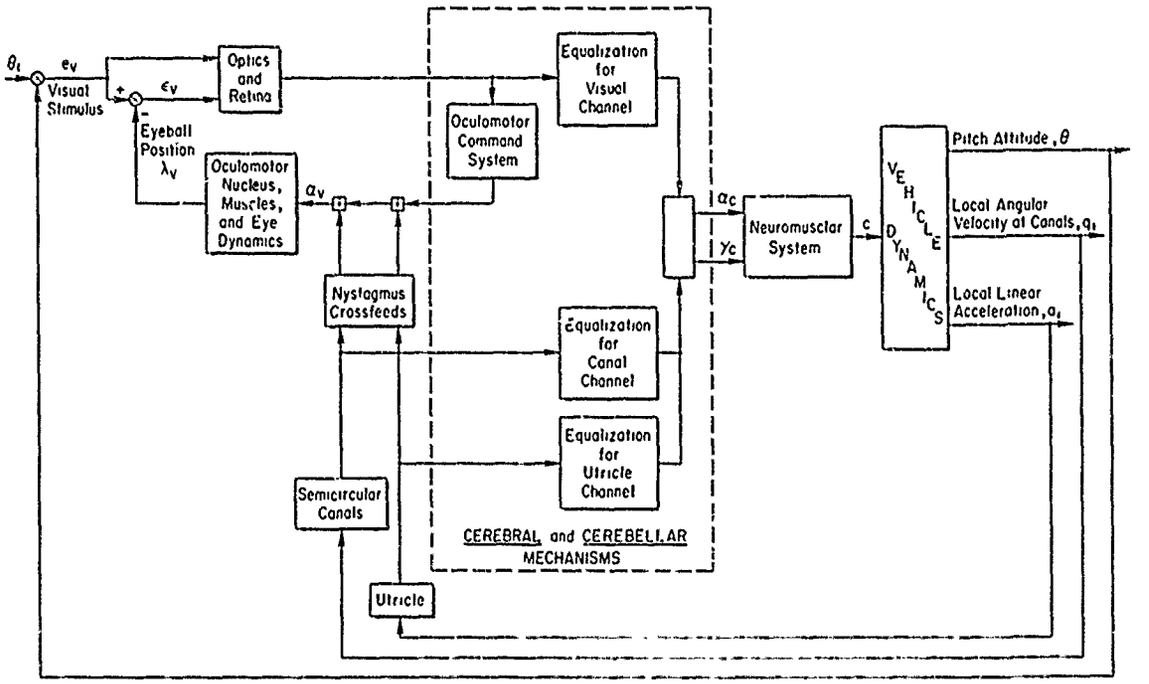

Figure 34. Pilot/Vehicle System for Head-Fixed, Pressure-Manipulator, Attitude Control Tasks

TABLE 10. EXAMPLES OF POSSIBLE MOTION ARTIFACTS IN THE PILOT/VEHICLE SYSTEM

SITUATION	VESTIBULAR SENSORS PRIMARILY INVOLVED		REMARKS
	UTRICLE (G_u)	SEMICIRCULAR CANALS (G_{sc})	
Steady turn	×	×	Illusion of straight and level flight; G_{sc} and G_u terms are washed out.
Straight and level after steady turn		×	Sensation opposite of turning; visual sensation of tilt. G_{sc} and G_{vc} are dominant in creating these sensations.
Steady acceleration in horizontal flight, pushover from steady climb	×		Sensation of nose-up change in attitude.
Deceleration	×		Sensation of pitch-down change in attitude.
Straight and level after high angular path (> 60 deg/sec) aerobatics		×	Sensation of turning.
Straight flight after long time high rate rolls		×	Nystagmus, blurred vision, reversal of background.
High-frequency pitching rotations, etc.		×	Blurred vision

E. MULTILOOP PILOT RATING CONSIDERATIONS

A number of schemes to obtain multiloop pilot ratings from single-loop considerations have been proposed (Ref. 37); at present the most promising (Ref. 119) is based on excess control capacity concepts. Assume that the relationship between pilot rating and excess control capacity, $\lambda_n \equiv \lambda_s/\lambda_c$, given by Fig. 29 is applicable to each loop of a multiloop manual control system. Then, for each such loop a pilot rating, R, can be estimated using the single-loop correlates previously discussed (Fig. 27) or, when available, rating functionals like those in Fig. 26 and an excess control capacity, λ_n, assigned accordingly.

Single-axis capacity, or attention, values can be combined to yield the combined axis value by a multiplication process (Ref. 120), i.e., the multiaxis excess capacity, λ_{n_m}, is given by the product of the excess capacities for the individual axes:

$$\lambda_{n_m} = \prod^{m} \lambda_{n_i} \tag{42}$$

and for $R = A + B\lambda_n$ as a linear fit of the Fig. 29 data:

$$R_m = A + B\lambda_{n_m} = A + B\prod^{m}\lambda_{n_i} = A + B\prod^{m}\left(\frac{R_i - A}{B}\right)$$

$$R_m = A + \frac{1}{B^{(m-1)}}\prod^{m}(R_i - A) \tag{43}$$

Combined ratings are always greater than (or equal to) individual ratings, since combined λ_n's are always less than any individual λ_n. Also, the maximum value of R_m never exceeds A, i.e., for large $R_i < A$, $\prod^{m}(R-A) \rightarrow 0$.

The logical value for A is 10.0; B is determined, using the empirical data to be equal to −8.3. This results in a good overall fit to all the available multiloop rating data (Ref. 119).

CHAPTER VI

RECONFIGURING MANUAL CONTROL SYSTEMS: BY DESIGN AND BY PILOT ADAPTATION

In Chapter I the stage was set for subsequent elaborations by presenting some of the caveats which historically confronted efforts to model the human pilot mathematically. This pessimism was based on the human pilot's manifest ability to learn new modes of behavior and to adapt them to the changing demands of the vehicle of which he was in control — an ability which is strongly nonlinear when compared with the responses of the inanimate components of the control system. It is pilot abilities such as the foregoing together with multimodal sensory perception and output behavior which lead to a number of possible control loop structures for piloted vehicles in any given situation. Through higher-order processes, such as judgment and memory, the pilot can evolve and modify his performance criteria, select relevant inputs, decide between competing control loop structures, and optimize his fine-grained behavior with respect to several criteria. Clearly, these are marvelous abilities, and, in fact, the reasons for the versatility and effectiveness of manned control systems. Understanding this behavior can serve to develop rules for the pilot/vehicle system analyst for selecting the pilot model appropriate to a given situation and can facilitate the development of system configurations which elicit and exploit this behavior. As we shall see, this development is an activity shared between the designer and the pilot. In what follows we describe a dual-channel controller and illustrate the compatibility of such a configuration with pilot behavior for both random-appearing and quasi-predictable inputs. A theory for the development of control skills is developed, and the stages in this development related to known capabilities of pilots. Finally, the behavior of the pilot in responding to transient inputs is placed within this context for skilled control.

A. SOME PROPERTIES OF A DUAL-CHANNEL CONTROLLER

The well-developed theory for pilot single-loop control behavior presented hitherto has treated the pilot as if he were responding to information arising from e(t) alone. Precise input/output measurements were made for this single input channel mode of behavior, but these measurements were not capable of distinguishing different cognitive operations which the pilot might elect to perform upon his inputs. In Chapters III and IV we showed how a model for neuromuscular control and actuation could be developed from physiological data and measurements on the intact, non-physiologically-instrumented, pilot. We will now present models for the internal cognitive organization of the pilot's information used for control.

Consider a situation in which both the forcing function, i(t), and the error, e(t), are available for use in control. Figure 35 presents this situation, where Y_{p_i} operates on the input channel and Y_{p_e} on the error channel.

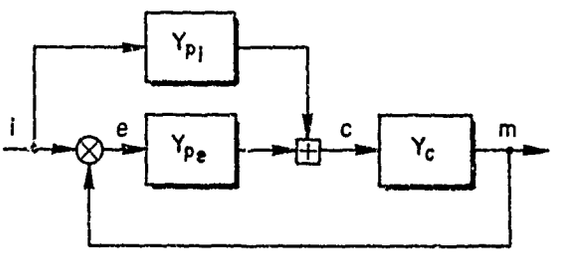

Figure 35. A Dual-Channel Controller

If a systems analyst were presented the controller in Fig. 35, as an unknown to be identified, he would proceed as discussed in Chapter III and compute describing functions, one of which we will call Y_β.

$$Y_\beta = \frac{\Phi_{im}}{\Phi_{ie}} = \frac{Y_c(Y_{p_i} + Y_{p_e})}{1 - Y_c Y_{p_i}} \tag{44}$$

Were the controller responding to e(t) alone, i.e., $Y_{p_i} = 0$, then $Y_\beta / Y_c = Y_{p_e} = Y_p$. In the dual-channel mode the closed-loop, M/I, and error/input describing function, E/I, are the following:

$$\frac{M}{I} = \frac{Y_\beta}{1 + Y_\beta} = \frac{Y_c(Y_{p_i} + Y_{p_e})}{1 + Y_c Y_{p_e}} \tag{45}$$

$$\frac{E}{I} = \frac{1}{1 + Y_\beta} = \frac{1 - Y_c Y_{p_i}}{1 + Y_c Y_{p_e}} \tag{46}$$

Subject to the constraints imposed by stabilization demands we would like Y_β to be very large so that $|M| / |I| \to 1$ and $|E| / |I| \to 0$. This could be accomplished if the block Y_{p_i} were "smart" enough to adjust

itself so that $Y_{pi}Y_c \doteq 1$. Increasing Y_{pe} to achieve the same end would be both potentially destabilizing and an inefficient use of information. For Y_{pi} to be calibrated to Y_c, functional knowledge of Y_c would have to be in Y_{pi}'s "memory." This knowledge could be wired in or it could evolve with experience.

If the systems analyst were to suspect that he was measuring a controller capable of acting in a dual-channel mode, he could make predictions about the form of Y_{pi}. He would expect the compensatory Y_{pe} to be present and active if the controlled element were unstable or if the forcing function were such as inherently to induce a remnant (e.g., random-appearing). In these events the Y_{pe} loop would have to be closed. On the other hand, if the controller had a functional knowledge of Y_c so as to compensate for system lags, and knew i(t) sufficiently well to enable "prediction" of its future course, Y_{pe} could be negligible for varying intervals of time and $Y_{pi}Y_c \doteq 1$. A feedforward of this sort could exhibit prodigious performance by acting on estimates of the future input to compensate for lags in itself and the plant under control.

The hypothetical behavior described has parallels in human pilot operations. There are various means by which this pilot dual-channel multimode behavior can be facilitated. In the following sections we will review these means.

B. THE PURSUIT DISPLAY

The most direct means for helping the pilot become a dual-channel controller — bearing in mind that the dual channels are cognitive organizations of input information which can be facilitated and supported but not compelled by engineering design — is to present the necessary inputs to him. The pursuit display does this by presenting the pilot a moving target which he pursues in an effort to capture it with a cursor he commands through the vehicle dynamics. Figure 36 is a schematic of this display. Three possible inputs are illustrated in Fig. 36, but only two are independent; so that the dual-channel model does not result in any loss of generality. Although the body of research on pursuit display tracking for which dynamic measurements exist is limited, there are measurements from which we can determine whether the pilot is capable of generating operations which enhance the performance of a dual-channel controller.

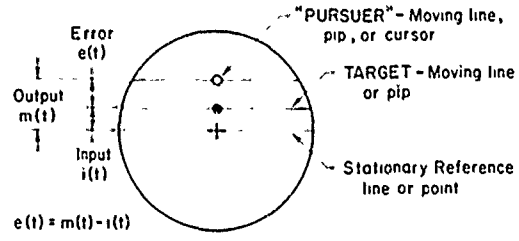

Figure 36. Pursuit Display

1. Random-Appearing Inputs

In order to measure the elements in Fig. 4, one must contrive situations which a priori make one or the other block dominant (Refs. 21 and 121), make assumptions about the form of Y_{pi} or Y_{pe} (Ref. 122), or introduce an additional uncorrelated input so as to be able to solve for two unknown blocks (Refs. 67 and 78). The first approach has been used for data with a pure-gain controlled element for $\omega_i < 4$ rad/sec inputs; with the assumption that since the task was quite easy and the error small, signals fed back through Y_{pe} were negligible. Under these circumstances measurements of M/I, the closed-loop transfer function, are identical with measurements of the feedforward, Y_{pi}, and the pure-gain plant. On Fig. 37a, the fidelity

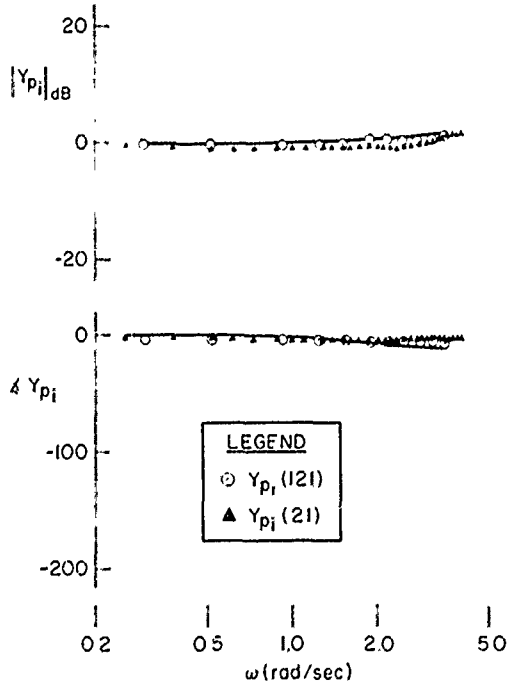

Figure 37a. Y_{pi}, Inferred, for $Y_c = K_c$

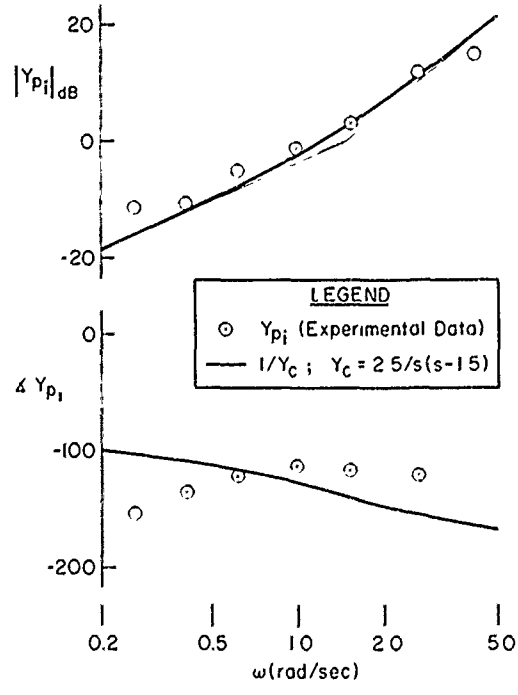

Figure 37b. Indirectly Measured Y_{pi}

with which Y_{pi} approximates $Y_c = K$ (0 dB, 0 deg phase) over a large range is remarkable. The data were generated in different laboratories, but were analyzed to the same end — to determine whether Y_{pi} could be fit by an optimal linear predictor in the minimum mean-square sense which operated only upon the position and velocity of the input signal. It was demonstrated (Refs. 21 and 121) that:

$$Y_{pi} = (\alpha + \beta j\omega)e^{-T_p j\omega} \tag{47}$$

where the prediction interval, T_p, was 0.2 sec. When α/β was less than about 5, $Y_{pi} \doteq Y_c^{-1}$. As the task increased in difficulty, the approximations which led $M/I \doteq$ no longer held, since the error loop became significant.

On the assumption that the feedback, Y_{pe}, in a dual channel does not differ significantly from the Y_p of a single-channel compensatory mode for the same subject with similar Y_c and ω_i, the feedforward for the pursuit case can be determined as:

$$Y_{p'} = \frac{Y_\beta - Y_c Y_p}{Y_c(1 + Y_\beta)} \tag{48}$$

Here, Y_β is measured in the pursuit situation and Y_p for the corresponding compensatory case.

This calculation has been made for several controlled elements. On Fig. 37b, which was generated using an unstable second-order system, we note a close correpondence between predicted and computed Y_{pi} magnitudes (Ref. 122). Certain data have indicated that when the pilot-generated feedforward cannot effect an adequate prediction of i(t) so as to allow a lag-free inversion of Y_c, a delay is present, i.e.:

$$Y_{p_i} Y_c = e^{-j\Phi(\omega)} \tag{49}$$

This effect accounts for the relatively poor phase match on Fig. 37b.

The substitution of Y_i for Y_{pe} in the calculations of Fig. 37b was justified by measurements using an additional uncorrelated input — the third technique (Ref. 67). That is, a disturbance, d(t), added to e(t) in Fig. 35 served to specify:

$$Y_{pe} = \frac{\Phi_{dc}}{\Phi_{de}} \tag{50}$$

and an open-loop describing function for the dual-channel controller, which can be designated $Y_{\beta p}$, was specified by i(t):

$$Y_{\beta p} = \frac{\Phi_{ic}}{\Phi_{ie}} = \frac{Y_{pi} + Y_{pe}}{1 - Y_c Y_{pi}} \tag{51}$$

Equations 50 and 51 were then solved for Y_{pe} and Y_{pi}. The pilot's pursuit behavior was scarcely affected by the additional input (Ref. 67). Y_{pe} exhibited a somewhat lower ω_c and greater phase margin than Y_p. This could account for some of the discrepancies in Fig. 37b.

2. Predictable Inputs

The most effective operation of the feedforward requires that i(t) be predictable. As predictability deteriorates, or involves more internal data processing, the lag in Eq. 49 becomes irreducible. Thus, although Fig. 37a indicates only minor phase lags at frequencies less than 4 rad/sec, it is clear from Eq. 47 that the prediction interval, $T_p = 0.2$ sec, must generate phase lags of increasing impact at higher frequencies. The data at higher frequencies bear this out. The lags inherent in generating a prediction of the input signal are analogous to the dynamic costs of low-frequency lead generation illustrated in Fig. 15.

There exists in practice a large number of examples of quasi-predictable inputs which the pilot might be able to reproduce with sufficient fidelity so as to minimize or perhaps eliminate these time costs for predictions. Such inputs arise in a variety of piloting tasks. Examples are: following the optical landing beam of an aircraft carrier plunging through deep ocean swells; compensating for low-frequency, lightly-damped vehicle modes; fighting pilot-induced oscillations; terrain-following flight over rolling countryside, etc. An example of such quasi-predictable inputs are the actual ship motion time histories shown in Fig. 38. A carrier pilot would like to match perfectly the corresponding deck motions with his aircraft landing gear if this could be accomplished through adequate vehicle response bandwidth and suitable displays and controls.

There are many examples of how well the pilot can match similar quasi-predictable motion. Pure sinewaves or simple combinations of a few sinewaves are subjectively and actually clearly predictable and, as such, thus provide an upper limit for the pilot's feedforward operation. A striking example of how well the pilot can generate a prediction of i(t) is presented in Fig. 39, where the human continued to produce

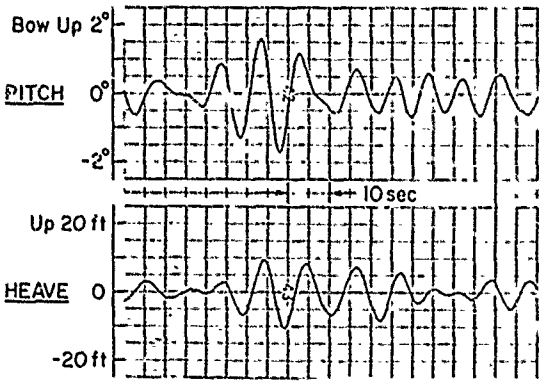

Figure 38. A Typical Quasi-Predictable Input; Ship Motion Time Histories (Ref. 123)

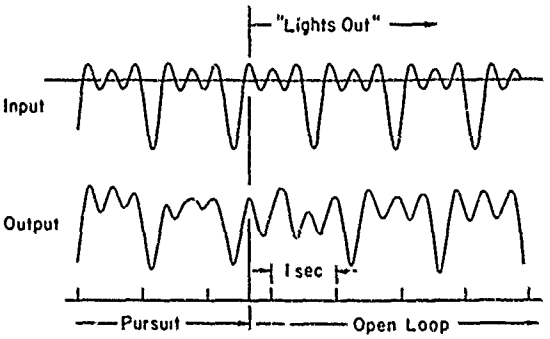

Figure 39. Demonstration of Pattern Generation (Adopted from Ref. 124)

a highly similar, though phase-shifted, version of the original harmonic signal when he could no longer see either i(t), e(t), or m(t) (Ref. 124). Further evidence of such internal signal generation is found in Refs 123, 125, and 126).

Data from the various previous studies of pure sinewave tracking (Refs. 37, 75, and 127) can be coalesced and presented in describing function form to illustrate the pilot's ability in this extreme case of signal predictability (see Fig. 40). Limiting conditions exist at the low-frequency end where the signal's rate of change is so low as to require the pilot to use the Y_{pe} loop for continual correction, and above ~20 rad/sec where neuromuscular limitations come into play. This range of high fidelity in frequency generation (note the essentially zero phase lags) is corroborated by a variety of pursuit tapping output studies in response to either auditory or visual inputs (Ref. 125). It was found that the standard deviation of the time intervals between i(t) and m(t), analogous to phase variations, ranged from 4 to 6 percent of the command tapping rate up to a commanded period of about 300 ms.

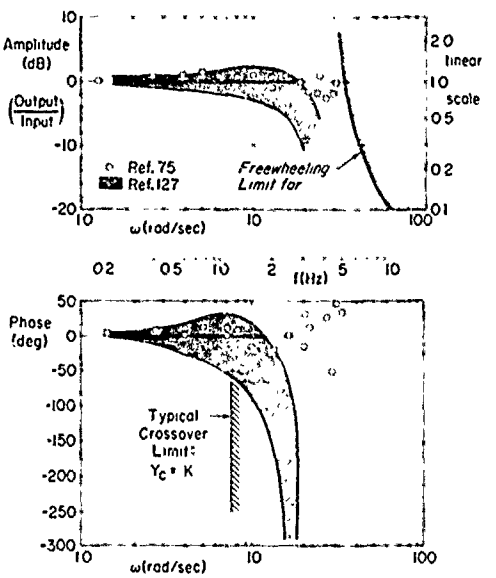

Figure 40. Frequency Response Data for a Single Sinewave Input at Various Frequencies

The foregoing can be summarized in the following rules for pilot tracking of sinewave inputs.

- In the region below about 0.5 Hz, it is advantageous to use a $Y_{pi} = 1/Y_c$ feedforward operation, with Y_{pe} present for vernier corrections and remnant suppression. In this region rhythms are hard to reproduce accurately. At very low frequencies (below 0.1 Hz) the operator operates to reduce the error, i.e., uses the Y_{pe} compensatory block solely.

- From 0.5 to about 1.0 Hz, rhythm detection permits activation of an internal "pattern generator" block, probably using proprioceptively perceived patterns. The feedforward block, Y_{pi}, aids in producing the "pattern generator" response. The compensatory loop, Y_{pe}, can still be closed tightly to phase lock the output and suppress remnant.

- From about 1 to just under 2 Hz, the pattern generator loop is active, but as the frequency exceeds the operator's compensatory crossover limit he must open the compensatory loop to avoid exciting undue overshoot errors. In this region control approaches ultimate predictive behavior with Y_{pe} acting intermittently to prevent frequency drift, but unable to prevent random phase and amplitude errors.

- From about 2 Hz to the neuromuscular response limit of 5 to 10 Hz, the operator only uses an internal pattern generator loop to roughly approximate the displayed amplitude and frequency, usually undershooting both.

Inputs can be scaled for subjective predictability along the dimension of signal shape or waveform features and their "coherence" or waveform time variations; such scaling, however, is not highly developed. This scaling of expected inputs would be helpful to the analyst and to the designer who might be able to either specify or induce Y_{pi} forms and control configurations appropriate to classes of signals. Because of their apparent similarity to such practical inputs as are illustrated on Fig. 38, bandpassed random noise provides an attractive idealization of an input of varying predictability. Examining its properties could assist the analyst in predicting the performance of control systems. It has been found (Ref. 123) that an effective rating for subjective predictability can be computed from the bandpass (half-power width),

Δ, and center frequency, f_o, of the narrowband filter through which the random process is passed. The properties of the ratio, $\nu = \Delta/f_o$, determine subjective predictability as follows:

Predictable $\quad \nu < 0.3$

Non-predictable $\quad \nu > 0.8$

For inputs with $\nu < 0.3$, there is evidence that the pilot generates a feedforward acting like a Kalman filter predictor for $Y_c = K_c$:

$$Y_{pi} = \frac{\sin \pi\nu}{\pi\nu} \frac{e^{-j\omega T_o}}{Y_c} \tag{52}$$

where $1/T_o$ is the center frequency of the narrowband filter. The prediction interval, T_o, is the cost imposed on the pilot by conditions under which he cannot internally generate the appropriate prediction but must operate upon the signal instead.

3. Are Pursuit Displays Desirable?

Whether a designer should attempt to facilitate the generation by the pilot of a feedforward loop by presenting him with a pursuit display is not an easily answered question. Ambiguities arise because the physical display does not guarantee the extent to which the pilot will utilize the added information channels. Table 11 lists the available data comparing pursuit and compensatory displays for which describing functions have been measured. Such comparison data which are in the form of performance measures alone have not been listed, because there is no way by which the selected pilot control structure can be adduced. For example, in Ref. 78 it was found that the influence of the Y_{pi} loop was negligible in the control of a K_c/s, and that Y_{pe} predominated. In other words, there was very little cognitive difference between a physical compensatory and physical pursuit display under the measurement conditions. The performance data confirmed this indifference, but without the dynamic data these performance measures would have been uninterpretable. Comparisons based on relative mean-square error must be interpreted with care, because the pilot may respond to additional control criteria. With this in mind we can review comparisons based on e^2/i^2 from Refs. 21, 67, 78, and 127. The most definitive findings are for $Y_c = K_c$ where pursuit displays are superior to compensatory displays in the range from 1 to 10 rad/sec. Outside this range, where compensatory tracking is at all feasible the compensatory display is to be preferred. For K_c/s over the range of measurements there is not much difference based on performance measures alone. What little data exists for K_c/s^2 indicate a slight preference for the pursuit display. There is, however, evidence that the pilot requires less control movement for K_c/s^2 in the pursuit than compensatory configuration, and he appears to like this condition.

Other bases for comparison between the two displays are presented in Table 12. As it can be seen, there are many desiderata in selecting a control display configuration in addition to performance measures. Perhaps the most important for aircraft applications is the indication of status information as well as command and error present in the pursuit display.

TABLE 11

SUMMARY OF HUMAN DYNAMICS DATA FOR EXPLICIT PURSUIT DISPLAYS

INVESTIGATOR	NUMBER OF TYPES OF RANDOM-APPEARING INPUTS	INPUT REMARKS	ADDITIONAL DISTURBANCE INPUT	NUMBER OF TYPES OF CONTROLLED ELEMENTS	DIRECTLY COMPARABLE WITH EXPLICIT COMPENSATORY DATA	REMARKS; NUMBER OF SUBJECTS
Elkind (Ref. 21)	20	1" rms; (sum of sine-waves)	No	(1), $Y_c = K_c$, pencil-like manipulator	Yes	3
Wasicko, McRuer, and Magdaleno (Ref. 127)	5	0.25" to 1" rms; all 5 inputs were present to 3 of the controlled elements (sum of sine-waves)	No	(7), $Y_c = K_c$, K_c/s, K_c/s^2 $K_c/s(s - 0.5)$ $K_c/s(s - 1.5)$ $K_c/[(s + 0.25)/(s + 5.0)^2]$ Lateral side stick	Yes	1
Allen and Jex (Ref. 67)	1	0.4" rms, 3.2 rad/sec, dominant frequency (sum of sinewaves)	Yes	(2), K_c/s, K_c/s^2 Lateral side stick	Yes	4 Obtained comments
Reid (Ref. 78)	4	Filtered noise, ω_{i_c} = 1.3, 1.4, 2.8 deg, 4.3 rad/sec 3 inputs had high-frequency shelves	Yes	(2), K_c, K_c/s Low inertia Restraint free stick	Yes	8 Disturbance magnitude:input magnitude
Ware (Ref. 121)	4	Filtered noise ω_{i_c} = 1.2, 1.4, 2.3, and 2.8 rad/sec	No	(1), $Y_c = K_c$ Force stick	No	3

TABLE 12

COMPENSATORY VERSUS PURSUIT DISPLAYS

COMPENSATORY	PURSUIT
Advantages	Advantages
1. Simple to build instruments, and to simulate. Most reliable.	1. Shows more of available information; permits operator to adopt separate control criteria for tracking versus regulation; enhances the ability to control quasi-predictable inputs
2. Expanded scale possible; easy to detect small errors.	2. Operator can develop a feedforward path (Y_{p_i}) operating directly on the input to minimize the closed-loop errors. Results in reduced τ_{eff} and higher overall system bandwidth, with lower gain and fewer stability problems in the compensatory loop.
3. Simple to interpret; only one form of action and/or Y_p is required.	3. Improved "conformability," i.e., a proper pursuit instrument is a closer analog to the visual field, permitting easier VFR and IFR transitions.
4. Can be easily optimized and equalized using pilot/vehicle systems analysis.	4. Less control motion required for higher-order controlled elements
5. Only type feasible for pure regulation tasks (e.g., suppress gust disturbances).	
Disadvantages	Disadvantages
1. Cannot separate disturbances from commands; leads to conservative closed-loop stability criteria and larger tracking errors for low-frequency inputs.	1. Scaling set by largest input command; may result in errors being too small to use effectively.
2. Error may not agree with secondary cues (e.g., normal accelerations versus $\ddot{e}$, while tracking a maneuvering target).	2. Harder to put inputs on instruments, e.g., maneuvering target position in space is hard to derive except from direct visual field.
3. Command patterns may be masked by remnant-induced errors, thereby impeding improvements due to more effective signal prediction.	3. No improvement for regulation against disturbances (for zero inputs cases).
	4. More difficult to interpret; Y_{p_i} and Y_{p_e} involved.
	5. More complex to build; less reliable.

C. SUCCESSIVE ORGANIZATIONS OF PERCEPTION

In the preceding discussion of the dual-input configuration we noted instances in which the pilot responded to the input signal as if it were a trigger to release a stored or self-generated program. Such instances occurred for the perfectly predictable sinewave or simple compound sinewave inputs. The pilot acts as if the only signals he requires, once he is fully familiar with the input and controlled element and knows when to begin, are those generated by the proprioceptors involved in his control movements. The level of skill is akin to that exhibited by a trained motorist applying controlled foot pressure to his vehicle's brakes on seeing a red signal light ahead, or overtaking and passing another car. In these examples the control skills constitute repertories of action which are called up at the appropriate moment and released. In this manner a variety of different criteria can be realized. The controller may elect a minimum effort maneuver, a minimum time maneuver, a minimum error maneuver, or he may apply his own relative weights to the foregoing and other considerations. As with any predictive control technique, this type of behavior requires the rest of the world to maintain its position during the maneuver. If, for example, after pulling out of the lane and drawing alongside of the car to be passed in a preprogrammed maneuver the passing vehicle is confronted by a change in lateral position or a forward acceleration by the vehicle being passed, deep trouble could result. It is the need to watch the rest of the world — or maintain an intermittent Y_{p_e} — which can contribute apprehension and add to the workload of otherwise simple tasks. If the Y_{p_e} loop is closed too tightly about lateral position, for example, the skilled passing maneuver is almost impossible to achieve. On the other hand, a monitoring mode is essential to prevent disaster — however unlikely the contributing events may be. The kind of intermittent open-loop behavior which we have been describing is called precognitive, and it represents the highest level in a progressive development of motor skill by stages of information exploitation which are Successive Organizations of Perception (SOP). The theory has been expounded elsewhere (Refs. 37, 74, 125, 128, and 129) and will only be summarized here. Figure 41, where remnants and disturbances have been omitted, will be useful in this regard.

- The initial phase is the familiar compensatory display. The pilot is capable of acting only in response to the error signal. Some analogies to this level of skill are: a blind man feeling his way with a cane across stepping stones; a motorist proceeding in a dense fog by hugging the cartway guideline; or a very drunken motorist, having generated a dense internal fog, cautiously proceeding by edging along the curb. The last is an example of a regression from a higher to a lower level of skill.

- The second phase is an elaboration upon the dual-channel configuration which we have discussed in detail. The additional channels are Y_{p_p}, the proprioceptive feedback which is particularly useful in committing simple periodic inputs to a memory of motor responses, and Y_{p_m}, an operator on the system output. Although a controller can conceivably develop all three of the transfer characteristics, Y_{p_e}, Y_{p_i}, Y_{p_m}, any two are adequate to describe the control process. An explicit pursuit display enables the pilot to more readily advance to the final phase of skill.

- The final or precognitive phase can be conveniently, but not usefully in terms of operationally defined measurements, conceived as a series of decision rule algorithms and stored programs. Phase three is the graceful or adept maneuver mode of behavior — skilled gymnastic evolutions, batting a ball, etc. The components are a stored repertory and a knowledge of which cues to use in releasing this repertory in a timely fashion. The open-loop sequences may be short, as a timely bang-bang control, or long as in generating a synchronous sinewave.

Hitherto we have emphasized the pilot's predictive ability as the essential element in achieving the state of precognitive grace — for however briefly. It should be clear from the description of precognitive control that an additional element, the dynamics of programmed responses in the pilot's repertory, must also be considered. These responses are those which may be called up while the pilot is engaged in some form of steady-state behavior such as continuous tracking or daydreaming. It has been found (Ref. 74) that such combined transient and stationary situations can adequately be modeled with a single input channel dual-mode structure such as that shown in the simplified diagram of Fig. 42. To represent a multiloop situation the signals shown in this block diagram could be considered as vector quantities. The quasi-linear steady-state path is the one used for tracking random inputs or disturbances. It is the same model described in great detail in previous chapters. The feedforward element operates on the transient inputs provided either from the system, such as a random-occurring step sequence, or induced by an internal command repertory from the pilot.

The nature of the switching and the feedforward element is, in the simplest terms, such as to divide the total pilot behavior into temporal phases, each having a different system organization. As an elementary example, consider the typical system step response shown in Fig. 43. In the first or time delay phase, nothing happens. This is followed by a rapid response phase and finally by a more or less oscillatory error reduction phase. The feedforward element provides the major component of the pilot's output, c, during the rapid response phase. The quasi-linear steady-state model is predominant in the error reduction phase (and in general during the time delay phase if the system is continuously excited by random disturbances or inputs other than the step assumed here).

The output of the feedforward element for a skilled pilot is peculiar to each controlled element form. Some appreciation for this variation with controlled element dynamics can be gained from the responses shown in Fig. 44. These are sample large maneuver responses to step commands for effective controlled elements given by K_c, K_c/s, K_c/s^2, and K_c/s^3, proceeding from left to right, respectively. The most important aspect immediately apparent from these data is the pulse-like bang-bang nature of the stick deflection control movements. In fact, the pilot's control, c, is a remarkably good approximation to the controller properties of the nth order (n = 0 to 3), single-input, single-output, time-optimal control system with $|c(t)| \leq M$. Here, the scaler, M, may represent either a physical limit on the stick deflection or, more likely in the piloted case, an implicit restraint imposed by the pilot for the given situation. Ideal time-optimal traces for comparison with the actual piloted conditions are shown in Fig. 45.

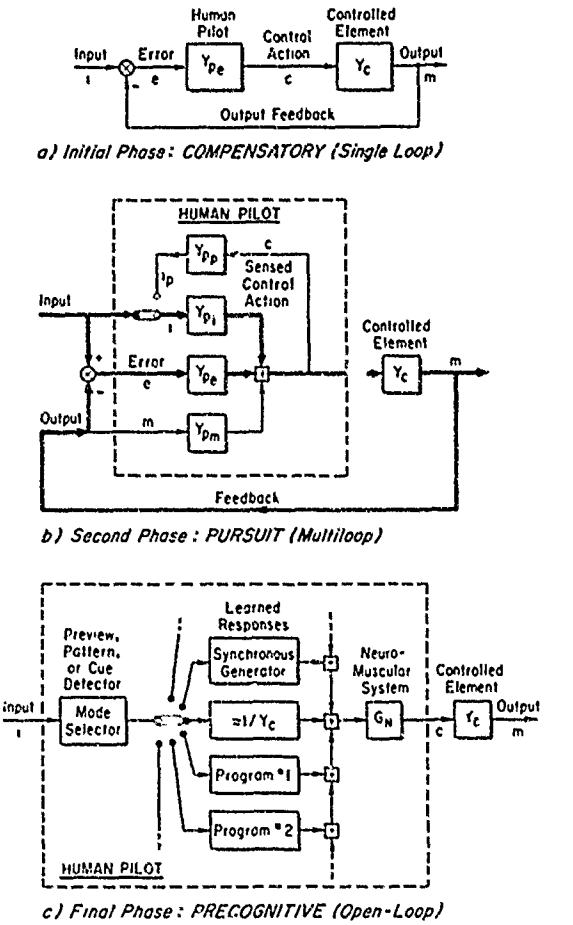

a) Initial Phase: COMPENSATORY (Single Loop)

b) Second Phase: PURSUIT (Multiloop)

c) Final Phase: PRECOGNITIVE (Open-Loop)

Figure 41. The Three Main Phases in the Successive Organization of Perception (SOP)

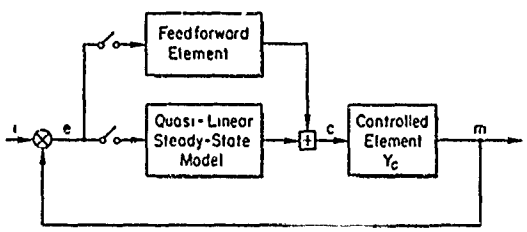

Figure 42. Structure of the Dual-Mode Model

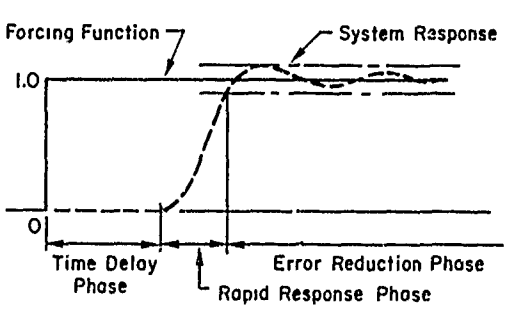

Figure 43. Typical System Step Response

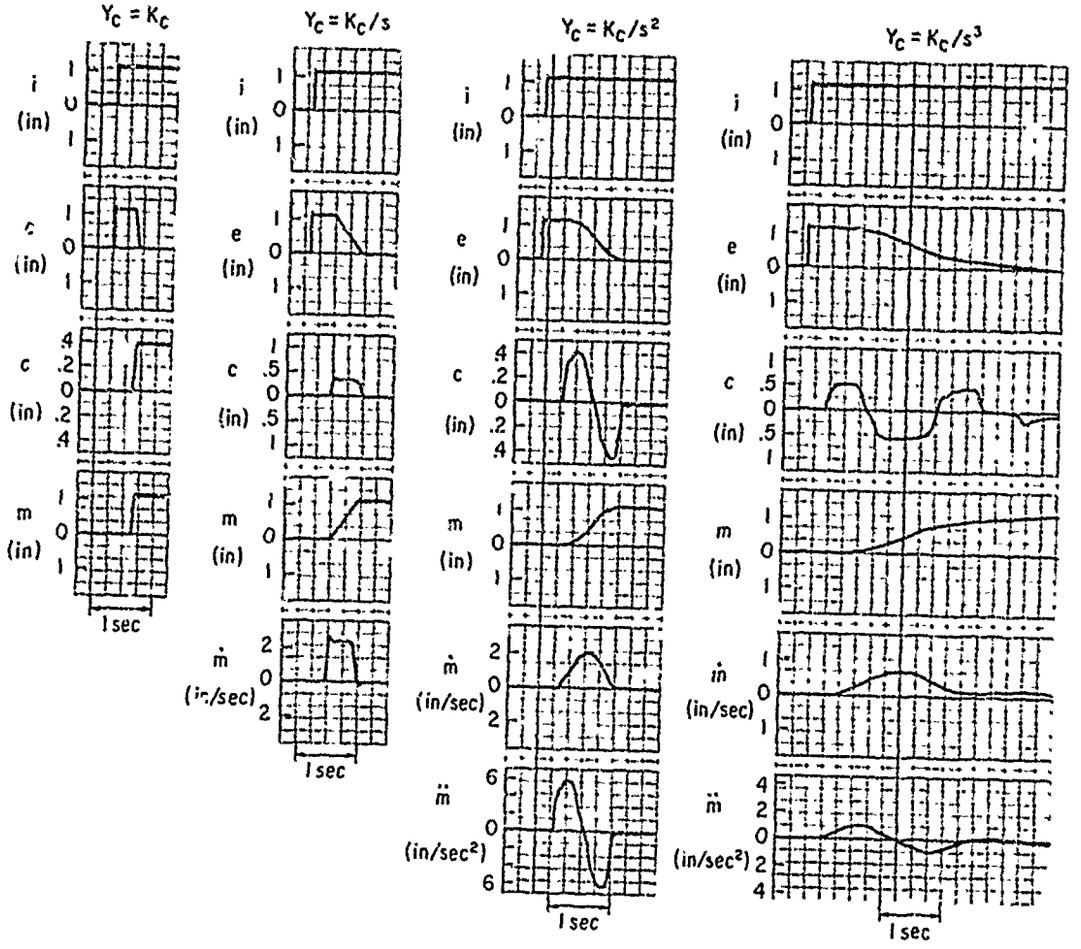

Figure 44. Sample Large Maneuver Response Data for Several Idealized Controlled Elements

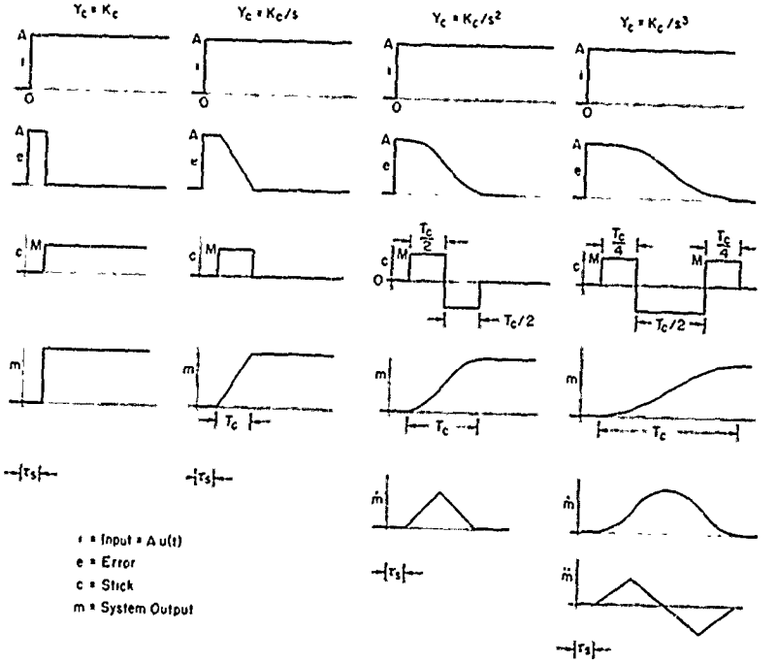

Figure 45. Ideal Time-Optimal Response Characteristics

A dual-mode pilot maneuvering model which serves to explain all the available data is presented in Fig. 46. The nonlinear error sensing blocks automatically route the error signal through the appropriate channel based upon whether the error is greater or less than some threshold magnitude of error, e_T. The control logic for each different controlled element and as a function of the error state, $\underline{e}[e = col\ (e, \dot{e}, \ldots)]$, is given in Table 13 for time-optimal response. Note that M, the constraint on the control input, is some function of the step input height, controlled element gain, and its order. The decision logic model behaves like a function switch (FSW) and accounts for the initial increase in the time delay (beyond that due to quasi-linear tracking) in response to a step input.

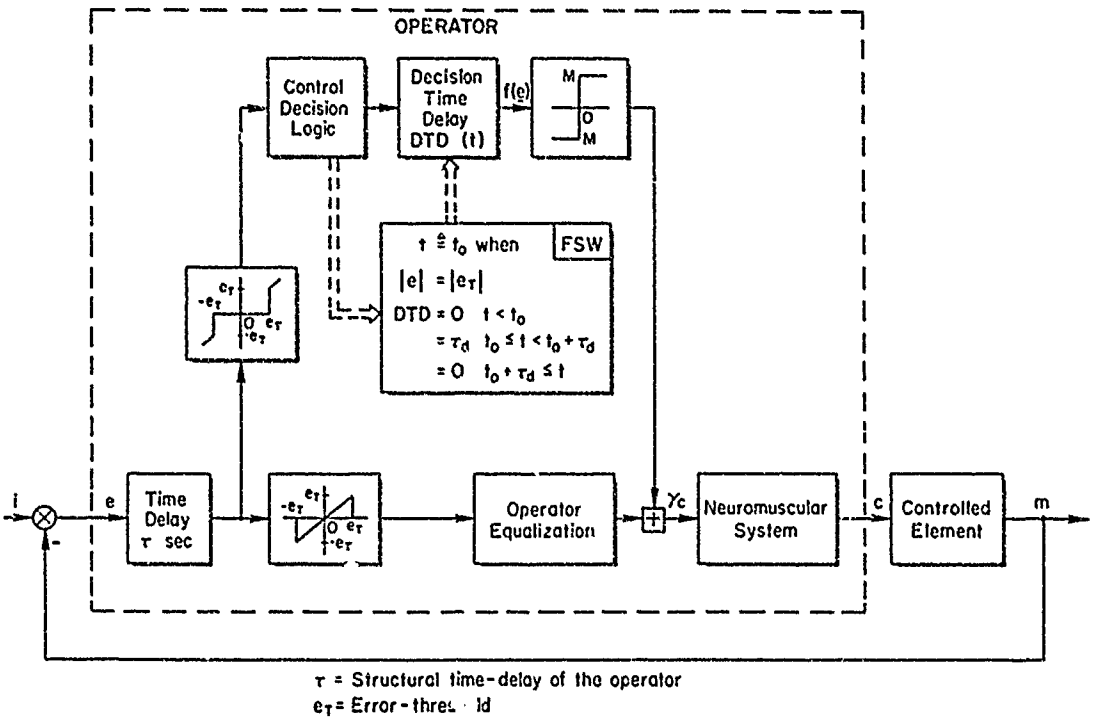

Figure 46. Dual-Mode Controller Model

TABLE 13

CONTROL LOGIC FOR VARIOUS CONTROLLED ELEMENTS

CONTROLLED ELEMENT Y_c	CONTROL LOGIC $f(\underline{e})$
K_c	$(A/MK_c)e(t)$
K_c/s	$e(v)$
K_c/s^2	$\dot{e} + \sqrt{2MK_c\lvert e\rvert}\ \text{sgn}\ e$
K_c/s^3	$e + (1/3)\dddot{e}^2 + W\ddot{e}\dddot{e} + W[(1/2)\ddot{e}^2 + W\dot{e}]^{3/2}$ $W = +1$ for $[\dot{e} + (1/2)\ddot{e}\lvert\ddot{e}\rvert] > 0$ $= -1$ for $[\dot{e} + (1/2)\ddot{e}\lvert\ddot{e}\rvert] < 0$ (Ref. 74)

This same model is appropriate when the step function or other transient input is initiated "inside" the pilot. In this instance, of course, the internal stimulus is indiscernible; only the response after any time delay can be seen. Yet the skilled pilot's output in programmed maneuvers exhibits at least the timing of this dual-mode, quasi-time-optimal character.

The decision time delay called out in Fig. 46 includes the decision interval during which the pilot determines the parameters of his preprogrammed response. This interval may contain wild fluctuations under conditions of suddenly failing dampers, autopilots, or other controlled element transitions. An extensive review of findings under such circumstances has been carried out (Ref. 130). Simple transitions, such as ± changes in gain for $Y_c = K_c$ are detected, and an appropriate response begun within about 0.5 sec

and the error stabilized at its pretransition value in about 1 sec. For transitions from $Y_c = K_c$ to $Y_c = K_c/s^2$, detection and correction occur within about 1 sec, but there may be an extensive period devoted to compensating for the dynamics of the new controlled element. Oscillations from 6-20 sec are not uncommon. These examples serve to leave the reader with a caveat about the desirability of operating at the highest level of skill when controlling an unstable plant. The pilot should monitor his control with Y_{pe} at periods such that any potentially disastrous divergences can be apprehended and controlled. This imposes a practical limit on the duration that the open-loop mode in Fig. 41c can be maintained.

CHAPTER VII

BRIEF REVIEW OF PILOT MODEL APPLICATIONS

Since its first tentative and rudimentary applications in the early 1950s, the use of pilot models in pilot/vehicle system analysis has grown exponentially to the point where it is now commonly applied to consider a very wide range of problems. Some appreciation of the scope of application efforts is revealed in the bibliography which constitutes the second half of this chapter. There, the applications are classified under five headings:

1. Pilot/aircraft system single- and multi-loop regulation and control.
2. Pilot/space-vehicle regulation and control.
3. Limits of piloted control.
4. Instabilities of pilot/aircraft systems.
5. Flight control system display design.

This classification selection resulted in a minimum number of repetitive entries, although a few still exist. To make the bibliography as comprehensive as possible for the benefit of specialists, the references presented are ordinarily the original documents. These, more often than not, are limited distribution but usually available government or company reports. For some of the entries condensed versions in the form of archival journal articles are available.

The analytical techniques used to exercise existing pilot models in these applications can be classified under three headings. These are:

1. Conventional Flight Control System Analysis — The vast majority of application results have been accomplished using conventional feedback system analysis techniques as specialized for aircraft flight control purposes. The techniques and procedures used include conventional Bode and root locus analysis, coupled with Bode root loci, pole-zero sensitivity, and multiloop analysis procedures lumped under the general heading of Unified Servo Analysis Methods (USAM). A comprehensive summary of these techniques with many application examples for automatic control systems is provided in Ref. 102. With these methods pilot/vehicle analysis is accomplished by substituting pilot models wherever controller properties are required and taking into account pilot ratings as well as dynamic and system performance characteristics.

2. Parameter Optimization Techniques — In these procedures, the form of the pilot model is assumed a priori, hopefully to one pertinent to the control tasks being considered (e.g., by use of the pilot model forms of Chapters IV and V adjusted appropriate to the controlled elements of interest). The pilot parameters are then adjusted via a parameter optimization scheme to minimize some performance index. In some cases this performance index can be pilot rating itself with the criterion then being to adjust pilot parameters such that pilot rating is minimized (Refs. 96-100).

3. Quadratic Optimal Control — In these formulations, conventional optimal control theory is modified to permit a pure time delay and observation noise (remnant) to be given quantities along with the plant characteristics. A "reasonable" performance criterion is selected for minimization, and the results of computer-based optimization procedures are the closed-loop dynamics and system performance (Refs. 131-135).

Each of these approaches has a common basis in the experimental data and mathematical pilot models described in previous chapters, although the basic information about the models may be applied in quite different forms. Among the cognoscenti there are proponents of each approach, but the authors' view is that of the middleman, i.e., all have merit and tend to supplement each other rather than compete. In fact, all three procedures share in the most significant single statement that can be made about the rise of pilot/vehicle analysis, that it has been established as a fundamental mode of thinking on the part of technical practitioners in the fields of aircraft flying qualities, pilot/vehicle control system integration, display synthesis, and associated fields.

Although the bibliography titles alone give a cross section of applications, these may not be as readily appreciated as a more direct statement of pilot/vehicle system problems which have been addressed using mathematical models. To illustrate applications in these ways, we have divided the problems into three categories for convenience, and have presented them in outline form in Tables 14-16 (Ref. 138).

1. Flight Test Problems (Table 14). The first category is also the smallest because it lists problems initially encountered far down the line in an aircraft development, i.e., in the flight test phase. In all of these cases the application of the pilot/vehicle analysis procedures led to a delineation of the cause of the troubles and further application of the procedure led to solutions.

2. Design Problems (Table 15). By far the most widespread use of any good predictive technique is in the design phase. Here, specific instances are too numerous to list, so more general classifications are used in Table 15.

3. Simulation Problems (Table 16). In simulation experiments the theory is ideal for program planning before the experiment, and data interpretation and generalization afterwards. Like all good theories it has the supreme attribute of focusing the experimental effort on critical issues. And again, like all good theories, it has the characteristic which permits the fitting of experimental data into a broader, more general, context. These generalizations not only describe the use of pilot mathematical models in simulation problems but also serve as a suitable windup for the entire discussion.

TABLE 14

SOME PAST APPLICATIONS OF PILOT-VEHICLE SYSTEM ANALYSES
FLIGHT ENCOUNTERED PROBLEMS

SITUATION	CONTROL PROBLEM	CAUSES
Pilot-Induced Oscillations	Pitch (Single Loop) Roll (Single Loop)	Sensitivity; Bobweight/Feel Spring; Loss of Pilot Lag, Elevator Rate Limiting ω_ϕ/ω_d Effect; Lateral Bobweight
Weapon Delivery	Heading Aim Wander (3 loops)	Loss of Roll Loop; Lateral-Directional Multiloop Cross Coupling
Carrier Landing	Path Control-Inability to arrest Rate of Sink (2 and 3 loops)	Dynamic Reversal in Path
Attitude Control	Pitch (Single Loop)	Improper Pilot / Stability Augmenter Matching

TABLE 15

PILOT-VEHICLE-DISPLAY SYSTEM ANALYSES:
DESIGN

SITUATION	ANALYSIS RESULTS
Basic Airframe and Primary Control System	Predict multiple, closed-loop pilot-vehicle system problem areas and assess possible solutions
Pilot / Stability Augmentation Tradeoffs	Candidate stability augmentation systems, pilot behavior and workload, system performance and compromises, reliability, redundancy, etc
SAS Failure Effects	Pilot actions and resulting aircraft excursions
Competing Pilot Display Formats Manual Control AFCS Monitoring	Information requirements, scan patterns, workload, assessment factors and criteria
Flight Director	Command display laws, status information requirements, flight director/pilot/stability augmentation tradeoffs
Carrier Landing Aids	Optimum FLOLS control and stabilization
Categories II and III Landing System	Probability of approach success, decision "state windows", touchdown statistics, manual/automatic tradeoffs, guidance sampling
Energy-Trim Management	Simplified controls/displays

TABLE 16

SOME PAST APPLICATIONS OF
PILOT-VEHICLE-DISPLAY SYSTEM ANALYSIS:
SIMULATION

SITUATION	ANALYSIS RESULTS
Pre-Experimental Analysis	Predict critical areas and parameters, guidance for experimental design, pilot briefing, questionnaire
Post-Experimental Analysis	Interpretation and generalization of results
Competing Piloting Techniques	Pilot control procedures, system performance and safety margin differences. Control system refinements to simplify piloting technique
Motion-Cue Simulation	Task-dependent motion sensitivity, optimum washout design

BIBLIOGRAPHY OF APPLICATIONS OF PILOT/VEHICLE CONTROL THEORY

1. Pilot/Aircraft System Single- and Multi-Loop Regulation and Control

Northrop Aircraft, Inc., Artificial Feel System, BuAer Rept. AE-61-4, Vol. V, May 1953.

Decker, J. L., "The Human Pilot and the High-Speed Airplane," J. Aeron. Sci., Vol. 23, No. 8, Aug. 1956, pp. 765-770.

Hall, I. A. M., Effects of Controlled Element on the Human Pilot, WADC-TR-57-509, Aug. 1958.

Sadoff, M., The Effects of Longitudinal Control-System Dynamics on Pilot Opinion and Response Characteristics as Determined from Flight Tests and from Ground Simulator Studies, NASA Memo 10-1-58A, Oct. 1958.

Ashkenas, I. L., and D. T. McRuer, The Determination of Lateral Handling Quality Requirements from Airframe/Human-Pilot System Studies, WADC-TR-59-135, June 1959.

McRuer, D. T., I. L. Ashkenas, and C. L. Guerre, A Systems Analysis View of Longitudinal Flying Qualities, WADD-TR-60-43, Jan. 1960.

Jex, H. R., and C. H. Cromwell, Theoretical and Experimental Investigation of Some New Longitudinal Handling Quality Parameters, ASD-TR-61-26, Mar. 1961.

Frost, G. G., An Application of a Dynamic Pilot-Model to System Design, ASD-TN-61-57, Apr. 1961.

Ashkenas, I. L., and D. T. McRuer, "A Theory of Handling Qualities Derived from Pilot-Vehicle System Considerations," Aerospace Eng., Vol. 21, No. 2, Feb. 1962, pp. 60, 61, 83-102.

Caporali, R. L., J. P. Lamers, and J. R. Totten, A Study of Pilot Induced Lateral-Directional Instabilities, Princeton, N. J., Princeton Univ., Aeronautical Engineering Dept., Rept. 604, May 1962.

Cromwell, C. H., and I. L. Ashkenas, A Systems Analysis of Longitudinal Piloted Control in Carrier Approach, Systems Technology, Inc., Tech. Rept. 124-1, June 1962.

Durand, T. S., and H. R. Jex, Handling Qualities in Single-Loop Roll Tracking Tasks: Theory and Simulator Experiments, ASD-TDR-62-507, Nov. 1962.

Sadoff, M., A Study of a Pilot's Ability to Control During Simulated Stability Augmentation System Failures, NASA TN D-1552, Nov. 1962.

Hall, I. A. M., "Study of the Human Pilot as a Servo-Element," J. Royal Aeron. Soc., Vol. 67, No. 630, June 1963, pp. 351-360.

Lollar, T. E., A Rationale for the Determination of Certain VTOL Handling Qualities Criteria, AGARD Rept. 471, July 1963.

Ashkenas, I. L., and T. S. Durand, "Simulator and Analytical Studies of Fundamental Longitudinal Control Problems in Carrier Approach," AIAA Simulation for Aerospace Flight Conf., Aug. 1963, pp. 16-34.

Durand, T. S., and G. L. Teper, An Analysis of Terminal Flight Path Control in Carrier Landing, Systems Technology, Inc., Tech. Rept. 137-1, Aug. 1964.

Durand, T. S., Theory and Simulation of Piloted Longitudinal Control in Carrier Approach, Systems Technology, Inc., Tech. Rept. 130-1, Mar. 1965.

Stapleford, R. L., J. Wolkovitch, R. E. Magdaleno, C. P. Shortwell, and W. A. Johnson, An Analytical Study of V/STOL Handling Qualities in Hover and Transition, AFFDL-TR-65-73, May 1965.

Stapleford, R. L., D. E. Johnston, G. L. Teper, and D. H. Weir, Development of Satisfactory Lateral-Directional Handling Qualities in the Landing Approach, NASA CR-239, July 1965.

Gould, D. G., Results of Recent Investigations of V/STOL Control and Response Requirements Using Variable Stability Helicopters, National Research Council of Canada, Aero Rept. LR-434, Sept. 1965.

Ashkenas, I. L., A Study of Conventional Airplane Handling Qualities Requirements. Part I: Roll Handling Qualities. Part II: Lateral-Directional Oscillatory Handling Qualities, AFFDL-TR-65-138, Oct. 1965.

Schweizer, G., Pilot Behavior in VTOL Aircraft, AGARD Rept. 521, Oct. 1965.

Wolkovitch, J., and D. E. Johnston, Automatic Control Considerations for Helicopters and VTOL Aircraft With and Without Sling Loads, Systems Technology, Inc., Tech. Rept. 138-1, Nov. 1965.

Gallagher, J. T., and F. B. O'Donnell, "Investigation of the Application of Direct Translational Control to VTOL Aircraft," J. Aircraft, Vol. 2, No. 6, Nov.-Dec. 1965, pp. 538-545.

Smith, R. H., "VTOL Control Power Requirements Reappraised," J. Aircraft, Vol. 3, No. 1, Jan.-Feb. 1966, pp. 11-17.

Ashkenas, I. L., Some Open- and Closed-Loop Aspects of Airplane Lateral-Directional Handling Qualities, AGARD Rept. 533, May 1966.

Peters, R. A., and F. R. Alex, Pilot Relief Mode Synthesis for a Helicopter During Terrain-Following, Systems Technology, Inc., Tech. Rept. 153-1, Aug. 1966.

Wasicko, R. J., Application of Approach Speed Criteria Derived from Closed-Loop Pilot-Vehicle Systems Analysis to an Ogee Wing Aircraft, NASA CR-579, Oct. 1966.

Durand, T. S., Carrier Landing Analyses, Systems Technology, Inc., Tech. Rept. 137-2, Feb. 1967.

Vinje, E. W., and D. P. Miller, Interpretation of Pilot Opinion by Application of Multiloop Models to a VTOL Flight Simulator Task, United Aircraft Research Labs., Rept. UAR-F20, Mar. 1967.

Stapleford, R. L., and I. L. Ashkenas, "Longitudinal Short-Period Handling Quality Requirements," and "Altitude Control During Approach and Other Topics," Analysis of Several Handling Quality Topics Pertinent to Advanced Manned Aircraft, AFFDL-TR-67-2, Sections IV and V, June 1967.

Seckel, E., H. Breul, T. Keller, et al., A Study of the Mechanics of Human Balancing for Potential Application to the Control of Vehicles. Part II: Toward a Mathematical Model of Vertical Balancing in Earth Gravity, Grumman Aircraft Engineering Corp., Research Dept. Rept. RM-369, July 1967.

Walton, R. P., and I. L. Ashkenas, Analytical Review of Military Helicopter Flying Qualities, Systems Technology, Inc., Tech. Rept. 143-1, Aug. 1967.

Roberts, L. D., Analysis of Helicopter Control in Landing Approach, Princeton Univ., Aerospace and Mechanical Sciences Dept., Master's Thesis, Dec. 1967.

Miller, D. P., and E. W. Vinje, Fixed-Base Flight Simulator Studies of VTOL Aircraft Handling Qualities in Hovering and Low Speed Flight, AFFDL-TR-67-152, Jan. 1968.

Bergeron, H. P., J. J. Adams, and G. J. Hurt, Jr., Analysis of Human Response in Combined Control Tasks, NASA TN D-4356, Mar. 1968.

DiCarlo, D. J., J. R. Kelley, and R. W. Sommer, Flight Investigation to Determine the Effect of Longitudinal Characteristics on Low-Speed Instrument Operations, NASA TN D-4364, Mar. 1968.

McRuer, D. T., H. R. Jex, W. F. Clement, and D. Graham, A Systems Analysis Theory for Displays in Manual Control, Systems Technology, Inc., Tech. Rept. 163-1, June 1968.

Weir, D. H., and W. A. Johnson, Pilot Dynamic Response to Sudden Flight Control System Failures and Implications for Design, NASA CR-1087, June 1968.

Lollar, T. E., and G. K. L. Kriechbaum, "VTOL Handling Qualities Criteria and Control Requirements — Analysis and Experiment," J. American Helicopter Soc., Vol. 13, No. 3, July 1968, pp. 20-29.

Frohlich, H., W. Kreil, G. Schweizer, and K. Stopfkuchen, New Techniques in Investigating Handling Qualities, NASA TT F-11,844, July 1968.

Adams, J. J., and H. P. Bergeron, A Synthesis of Human Response in Closed-Loop Tracking Tasks, NASA TN D-4842, Oct. 1968.

Craig, S. J., and A. Campbell, Analysis of VTOL Handling Qualities Requirements. Part I: Longitudinal Hover and Transition, AFFDL-TR-67-179, Part I, Oct. 1968.

Clement, W. F., H. R. Jex, and D. Graham, "A Manual Control Display Theory Applied to Instrument Landing of a Jet Transport," IEEE Trans., Vol. MMS-9, No. 4, Dec. 1968, pp. 93-110.

Vinje, E. W., "An Analysis of Pilot Adaptation in a Simulated Multiloop VTOL Hovering Task," IEEE Trans., Vol. MMS-9, No. 4, Dec. 1968, pp. 110-120.

Vinje, E. W., and D. P. Miller, Analytical and Flight Simulator Studies to Develop Design Criteria for VTOL Aircraft Control Systems, AFFDL-TR-68-165, Apr. 1969.

Johnston, D. E., R. L. Stapleford, G. L. Teper, and G. Chuck, Investigation of Improved Weapon Delivery by Means of Aircraft Handling Modifications, Systems Technology, Inc., Tech. Rept. 173-1, Apr. 1969.

Clement, W. F., and L. G. Hofmann, A Systems Analysis of Manual Control Techniques and Display Arrangements for Instrument Landing Approaches in Helicopters. Vol. I: Speed and Height Regulation, Systems Technology, Inc., Tech. Rept. 183-1, July 1969 (also JANAIR Rept. 690718).

Teper, G. L., I. L. Ashkenas, A. Campbell, and T. S. Durand, Carrier Landing Performance; An Analysis of Flight Tests Under Simulated Pitching Deck Conditions, Systems Technology, Inc., Tech. Rept. 137-4, Oct. 1969.

Adams, J. J., and M. W. Goode, Application of Human Transfer Functions to System Analysis, NASA TN D-5478, Oct. 1969.

Craig, S. J., A. Campbell, and R. H. Klein, Analysis of VTOL Handling Qualities Requirements. Part II: Lateral-Directional Hover and Transition, AFFDL-TR-67-179, Feb. 1970.

Anderson, R. O., A New Approach to the Specification and Evaluation of Flying Qualities, AFFDL-TR-69-120, June 1970.

Craig, S. J., and I. L. Ashkenas, Background Data and Recommended Revisions for MIL-F-8785B(ASG), "Military Specification — Flying Qualities of Piloted Airplanes", Systems Technology, Inc., Tech. Rept. 189-1, June 1970.

Drake, D. E., R. A. Berg, G. L. Teper, and W. A. Shirley, A Flight Simulator Study of STOL Transport Lateral Control Characteristics, FAA-RD-70-61, Sept. 1970.

Neal, T. P., and R. E. Smith, An In-Flight Investigation to Develop Control System Design Criteria for Fighter Airplanes, AFFDL-TR-70-74, Dec. 1970.

Adams, J. J., and H. G. Hatch, Jr., An Approach to the Determination of Aircraft Handling Qualities by Using Pilot Transfer Functions, NASA TN D-6104, Jan. 1971.

Anderson, R. O., A. J. Connors, and J. D. Dillow, Paper Pilot Ponders Pitch, AFFDL/FGC-TM-70-1, Jan. 1971.

Graham, D., W. F. Clement, and L. G. Hofmann, Investigation of Measuring System Requirements for Instrument Low Visibility Approach, AFFDL-TR-70-102, Feb. 1971.

Onstott, E. D., and E. P. Salmon, Airplane Flying Characteristics in Turbulence, AFFDL-TR-70-143, Feb. 1971.

Dillow, J. D., The "Paper Pilot" — A Digital Computer Program to Predict Pilot Rating for the Hover Task, AFFDL-TR-70-40, Mar. 1971.

Craig, S. J., R. F. Ringland, and I. L. Ashkenas, An Analysis of Navy Approach Power Compensator Problems and Requirements, Systems Technology, Inc., Tech. Rept. 197-1, Mar. 1971.

Franklin, J. A., Turbulence and Lateral-Directional Flying Qualities, NASA CR-1718, Apr. 1971.

Ashkenas, I. L., "Summary and Interpretation of Recent Longitudinal Flying Qualities Results," J. Aircraft, Vol. 8, No. 5, May 1971, pp. 324-328.

Berg, R. A., W. A. Shirley, G. L. Teper, and S. J. Craig, A Flight Simulator Study of STOL Transport Directional Control Characteristics, FAA-RD-71-81, June 1971.

Hollis, T. L., Optimal Selection of Stability Augmentation System Parameters to Reduce the Pilot Ratings for the Pitch Tracking Task, AF Institute of Technology, AFIT GGC/EE/71-10, June 1971.

Franklin, J. A., Turbulence and Longitudinal Flying Qualities, NASA CR-1821, July 1971.

Hofmann, L. G., K. V. Shah, and D. Graham, Analysis of Limited Authority Manual Control Systems, AFFDL-TR-71-6, July 1971.

Miller, G. E., and R. L. Traskos, Flight Evaluation of Engine Response, Flight Path Stability, Tail Lift, and Direct Lift Control, Princeton Univ., Aerospace and Mechanical Sciences Dept., Rept. 888, Aug. 1971.

Stapleford, R. L., D. T. McRuer, R. H. Hoh, D. E. Johnston, and R. K. Heffley, Outsmarting MIL-F-8785B(ASG), The Military Flying Qualities Specification, Systems Technology, Inc., Tech. Rept. 190-1, Aug. 1971.

Dillow, J. D., "Super Pilot" — A Revised Version of Paper Pilot, AFFDL/FGC-TM-71-9, Oct. 1971.

Kleinman, D. L., and S. Baron, Analytic Evaluation of Display Requirements for Approach to Landing, NASA CR-1952, Oct. 1971.

Ringland, R. F., R. L. Stapleford, and R. E. Magdaleno, Motion Effects on an IFR Hovering Task — Analytical Predictions and Experimental Results, NASA CR-1933, Nov. 1971.

Hofmann, L. G., W. F. Clement, D. Graham, et al., Investigation of Measuring System Requirements for Low Visibility Landing, AFFDL-TR-71-151, Dec. 1971.

Levison, W. H., and D. L. Kleinman, Analysis of Pilot/System Performance in Carrier Approach, Naval Air Development Center, NADC-CS-7132, 30 Dec. 1971.

Baron, S., and D. L. Kleinman, "Prediction and Analysis of Human Performance in a VTOL Hover Task," 7th Annual Conf. on Manual Control, Washington, D. C., NASA SP-281, 1972, pp. 247-256.

Onstott, E. D., E. P. Salmon, and R. L. McCormick, Prediction and Evaluation of Flying Qualities in Turbulence, AFFDL-TR-71-162, Feb. 1972.

Giles, R. F., "An Analytical Investigation of Short-Period Flying Qualities," J. Aircraft, Vol. 9, No. 2, Feb. 1972, pp. 103-107.

Chen, R. T. N., A Preliminary Analysis on the Pilot-STOL Aircraft System in Landing Approach, Cornell Aeronautical Laboratory, Inc., Flight Research Dept., Rept. VTOL H.Q. TM-30, 11 Feb. 1972.

Leondes, C. T., and R. R. Rankine, Jr., "Modeling the Effects of Pilot Performance on Weapon Delivery Accuracy," J. Aircraft, Vol. 9, No. 4, Apr. 1972, pp. 286-293.

Teper, G. L., An Assessment of the "Paper Pilot" — An Analytical Approach to the Specification and Evaluation of Flying Qualities, AFFDL-TR-71-174, June 1972.

Craig, S. J., I. L. Ashkenas, and R. K. Heffley, Pilot Background and Vehicle Parameters Governing Control Techniques in STOL Approach Situations, FAA-RD-72-69, June 1972.

Ashkenas, I. L., and S. J. Craig, Multiloop Piloting Aspects of Longitudinal Approach Path Control, New York, International Council of the Aeronautical Sciences, ICAS Paper No. 72-46, Aug. 1972.

Naylor, F. R., Predicting Roll Task Flying Qualities with "Paper Pilot", AF Institute of Technology, AFIT GAM/MA/73-1, Sept. 1972.

Denaro, R. P., and G. L. Greenleaf, Selection of Optimal Stability Augmentation System Parameters for a High Performance Aircraft Using Pitch Paper Pilot, AF Institute of Technology, AFIT GGC/EE/73-3, Oct. 1972.

Hollis, T. L., R. A. Hannen, and J. D. Dillow, "The Sensuous SAS by Paper Pilot," Proc. of the 8th Annual Conf. on Manual Control, Wright-Patterson AFB, Ohio, AFFDL-TR-72-92, 1973, pp. 413-429.

Gerken, G. J., F. E. Unfried, J. A. Johnson, et al., A Piloted Power Approach Simulation, Vols. I and II, AFFDL-TR-73-27, Vols. I and II, Mar. 1973.

Arnold, J. D., An Improved Method of Predicting Longitudinal Handling Qualities Based on the "Minimum Rating Concept" (Draft), AF Institute of Technology, AFIT GGC/MA/73-1, June 1973.

Ashkenas, I. L., R. H. Hoh, and S. J. Craig, Recommended Revisions to Selected Portions of MIL-F-8785B(ASG) and Background Data, AFFDL-TR-73-76 (forthcoming).

2. Pilot/Space-Vehicle Regulation and Control

Stapleford, R. L., and H. R. Jex, A Study of Manual and Automatic Systems for the Terminal Phase of Orbital Rendezvous, ASD-TDR-62-82, June 1962.

Muckler, F. A., and R. W. Obermayer, The Use of Man in Booster Guidance and Control, NASA CR-81, July 1964.

Young, L. R., and J. L. Meiry, "Manual Control of an Unstable System with Visual and Motion Cues," IEEE International Convention Record, Vol. 13, Pt. 6, 1965, pp. 123-127.

Kilpatrick, P. S., Bending Mode Acceleration Influence on Pilot Control of Flexible Booster Dynamics, MIT Man-Vehicle Control Laboratory, Rept. T-65-2, Sept. 1965.

Jex, H. R., G. L. Teper, D. T. McRuer, and W. A. Johnson, A Study of Fully-Manual and Augmented-Manual Control System for the Saturn V Booster Using Analytical Pilot Models, NASA CR-1079, July 1968.

Denery, D. G., and B. Y. Creer, Evaluation of a Pilot Describing Function Method Applied to the Manual Control Analysis of a Large Flexible Booster, NASA TN D-5199, Apr. 1969.

Stapleford, R. L., R. H. Klein, and R. H. Hoh, Handling Qualities Criteria for the Space Shuttle Orbiter During the Terminal Phase of Flight, NASA CR-2017, Apr. 1972.

3. Limits of Piloted Control

Creatham, D. C., A Study of the Characteristics of Human-Pilot Control Response to Simulated Aircraft Lateral Motions, NACA Rept. 1197, 1954.

McRuer, D. T., I. L. Ashkenas, and C. L. Guerre, A Systems Analysis View of Longitudinal Flying Qualities, WADD-TR-60-43, Jan. 1960.

Jex, H. R., C. H. Cromwell III, and R. K. Siskind, Correlation of Experimental and Theoretical Limits for Pilot Control of Unstable Second-Order Systems, Systems Technology, Inc., TM-56, July 1960.

Taylor, W., Jr., and R. E. Day, Flight Controllability Limits and Related Human Transfer Functions as Determined from Simulator and Flight Tests, NASA TN D-746, May 1961.

Jex, H. R., and C. H. Cromwell III, Theoretical and Experimental Investigation of Some New Longitudinal Handling Quality Parameters, ASD-TR-61-26, Mar. 1961.

Kohlhaas, R. L., Limits of Pilot Controllability of a Two-Axis Unstable, Second-Order System, AF Institute of Technology, Master's Thesis, Mar. 1962.

Smith, R. H., "On the Limits of Manual Control," IEEE Trans., Vol. HFE-4, No. 1, Sept. 1963, pp. 56-59.

Washizu, K., and K. Miyajima, "Controllability Limit of a Human Pilot," AIAA J., Vol. 3, No. 5, May 1965, pp. 941-947.

Smith, R. H., "Comment on 'Controllability Limit of a Human Pilot'," AIAA J., Vol. 3, No. 10, Oct. 1965, pp. 1980-1981.

Washizu, K., and K. Miyajima, "Reply by Authors to R. H. Smith," AIAA J., Vol. 3, No. 10, Oct. 1965, p. 1981.

Adams, J. J., K. Kincaid, and H. P. Bergeron, Determination of Critical Tracking Tasks for a Human Pilot, NASA TN D-3242, Feb. 1966.

Jex, H. R., J. D. McDonnell, and A. V. Phatak, A "Critical" Tracking Task for Man-Machine Research Related to the Operator's Effective Delay Time. Part I: Theory and Experiments with a First-Order Divergent Controlled Element, NASA CR-616, Oct. 1966.

McDonnell, J. D., and H. R. Jex, A Critical Task for Man-Machine Research Related to the Operator's Effective Time Delays. Part II: Experimental Effects of System Input Spectra, Control Stick Stiffness, and Controlled Element Order, NASA CR-674, Jan. 1967.

4. **Instabilities of Pilot/Aircraft Systems**

Terrill, W. H., L. R. Springer, and J. G. Wong, Investigation of Pilot-Induced Longitudinal Oscillation in the Douglas Model A4D-2 Airplane, Douglas Aircraft Co., Inc., Rept. LB-25452, May 1957.

Phillips, W. H., B. P. Brown, and J. T. Matthews, Jr., Review and Investigation of Unsatisfactory Control Characteristics Involving Instability of Pilot-Airplane Combination and Methods for Predicting These Difficulties from Ground Tests, NACA TN 4064, Aug. 1957.

Taylor, L. W., Jr., Analysis of a Pilot-Airplane Lateral Instability Experienced with the X-15 Airplane, NASA TN D-1059, Nov. 1961.

Ashkenas, I. L., H. R. Jex, and D. T. McRuer, Pilot-Induced Oscillations: Their Cause and Analysis, Northrop Corp., Norair Div., Rept. NOR 64-143, June 1964 (AD 481994).

Wolowicz, C. H., Analysis of an Emergency Deceleration and Descent of the XB-70-1 Airplane Due to Engine Damage Resulting from Structural Failure, NASA TM X-1195, Mar. 1966.

5. **Flight Control System Display Design**

Bliss, J. C., "Human Operator Describing Functions with Visual and Tactile Displays," 3rd Annual NASA-Univ. Conf. on Manual Control, Washington, D. C., NASA SP-144, 1967, pp. 67-79.

McRuer, D. T., H. R. Jex, W. F. Clement, and D. Graham, A Systems Analysis Theory for Displays in Manual Control, Systems Technology, Inc., Tech. Rept. 163-1, Oct. 1967 (revised June 1968).

Sower, W. A., and J. E. Wanamaker, Extension of Pilot Describing Functions to Multiple Compensatory Tracking Tasks, AF Institute of Technology, AFIT GE/EE/69-18, Mar. 1969.

Weir, D. H., and R. H. Klein, The Measurement and Analysis of Pilot Scanning and Control Behavior During Simulated Instrument Approaches, NASA CR-1535, June 1970.

Van Houtte, N. A. J., Display Instrumentation for V/STOL Aircraft in Landing, MIT Man-Vehicle Laboratory, Rept. MVT-70-2, June 1970.

Levison, W. H., The Effects of Display Gain and Signal Bandwidth on Human Controller Remnant, Bolt, Beranek and Newman, Inc., Rept. 1968, 15 Aug. 1970.

Weir, D. H., R. H. Klein, and D. T. McRuer, Principles for the Design of Advanced Flight Director Systems Based on the Theory of Manual Control Displays, NASA CR-1748, Mar. 1971.

Kleinman, D. L., and S. Baron, Manned Vehicle Systems Analysis by Means of Modern Control Theory, NASA CR-1753, June 1971.

Jex, H. R., R. W. Allen, and R. E. Magdaleno, Display Format Effects on Precision Tracking Performance, Describing Functions, and Remnant, Aerospace Medical Research Laboratory, AMRL-TR-71-63, Aug. 1971.

Clement, W. F., R. W. Allen, and D. Graham, Pilot Experiments for a Theory of Integrated Display Format, Systems Technology, Inc., Tech Rept. 183-2, Oct. 1971 (JANAIR Rept. 711107).

Vinje, E. W., and E. T. Pitkin, "Human Operator Dynamics for Aural Compensatory Tracking," 7th Annual Conf. on Manual Control, Washington, D. C., NASA SP-281, 1972, pp. 339-348.

Duning, K. E., C. W. Hickok, K. C. Emerson, and W. F. Clement, Control-Display Testing Requirements Study, AFFDL-TR-72-122, Dec. 1972.

Klein, R. H., and W. F. Clement, Application of Manual Control Display Theory to the Development of Flight Director Systems for STOL Aircraft, AFFDL-TR-72-152 (forthcoming).

CHAPTER VIII

CURRENT STATUS OF PILOT MODELING AND FURTHER REQUIREMENTS

In the foregoing chapters we have emphasized the application of quasi-linear models to a large and useful class of pilot control situations while also presenting appropriate time-dependent models for transient and mode-switching behavior.

As Chapter I indicates, quasi-linear models for human controller behavior trace their history to World War II. They have been questioned and criticized from their inception to the present. Yet they are still with us and continue to be applied effectively to a large variety of problems. Our previous chapters provide insight into why this is the case. Consider the assumptions upon which applications of the model rest:

- The forcing function is a stationary, random-appearing process.
- The time-averaged dynamic properties of the pilot are statistically stable.
- The controlled element characteristics are time-invariant.
- The quasi-linear operator portion of the model characterizes a usefully large portion of the pilot's behavior.
- Remnant, when accounted for as a pilot-induced noise, does not "hide" more fundamental phenomena which may be important in an overall pilot/vehicle system context.

The first and second assumptions require a minimum time duration of 5-10 sec for the generation of meaningful measurements and the correspondingly meaningful application of the model. This is readily realized in a very large number of practically useful cases. The third assumption is realized for the overwhelming majority of non-emergency conditions. Together these assumptions enable the calculation and use of the describing function for the quasi-linear model. It is the fourth and fifth assumptions which have been historic sources of criticism.

Early critics voiced the uneasy feeling that there was a lack of elegance or perhaps analytic power inherent in accepting a remnant term. The feeling prevailed that imposing the Procrustean bed of linearity, even though situation-specific, upon the pilot thwarted the exposition of interesting and uniquely human attributes. A criticism that could not be dealt with directly for many years suggested that more sophisticated and crafty model making could be expected to account for significant portions of the remnant by means of nonlinear operations. Chapters IV and V provide the basis for reducing this criticism to an ephemera. All the available data on the remnant make it clear that for single-loop systems it is dominantly due to random time variations of the parameters in the pilot's describing function and due to both this and visual scanning behavior for multiloop systems. The majority of the remnant is thus an irreducible stochastic variability characteristic of the pilot which depends on the four classes of variables influencing control task behavior. The remnant contributes to system error and can superpose small system oscillations, but it is the pilot's transfer characteristics which determine the system's basic dynamic stability and provide an estimate of what is usually the major component of the error signal. From our present understanding of the components of the quasi-linear model, its long history of applicability is not surprising; it should work and it does.

For most practical concerns related to pilot/vehicle system analysis, there are no further critical research issues for this model. It is in transition from the domain of research to that of routine applications. There are, however, issues relevant to our basic understanding of human control processes, in general, and second-order effects in quasi-linear control, which remain to be addressed:

- The short time (less than 5-10 sec) behavior of the pilot cannot be described adequately by constant-coefficient describing functions. Current indications from remnant data are that the pilot's characteristics derive from a mathematical time-varying operator containing the terms:

$$[K_{p_o} + \Delta K(t)]e^{-[\tau_o + \Delta\tau(t)]s}$$

  where ΔK and $\Delta\tau$ are random processes. The distributions which characterize these random processes are not well known, and their definition and dependence on environmental, pilot-centered, and procedural variables constitute areas for further research.

- The inputs sensed for VFR conditions are currently estimated on the basis of control needs (i.e., what feedback paths are necessary or desirable for the closed-loop system). The actual quantities perceived are likely to be linear combinations of these, with the weightings between the independent inputs fixed by the geometry and perspective rather than being independently adjustable by the pilot. These aspects of perception can have profound effects on the closed-loop analysis of various maneuvers (e.g., approach, landing, dive bombing, etc.). There is a need to refine our understanding of the actual real-world cues used under VFR conditions so that more precise estimates of pilot dynamics, scanning behavior, and performance can be made for VFR conditions and for integrated displays.

- The dependence of the quasi-linear feedback model in its steady-state form upon task variables is fairly complete. For specific applications there is a need for codification of the influence of environmental, pilot-centered, and procedural (ϵ, σ, and π) variables on the model.

- Scanning behavior has been applied with considerable success in some multiloop control configurations, but the data base and models are still in a relatively rudimentary state. More complete data in general is needed wherein control and scanning behavior is measured. Changes in scanning behavior and in the induced remnant as functions of ϵ, π, and σ and the potential work overload and destabilizing influences need examination.

- Possible crossfeed elements of the quasi-linear model are presently based more on inference than on directly applicable measurements. The potential importance of such elements to a complete modeling of probably rare but demanding, highly coupled multiloop situations, warrants the development of a better experimental base therefor.

- Pilot opinion ratings, despite their utility and record of validation in the past, exhibit an artistic quality in their development. The physical continuum underlying the ratings is multidimensional, and the component dimensions have weightings which depend upon the aircraft's mission. The engineering foundation for this activity requires strengthening.

- Although a battery of extremely promising techniques based on critical task concepts is presently available for assessing pilot workload as an excess control capacity, the interactions between workload and pilot skill progression have not been quantified. There exists anecdotal material about the minimum effort characteristic of high skill, but the conceivable tradeoffs between such things as effort extended in training and potential subsequent savings in piloting effort are as yet undefined.

- Mode switching in response to either abrupt Y_c changes or nonstationary forcing functions has been modeled on an ad hoc basis. Our understanding of the pilot's decision rules, switching criteria, and the mating of transient models with steady-state models is incomplete.

- Our knowledge of the duration of intermittent open-loop behavior in precognitive and near-precognitive conditions is sketchy. There are a variety of research questions in determining in useful detail the parameters of subjective predictability so that tendencies toward precognitive behavior may be either encouraged or discouraged, depending on the risks involved from potentially catastrophic transients.

ACKNOWLEDGMENT

Many colleagues at Systems Technology, Inc., have played key roles in the development of the authors' views about the models and concepts described by this report. The authors especially acknowledge the contributions of R. W. Allen, I. L. Ashkenas, W. F. Clement, D. Graham, H. R. Jex, R. E. Magdaleno, R. L. Stapleford, R. J. Wasicko, and D. H. Weir. The authors are also grateful to R. O. Anderson and H. R. Jex for their critical and helpful review of portions of the manuscript.

REFERENCES

1. Signal Corps Specification, No. 486, Advertisement and Specification for a Heavier-than-Air Flying Machine, Washington, D. C., 2[illegible] Dec. 1907.

2. McFarland, M. W., ed., The Papers of Wilbur and Orville Wright, Vol. I, New York, McGraw-Hill, 1953, pp. 90-100.

3. Koppen, O. C., "Airplane Stability and Control from a Designer's Point of View," J. Aeron. Sci., Vol. 7, No. [illegible], Feb. 1940, pp. 131-140.

4. Crowley, W. L., and S. W. Skan, A Simplified Analysis of the Stability of Aeroplanes, Aeronautical Research Committee R&M No. 1333, Mar. 1930.

5. Tustin, A., "The Effects of Backlash and of Speed-Dependent Friction on the Stability of Closed-Cycle Control Systems," J. IEE, Vol. 94, Part IIA, No. 1, May 1947.

6. Tustin, A., An Investigation of the Operator's Response in Manual Control of a Power Driven Gun, Metropolitan-Vickers Electrical Co., Ltd., Attercliffe Common Works, Sheffield, England, C.S. Memorandum No. 169, 22 Aug. 1944.

7. Tustin, A., "The Nature of the Operator's Response in Manual Control and Its Implications for Controller Design," J. IEE, Vol. 94, Part IIA, No. [illegible], 1947.

8. James, H. M., N. B. Nichols, and R. S. Philipps, Theory of Servomechanisms, New York, McGraw-Hill, 1947, pp. 360-369.

9. Weiss, H. K., Recommended Tracking Ratios for T36 Director, Memo to President Antiaircraft Artillery Board, Sept. 1943.

10. Weiss, H. K., Improvement of Tracking with Disturbed Reticle Sights, Memo to President Antiaircraft Board, Fort Bliss, Texas, 1945.

11. A Proposal to Study the Dynamic Characteristics of Man as Related to the Man-Aircraft System, Goodyear Aircraft Corp., Rept. No. GER-3006-A, 2 May 1950.

12. Human Dynamic Study, Goodyear Aircraft Corp., Rept. No. GER-[illegible]70, 8 Apr. 1952.

13. Investigation of Vestibular and Body Reactions to the Dynamic Response of a Human Operator, Final Report, BuAer Rept. AE-61-[illegible] and Goodyear Aircraft Corp., Rept. No. GER-5492, 25 Nov. 1953.

14. Investigation of Control "Feel" Effects on the Dynamics of a Piloted Aircraft System, Goodyear Aircraft Corp., Rept. No. GER-6726, 2[illegible] Apr. 195[illegible].

15. Krendel, E. S., and G. H. Barnes, Interim Report on Human Frequency Response Studies, WADC-TR-54-370, June 1954.

16. Seckel, E., I. A. M. Hall, D. T. McRuer, and D. H. Weir, Human Pilot Dynamic Response in Flight and Simulator, WADC-TR-57-520, Oct. 1957.

17. Hall, I. A. M., Effects of Controlled Element on the Human Pilot, WADC-TR-57-509, Aug. 1958.

18. Hall, I. A. M., "Study of the Human Pilot as a Servo-Element," J. Royal Aeron. Soc., Vol. 67, No. 630, June 1963, pp. 371-370.

19. McRuer, D. T., and E. S. Krendel, Dynamic Response of Human Operators, WADC-TR-56-524, Oct. 1957.

20. Russell, Lindsay, Characteristics of the Human as a Linear Servo-Element, Master's Thesis, MIT, Dept. of Elec. Engr., 18 May 1951.

21. Elkind, J. I., Characteristics of Simple Manual Control Systems, MIT, Lincoln Lab., TR-111, 6 Apr. 1956.

22. Second Annual NASA-University Conference on Manual Control, Washington, D.C., National Aeronautics and Space Administration, NASA SP-128, 1966.

23. Third Annual NASA-University Conference on Manual Control, Washington, D. C., National Aeronautics and Space Administration, NASA SP-144, 1967.

24. Fourth Annual NASA-University Conference on Manual Control, Washington, D. C., National Aeronautics and Space Administration, NASA SP-192, 1969.

25. Fifth Annual NASA-University Conference on Manual Control, Washington, D. C., National Aeronautics and Space Administration, NASA SP-215, 1970.

26. Proceedings of the Sixth Annual Conference on Manual Control, Wright-Patterson Air Force Base, Ohio, Air Force Institute of Technology/Air Force Flight Dynamics Laboratory, 1970.

27. Seventh Annual Conference on Manual Control, Washington, D. C., National Aeronautics and Space Administration, NASA SP-281, 1972.

28. Proceedings of the Eighth Annual Conference on Manual Control, Wright-Patterson Air Force Base, Ohio, Air Force Flight Dynamics Laboratory, AFFDL-TR-72-92, Jan. 1973.

29. Costello, R. G., and T. J. Higgins, "An Inclusive Classified Bibliography Pertaining to Modeling the Human Operator as an Element in an Automatic Control System," IEEE Trans., Vol. HFE-7, No. 4, Dec. 1966, pp. 174-181.

30. Summers, L. G., and K. Ziedman, A Study of Manual Control Methodology with Annotated Bibliography, NASA CR-125, Nov. 1964.

31. McRuer, D. T., and D. H. Weir, "Theory of Manual Vehicular Control," Ergonomics, Vol. 12, No. 4, July 1969, pp. 599-633; also IEEE Trans., Vol. SMC-2, No. 5, Nov. 1972, pp. 638-643.

32. McRuer, D. T., and E. S. Krendel, "The Human Operator as a Servo System Element," J. Franklin Inst., Vol. 267, No. 5, May 1959, pp. 381-403; No. 6, June 1959, pp. 511-536.

33. Licklider, J. C. R., "Quasi-Linear Operator Models in the Study of Manual Tracking," in R. D. Luce, ed., Developments in Mathematical Psychology, The Free Press of Glencoe, Ill., 1960, pp. 169-279.

34. Sheridan, T. B., "The Human Operator in Control Instrumentation," Vol. I of R. H. Macmillan, T. J. Higgins, and P. Naslin, eds., Progress in Control Engineering, New York, Academic Press, 1962, pp. 141-187.

35. Elkind, J. I., "A Survey of the Development of Models for the Human Controller," in R. C. Langford and C. J. Mundo, eds., Guidance and Control – II, Vol. 13 of Progress in Astronautics and Aeronautics, New York, Academic Press, June 1964, pp. 623-643.

36. Young, L. R., and L. Stark, Biological Control Systems — A Critical Review and Evaluation, NASA CR-190, Mar. 1965.

37. McRuer, D. T., and H. R. Jex, "A Review of Quasi-Linear Pilot Models," IEEE Trans., Vol. HFE-8, No. 3, Sept. 1967, pp. 231-249.

38. Young, L. R., "Human Control Capabilities," Chap. 16 of J. F. Parker, Jr., and V. R. West, eds., Bioastronautics Data Book, 2nd Ed., NASA SP-3006, 1973, pp. 751-806.

39. Bartlett, F. C., "The Measurements of Human Skill," Occup. Psychol., Vol. 22, 1948, pp. 83-93.

40. Graham, D., and D. T. McRuer, Analysis of Nonlinear Control Systems, New York, Wiley, 1961 (New York, Dover, 1971).

41. Goodman, T. P., and J. B. Reswick, "Determination of System Characteristics from Normal Operating Records," Trans. ASME, Vol. 7, Feb. 1956, pp. 258-271.

42. Wingrove, R. C., and F. C. Edwards, "Measurement of Pilot Describing Functions from Flight Test Data with an Example from Gemini X," 4th Annual NASA-Univ. Conf. on Manual Control, Washington, D. C., NASA SP-192, pp. 119-134; also IEEE Trans., Vol. MMS-9, No. 3, Sept. 1968, pp. 49-55.

43. Wingrove, R. C., and F. G. Edwards, A Technique for Identifying Pilot Describing Functions from Routine Flight-Test Records, NASA TN D-5127, May 1969.

44. Seltzer, L. J., and D. T. McRuer, Survey of Analog Cross-Spectral Analyzers, WADC-TR-59-241, Dec. 1959.

45. Taylor, L. W., Jr., "Discussion of Spectral Human-Response Analysis," 2nd Annual NASA-Univ. Conf. on Manual Control, Washington, D. C., NASA SP-128, 1966, pp. 403-412.

46. Taylor, L. W., Jr., "A Comparison of Human Response Modeling in the Time and Frequency Domains," 3rd Annual NASA-Univ. Conf. on Manual Control, Washington, D. C., NASA SP-144, 1967, pp. 137-153.

47. Taylor, L. W., Jr., "Relationships Between Fourier and Spectral Analyses," 3rd Annual NASA-Univ. Conf. on Manual Control, Washington, D. C., NASA SP-144, 1967, pp. 183-186.

48. Taylor, L. W., Jr., "A Look at Pilot Modeling Techniques," Proc. of the 6th Annual Conf. on Manual Control, Wright-Patterson AFB, Ohio, 1970, pp. 871-896.

49. Whitbeck, R. F., and F. D. Newell, "Mean Square Estimation of Human Pilot Transfer Functions," 4th Annual NASA-Univ. Conf on Manual Control, Washington, D. C., NASA SP-192, 1969, pp. 35-45.

50. Allen, R. W., and H. R. Jex, "A Simple Fourier Analysis Technique for Measuring the Dynamic Response of Manual Control Systems," IEEE Trans., Vol. SMC-2, No. 5, Nov. 1972, pp. 638-643.

51. Magdaleno, R. E., "Serial Segments Method for Measuring Remnant," IEEE Trans., Vol. SMC-2, No. 5, Nov. 1972, pp. 674-678.

52. Shirley, R. S., "Application of a Modified Fast Fourier Transform to Calculate Human Operator Describing Functions," IEEE Trans., Vol. MMS-10, No. 4, Pt. 1, Dec. 1969, pp. 140-144.

53. Shirley, R. S., "A Comparison of Techniques for Measuring Human Operator Frequency Response, Proc. of 6th Annual Conf. on Manual Control, Wright-Patterson AFB, 1970, pp. 803-869.

54. Whitbeck, R. F., and J. R. Knight, "Some Recent Experimental Results Pertaining to the Estimation of Power Spectra Using Finite Lengths of Data," Proc. of the 8th Annual Conf. on Manual Control, AFFDL-TR-72-92, 1973, pp. 273-290.

55. McRuer, D. T., I. L. Ashkenas, and C. L. Guerre, A Systems Analysis View of Longitudinal Flying Qualities, WADD-TR-60-43, Jan. 1960.

56. McRuer, D., D. Graham, E. Krendel, and W. Reisener, Jr., Human Pilot Dynamics in Compensatory Systems: Theory, Models, and Experiments with Controlled Element and Forcing Function Variations, AFFDL-TR-65-15, July 1965.

57. Stapleford, R. L., D. T. McRuer, and R. E. Magdaleno, Pilot Describing Function Measurements in a Multiloop Task, NASA CR-542, Aug. 1966 (also IEEE Trans., Vol. HFE-8, No. 2, June 1967).

58. Magdaleno, R. E., and D. T. McRuer, Effects of Manipulator Restraints on Human Operator Performance, AFFDL-TR-66-72, Dec. 1966.

59. McRuer, D. T., and R. E. Magdaleno, Human Pilot Dynamics with Various Manipulators, AFFDL-TR-66-138, Dec. 1966.

60. Jex, H. R., J. D. McDonnell, and A. V. Phatak, A "Critical" Tracking Task for Man-Machine Research Related to the Operator's Effective Delay Time. Part I: Theory and Experiments with a First-Order Divergent Controlled Element, NASA CR-616, Nov. 1966.

61. McDonnell, J. D., and H. R. Jex, A "Critical" Tracking Task for Man-Machine Research Related to the Operator's Effective Delay Time. Part II: Experimental Effects of System Input Spectra, Control Stick Stiffness, and Controlled Element Order, NASA CR-674, Jan. 1967.

62. Smith, H. J., "Human Describing Functions Measured in Flight and on Simulators," 2nd Annual NASA-Univ. Conf. on Manual Control, NASA SP-128, 1966, pp. 289-290

63. Newell, F. D., and H. J. Smith, Human Transfer Characteristics in Flight and Ground Simulation for a Roll Tracking Task, NASA TN D-5007, Feb. 1969.

64. Newell, Fred D., and P. E. Pietrzak, "In-Flight Measurement of Human Response Characteristics," J. Aircraft, Vol. 5, No. 3, May-June 1968, pp. 277-284.

65. Levison, W. H., and Jerome I. Elkind, Studies of Multivariable Manual Control Systems: Two-Axis Compensatory Systems with Separated Displays and Controls, NASA CR-875, Oct. 1967.

66. Shirley, R. S., Motion Cues in Man-Vehicle Control, MIT, ScD Thesis, MVT-68-1, Jan. 1968 (also Shirley, R. W., and L. R. Young, "Motion Cues in Man-Vehicle Control: Effects of Roll-Motion Cues on Human Operator's Behavior in Compensatory Systems with Disturbance Inputs," IEEE Trans., Vol. MMS-9, No. 4, Dec. 1968, pp. 121-128).

67. Allen, R. W., and H. R. Jex, An Experimental Investigation of Compensatory and Pursuit Tracking Displays with Rate and Acceleration Control Dynamics and a Disturbance Input, NASA CR-1082, June 1968.

68. Gordon-Smith, M., "An Investigation into Some Aspects of the Human Describing Function While Controlling a Single Degree of Freedom," 5th Annual NASA-Univ. Conf. on Manual Control, NASA SP-215, 1970, pp. 203-240 (also An Investigation into Certain Aspects of the Describing Function of a Human Operator Controlling a System of One Degree of Freedom, Toronto, Can., Univ. of Toronto, Inst. for Aerospace Studies, Rept. 149, Feb. 1970.

69. Stapleford, R. L., S. J. Craig, and J. A. Tennant, Measurement of Pilot Describing Functions in Single-Controller Multiloop Tasks, NASA CR-1238, Jan. 1969.

70. Stapleford, R. L., R. A. Peters, and F. R. Alex, Experiments and a Model for Pilot Dynamics with Visual and Motion Inputs, NASA CR-1325, May 1969.

71. Magdaleno, R. E., and D. T. McRuer, Experimental Validation and Analytical Elaboration for Models of the Pilot's Neuromuscular Subsystem in Tracking Tasks, NASA CR-1757, Apr. 1971.

72. McRuer, D. T., D. Graham, and E. S. Krendel, "Manual Control of Single-Loop Systems," J. Franklin Inst., Vol. 238, No. 1, Jan 1967, pp. 1-29; No. 2, Feb. 1967, pp. 145-168.

73. Magdaleno, R. E., D. T. McRuer, and G. P. Moore, Small Perturbation Dynamics of the Neuromuscular System in Tracking Tasks, NASA CR-1212, Dec. 1968 (also "A Neuromuscular Actuation System Model," IEEE Trans., Vol. MMS-9, No. 3, Sept. 1968, pp. 61-71).

74. McRuer, D. T., L. G. Hofmann, H. R. Jex, et al., New Approaches to Human-Pilot/Vehicle Dynamic Analysis, AFFDL-TR-67-150, Feb. 1968.

75. Stark, L., Neurological Control Systems, New York, Plenum Press, 1968.

76. Boring, E., A History of Experimental Psychology, New York, Appleton-Century-Crofts, 1950.

77. McRuer, D. T., "Remarks on Some Neuromuscular Subsystem Dynamics," IEEE Trans., Vol. HFE-7, No. 3, Sept. 1966, pp. 129-130.

78. Reid, L. D., The Measurement of Human Pilot Dynamics in a Pursuit-Plus-Disturbance Tracking Task, Toronto, Can., Univ. of Toronto, Inst. for Aerospace Studies, Rept. 138, Apr. 1969.

79. Heifferon, J. C., and R. A. Hannen, "The Effects of Changes in Input Power Spectra on Human Operator Compensatory Tracking," Proc. of the 6th Annual Conf. on Manual Control, Wright-Patterson AFB, Ohio, AF Inst. of Technology/AF Flight Dynamics Lab., 1970, pp. 677-700 (also J. C. Heifferon, The Effects of Input Power Spectra on Human Operator Compensatory Tracking, Master's Thesis, AF Inst. of Technology, Mar. 1970).

80. Levison, W. H., S. Baron, and D. L. Kleinman, "A Model for Controller Remnant," IEEE Trans., Vol. MMS-10, No. 4, Dec. 1969, pp. 101-108 (also Bolt, Beranek and Newman, Inc., Rept. 1731, 15 Oct. 1968).

81. Jex, H. R., and R. E. Magdaleno, "Corroborative Data on Normalization of Human Operator Remnant," IEEE Trans., Vol. MMS-10, No. 4, Dec. 1969, pp. 137-140.

82. Levison, W. H., and J. I. Elkind, "Two-Dimensional Manual Control Systems with Separated Displays," IEEE Trans., Vol. HFE-8, No. 3, Sept. 1967, pp. 202-209.

83. McRuer, D. T., "Human Operator System and Subsystem Dynamic Characteristics," in A. S. Iberall and A. C. Guyton, eds., Regulation and Control in Physiological Systems, Pittsburgh, Pa., Instrument Soc. of America, 1973, pp. 230-235 (published for International Federation of Automatic Control).

84. Wierwille, W. W., and G. A. Gagne, A Theory for the Optimal Deterministic Characterization of the Time-Varying Dynamics of the Human Operator, NASA CR-170, Feb. 1965.

85. McDonnell, J. D., "A Preliminary Study of Human Operator Behavior Following a Step Change in the Controlled Element," IEEE Trans., Vol. HFE-7, No. 3, Sept. 1966, pp. 125-128.

86. McRuer, D. T., D. Graham, E. S. Krendel, and W. C. Reisener, Jr., System Performance and Operator Stationarity in Manual Control Systems, presented at the 3rd Cong. of the International Federation of Automatic Control, London, 20-25 June 1966.

87. Schwiezer, G., "Some Contributions to the Theory of Linear Models Describing the Control Behaviour of the Human Operator," in R. K. Bernotat and K.-P. Gartner, ed., Displays and Controls, Amsterdam, Swets and Zeitlinger N.V., 1972, pp. 327-348.

88. Bekey, G. A., and J. M. Biddle, "The Effect of a Random-Sampling Interval on a Sampled-Data Model of the Human Operator," 3rd Annual NASA-Univ. Conf. on Manual Control, NASA SP-144, 1967, pp. 247-258.

89. Jex, H. R., R. W. Allen, and R. E. Magdaleno, Display Format Effects on Precision Tracking Performance, AMRL-TR-71-63, Aug. 1971.

90. Graham, D., Research on the Effect of Nonlinearities on Tracking Performance, AMRL-TR-67-9, July 1967.

91. Allen, R. W., W. F. Clement, and H. R. Jex, Research on Display Scanning, Sampling, and Reconstruction Using Separate Main and Secondary Tracking Tasks, NASA CR-1569, July 1970.

92. Jex, H. R., and R. W. Allen, "Research on New Human Dynamic Response Test Battery. Part I: Test Development and Validation. Part II: Psychophysiological Correlates," Proc. of the 6th Annual Conf. on Manual Control, Wright-Patterson AFB, Ohio, 1970, pp. 743-777.

93. Cooper, G. E., and R. P. Harper, Jr., The Use of Pilot Ratings in the Evaluation of Aircraft Handling Qualities, NASA TN D-5153, Apr. 1969.

94. Ashkenas, I. L., and D. T. McRuer, "A Theory of Handling Qualities Derived from Pilot-Vehicle System Considerations," Aerospace Eng., Vol. 21, No. 2, Feb. 1962, pp. 60, 61, 83-102.

95. McDonnell, J. D., Pilot Rating Techniques for the Estimation and Evaluation of Handling Qualities, AFFDL-TR-68-76, Dec. 1968.

96. Anderson, R. O., A New Approach to the Specification and Evaluation of Flying Qualities, AFFDL-TR-69-120, June 1970.

97. Dillow, J. D., The "Paper Pilot" — A Digital Computer Program to Predict Pilot Rating for the Hover Task, AFFDL-TR-70-40, Mar. 1971.

98. Anderson, R. O., A. J. Connors, and J. D. Dillow, Paper Pilot Ponders Pitch, AFFDL/FGC-TM-70-1, Nov. 1970.

99. Anderson, R. O., "Theoretical Pilot Rating Predictions," Handling Qualities Criteria, AGARD Conf. Proc. No. 106, June 1972, pp. 19-1 to 19-14.

100. Teper, G. L., An Assessment of the "Paper Pilot" — An Analytical Approach to the Specification and Evaluation of Flying Qualities, AFFDL-TR-71-174, June 1972.

101. Clement, W. F., D. T. McRuer, and R. H. Klein, "Systematic Manual Control Display Design," Guidance and Control Displays, AGARD CP-96, Feb. 1972, pp. 6-1 to 6-10.

102. McRuer, D. T., I. L. Ashkenas, and D. Graham, Aircraft Dynamics and Automatic Control, Princeton, N. J., Princeton Univ. Press, 1973.

103. Weir, D. H., and D. T. McRuer, Pilot Dynamics for Instrument Approach Tasks: Full Panel Multiloop and Flight Director Operations, NASA CR-2019, May 1972.

104. Miller, D. P., and E. W. Vinje, Fixed-Base Flight Simulator Studies of VTOL Aircraft Handling Qualities in Hovering and Low-Speed Flight, AFFDL-TR-67-152, Jan. 1968.

105. Onstott, E. D., and E. P. Salmon, Airplane Flying Characteristics in Turbulence, AFFDL-TR-70-143, AFFDL-TR-70-143, Feb. 1971.

106. Clement, W. F., R. W. Allen, and D. Graham, Pilot Experiments for a Theory of Integrated Display Format, Systems Technology, Inc., Tech. Rept. 183-2, Oct. 1971 (also JANAIR Rept. 711107).

107. Onstott, E. D., E. P. Salmon, and R. L. McCormick, Prediction and Evaluation of Flying Qualities in Turbulence, AFFDL-TR-71-162, Feb. 1972.

108. Teper, G. L., "An Effective Technique for Extracting Pilot Model Parameter Values from Multi-Feedback, Single-Input Tracking Tasks," Proc. of the 8th Annual Conf. on Manual Control, Wright-Patterson AFB, Ohio, AFFDL-TR-72-92, 1973, pp. 23-33.

109. Weir, D. H., and D. T. McRuer, "Measurement and Interpretation of Driver/Vehicle System Dynamic Response," Human Factors, Vol. 15, No. 4, Aug. 1973, pp. 367-378 (also SAE Paper 730098).

110. Levison, W. H., and J. I. Elkind, Studies of Multivariable Manual Control Systems: Four-Axis Compensatory Systems with Separated Displays and Controls, Cambridge, Mass., Bolt, Beranek and Newman, Rept. 1965, 14 Mar. 1969.

111. Levison, W. H., and J. I. Elkind, Studies of Multivariable Manual Control Systems: Two-Axis Compensatory Systems with Separated Displays and Controls, NASA CR-875, Oct. 1967.

112. McRuer, D. T., H. R. Jex, W. F. Clement, and D. Graham, Development of a Systems Analysis Theory of Manual Control Displays, Systems Technology, Inc., Tech. Rept. 163-1, Oct. 1967.

113. Weir, D. H., and R. H. Klein, The Measurement and Analysis of Pilot Scanning and Control Behavior During Simulated Instrument Approaches, NASA CR-1535, June 1970.

114. Bergen, A. R., "On the Statistical Design of Linear Random Sampling Systems," in J. F. Coales, et al., eds., Automatic and Remote Control (Proc. 1st International Cong. IFAC), Washington, D. C., Butterworth, 1961, pp. 430-436.

115. Jones, G. M., Disorientation in Flight, Air Ministry, Flying Personnel Research Committee, Farnborough, Eng., Memo. 96, Sept. 1958.

116. Peters, R A., Dynamics of the Vestibular System and Their Relation to Motion Perception, Spatial Disorientation, and Illusions, NASA CR-1309, Apr. 1969.

117. Meiry, J. L., The Vestibular System and Human Dynamic Space Orientation, MIT, Man-Vehicle Control Lab., Thesis No. T-65-1, June 1965.

118. Ringland, R. F., and R. L. Stapleford, Experimental Measurements of Motion Cue Effects on STOL Approach Tasks, NASA CR-114458, Apr. 1972.

119. Ashkenas, I. L., Requirements for Airplane Normal and Failure States, Systems Technology, Inc., Working Paper 1017-2, Aug. 1972.

120. Klein, R. H., W. F. Clement, R. H. Hoh, L. G. Hofmann, and R. K. Heffley, XC-142 Vehicle Analyses, Pilot Workload Models, Disturbance Characteristics, and Lateral-Directional Requirements Pertinent to the Design of a STOL Flight Director, Systems Technology, Inc., Interim Tech. Rept. 1011-1, 1 June 1971.

121. Ware, J. R., "An Input Adaptive, Pursuit Tracking Model of the Human Operator," 7th Annual Conf. on Manual Control, NASA SP-281, 1972, pp. 33-45.

122. Wasicko, R. J., D. T. McRuer, and R. E. Magdaleno, Human Pilot Dynamic Response in Single-Loop Systems with Compensatory and Pursuit Displays, AFFDL-TR-66-137, Dec. 1966.

123. Magdaleno, R. E., H. R. Jex, and W. A. Johnson, "Tracking Quasi-Predictable Displays," 5th Annual NASA-Univ. Conf. on Manual Control, NASA SP-215, 1970, pp. 391-428.

124. Vossius, G., "Der Kybernetische Aspekt der Willkurbewegung," Progress in Cybernetics, New York, Elsevier Pub. Co., 1965.

125. Krendel, E. S., and D. T. McRuer, "Psychological and Physiological Skill Development — A Control Engineering Model," 4th Annual NASA-Univ. Conf. on Manual Control, NASA SP-192, 1969, pp. 275-288.

126. Hess, R. A., The Human Operator as an Element in a Control System with Time Varying Dynamics, AFFDL-FDCC-TM-65-34, June 1965.

127. Muckler, F. A., R. O. Hookway, and H. H. Burke, "Manned Control of Large Space Boosters," Trans. 7th Symp. on Ballistic Missile and Space Technology, Vol. II, Los Angeles, Calif., Air Force Systems Command, Space Systems Div., 1962, pp. 149-188.

128. Krendel, E. S., and D. T. McRuer, "A Servomechanisms Approach to Skill Development," J. Franklin Inst., Vol. 269, No. 1, Jan. 1960, pp. 24-42.

129. McRuer, D. T., and H. R. Jex, "A Systems Analysis Theory of Manual Control Displays," 3rd Annual NASA-Univ. Conf. on Manual Control, NASA SP-144, 1967, pp. 9-28.

130. Young, L. R., "On Adaptive Manual Control," IEEE Trans., Vol. MMS-10, No. 4, Pt. II, Dec. 1969, pp. 292-331.

131. Elkind, J. I., P. L. Falb, D. Kleinman, and W. H. Levison, An Optimal Control Method for Predicting Control Characteristics and Display Requirements of Manned-Vehicle Systems, AFFDL-TR-67-187, June 1968.

132. Baron, S., D. L. Kleinman, et al., Application of Optimal Control Theory to the Prediction of Human Performance in a Complex Task, AFFDL-TR-69-81, Mar. 1970.

133. Kleinman, D. L., S. Baron, and W. H. Levison, "An Optimal Control Model of Human Response, Parts 1 and 2," Automatica, Vol. 6, No. 3, May 1970.

134. Kleinman, D. L., and S Baron, Manned Vehicle Systems Analysis by Means of Modern Control Theory, NASA CR-1753, June 1971.

135. Kleinman, D L., S. Baron, and W. H. Levison, "A Control Theoretic Approach to Manned-Vehicle Systems Analysis," IEEE Trans., Vol. AC-16, No. 6, Dec. 1971, pp. 824-832.

136. Levison, W. H., The Effects of Display Gain and Signal Bandwidth on Human Controller Remnant, Bolt, Beranek and Newman, Inc , Rept. 1968, 15 Aug. 1970.

137. Ringland, R. F., R. L. Stapleford, and R. E. Magdaleno, Motion Effects on an IFR Hovering Task — Analytical Predictions and Experimental Results, NASA CR-1933, Nov. 1971.

138. McRuer, D., "Development of Pilot-in-the-Loop Analysis," J. Aircraft, Vol. 10, No. 9, Sept. 1973, pp. 515-524.